2023

Spatiotemporal heterogeneity and bias in respiratory infection surveillance

BOSTON UNIVERSITY

SCHOOL OF PUBLIC HEALTH

Dissertation

SPATIOTEMPORAL HETEROGENEITY AND BIAS IN RESPIRATORY INFECTION SURVEILLANCE

by

BENJAMIN MATTHEW RADER

A.B., Washington University in St. Louis, 2014
M.P.H., Northwestern University, 2018

Submitted in partial fulfillment of the

requirements for the degree of

Doctor of Philosophy

2023

Approved by

First Reader

Matthew P. Fox, D.Sc., M.P.H.
Professor of Epidemiology
Professor of Global Health

Second Reader

Christina M. Astley, M.D., Sc.D.
Attending Physician
Boston Children's Hospital

Assistant Professor of Pediatrics
Harvard Medical School

Third Reader

John S. Brownstein, Ph.D.
Chief Innovation Officer
Boston Children's Hospital

Professor of Pediatrics
Harvard Medical School

Fourth Reader

Laura F. White, Ph.D.
Professor of Biostatistics

ACKNOWLEDGMENTS

This dissertation stands as a testament to the combined efforts of a multitude of individuals, institutions, and communities who have nurtured, guided, and challenged me along the way. First and foremost, I am deeply grateful to my parents, Neil and Dinah, who instilled in me a persistent sense of curiosity from my earliest memories. Equally important is my brother, LJ, whose relentless efforts to keep me grounded, sometimes literally, have been instrumental since day one.

I am profoundly grateful to Boston University for its vital contributions to my academic journey. I am particularly indebted to Matt Fox, who stood by me from the inception to the culmination of this excursion. His remarkable personification of epidemiological virtues has been a constant source of inspiration. Laura White, under whom I've had the unique privilege of learning in manifold capacities—as a student, a researcher, a teaching assistant, and inevitably, an epidemiologist in dire need of a biostatistician—has left an indelible impact on my academic growth.

The Boston University Department of Epidemiology: Martha Werler, Sherri Stuver, Shelley Barnes, the Epidemiology Doctoral Committee, together with others in the broader BU community including Elaine Nsoesie, Zhenwei Zhou, Solange Vinhas, and the entire quantitative TB modeling consortium, have contributed substantially to my doctoral experience. Their insights and expertise have enriched my understanding and approach towards this project and epidemiology in general.

The next phase of my journey led me to Boston Children's, where I was privileged to cross paths with Christina Astley, John Brownstein, and many other impactful

colleagues, mentors, and collaborators. I am beyond thankful to Christina for her kindness, extraordinary reservoir of knowledge, and dedication to helping me grow as a scientist and person. Words cannot express how grateful I am to John for his leadership, expertise, and friendship, all equally essential to my academic journey. This project is a testament to their invaluable guidance and mentorship.

I extend my deepest gratitude to the entire Computational Epidemiology research team and broader HealthMap family including Autumn Gertz, Kara Sewalk, Nikki Schultheiss, Emily Cohn, Chris Remmel, Gaurav Tuli, Tanner Varrelman, Jared Hawkins, Neil Sehgal, Yulin Hswen, and Moritz Kraemer. The SM research team including Laura Wronski, Jack Chen, Jon Cohen, Zoe Padgett, and Joe Brilliant; and the CDC influenza team (who had no direct involvement in the present research) including Danielle Iuliano and Carrie Reed also warrant special mention for their continual collaboration, without which this dissertation would be impossible.

I cannot overlook the myriad of mentors and teachers who have shaped my approach to scientific inquiry. Thank you to Marsel Mesulam, Emily Rogalski, Sandra Weintraub, Kevin Connolly, Michael Fagen, Gregory Phillips, Lisa Kuhns, Ryan Bogdan, David Clifford, Ian Dobbins, Diana Selmeczy, John Doris, Paul Ciancio, and the many others who have imparted wisdom and fostered growth.

To the many collaborators I have had the privilege of working with, thank you for sharing your intellect, insights, and support. To my family and friends, thank you for your inspiration and patience. To my cohort: Nedghie Adrien, Holly Crowe, Dom Leone, and Reese Sy, I could not be luckier to crawl this 4-, 5-, and approaching 6- year marathon

with you. Here's to many more years of indulging in big epi energy.

Most importantly, nothing I achieved would be possible without my family including my family by marriage, who, perhaps reluctantly, were forced to adopt me. My wife and best-friend, Katie, who has been a pillar of unwavering support and the foundation and balance necessary to pursue every last-minute audible that has come our way. My son, Percy, has been the source of joy required to stay sane throughout a graduate program. Lastly, to my radiant daughter Ellie, thank you for inspiring me to continue learning, exploring, and contributing to your world.

SPATIOTEMPORAL HETEROGENEITY AND BIAS IN RESPIRATORY INFECTION SURVEILLANCE

BENJAMIN MATTHEW RADER

Boston University School of Public Health, 2023

Major Professor: Matthew P. Fox, D.Sc., M.P.H., Professor of Epidemiology, Professor of Global Health

ABSTRACT

Parameter estimation of respiratory infection surveillance dynamics commonly utilize data aggregated over space and time. However, estimates derived from aggregated data may fail to account for biologically meaningful spatiotemporal heterogeneity of effects or to identify where and when transmissions occur. This dissertation shows that high-resolution temporal and spatial data can improve our understanding of heterogeneity while producing more valid and precise estimates of transmission parameters (e.g., contagiousness), behavioral trends (e.g., face mask utilization), and intervention effects (e.g., at-home test distribution). In three projects, we evaluate spatiotemporal heterogeneity in the context of two major respiratory pathogens: Tuberculosis and SARS-CoV-2.

First, in project one, we identify disease transmission hotspots from a tuberculosis case surveillance system in Greater Vitória, Brazil. Utilizing a human mobility model and recently developed method to quantify disease transmission, we overcome multiple methodological constraints that often obscure spatially and temporally accurate transmission measurements. We estimate that two cities in Greater Vitória, Vila Velha (reproductive number = 1.05, 95%CI: 1.03–1.07) and Vitória (reproductive number =

1.04, 95%CI: 1.02–1.06), help sustain tuberculosis transmission in the entire region and may be effective targets for intervention, while Cariacica (reproductive number = 0.95, 95%CI: 0.94–0.97) fell below the critical threshold of 1 required to sustain transmission alone.

Next, in project two, we utilize interrupted time series methods to estimate the effect of mask mandates on mask adherence using a nationally representative digital health survey on masking and a comprehensive database of pandemic-related government policies. The analysis focuses on improving previous attempts at measuring the effectiveness of mask mandates at the state level, by utilizing county-level exposure and outcome data. We find that mask mandates were associated with a large heterogeneity of effects, ranging from increasing masking approximately 8% in counties with low levels of prior masking to 1% or lower change in masking in places like the Northeast U.S. where masking levels were already high.

Last, in project three, we leverage the same nationally representative digital health survey to understand at-home testing patterns in the United States. We utilize two different economic measures of resource allocation and a regression model with autoregressive integrated moving average errors to examine if the Covidtests.gov government program reduced at-home testing inequities. We show that Covidtest.gov did increase at-home testing across all demographics; however, income-, geographic- and race-based disparities in at-home test utilization were heightened during periods when the program was active. Specifically, the regression results estimate that Theil's T, an economic metric used here to measure at-home testing disparities, was 53% (95%CI:

6%–121%) higher for household income, 214% (95%CI: 86%–429%) higher for race, and 90% (95%CI: 23%–193%) higher for geography during Covidtest.gov dissemination periods. Disparities were not elevated for age.

Together, these three projects demonstrate the substantial role that high-resolution data can play in improving our understanding of respiratory infection surveillance and informing effective public health interventions.

TABLE OF CONTENTS

LIST OF TABLES

LIST OF FIGURES

1. INTRODUCTION

The precise measurement of where and when an infection occurs is of fundamental importance in epidemiology and requires additional considerations for the study of infectious disease transmission. For example, the transmission of a respiratory virus such as SARS-CoV-2 between an infected and susceptible individual relies on the two people coming into contact during a period where the disease can successfully spread[1]. Separation in space (e.g., social distancing) or time (e.g., avoidance of "high-risk" shopping hours) can result in the prevention of disease transmission. SARS-CoV-2 has high pandemic potential because infected individuals can be contagious for multiple days and often with no symptoms, allowing for numerous effective contacts across a vast space[2,3]. This can be contrasted to SARS-CoV-1, where asymptomatic cases could not spread the disease and, in infected individuals, severe symptoms developed just 2–3 days following the mild ones, making cases easy to recognize, isolate, and quarantine contacts of[4]. Quick identification of infectious individuals limited the space and time the virus could transmit and resulted in the epidemic quickly dying out.

Study of infections and their disease dynamics therefore relies on precise quantification of both space and time relationships. Incorrect measurement of the place and time infection occurred also threatens the validity of effect measurements. For example, if a case was misclassified as occurring in a place with a face mask mandate intervention (when in fact it occurred elsewhere), it would bias the preventative effect of mandates towards the null and result in a misestimation of their beneficial effects.

Research into the dynamics of human infectious diseases often relies on a multitude

of data sources. These data streams each cater to understanding a different aspect of the "agent-host-environment" model, a key framework to understanding disease spread. This model refers to what pathogen is being spread (the agent), by whom (the host), and in what location (the environment)[1,5]. However, studies monitoring the occurrence of diseases often only have detailed measurements for one aspect of this model. For example, they might have laboratory reports of confirmed cases, providing clear data on the nature of the pathogen, but lack information about the movements of the infected individuals, making it hard to understand the environment the disease is spreading in. To overcome this gap and comprehend the influence of unmeasured variables, researchers often turn to publicly published datasets[6]. For example, data from public transportation usage or mobility trends collected from smartphones could provide insights into the host movements[7].

The repurposing of public data is highly efficient, but can lead to temporal and spatial resolution mismatches with the predictors and outcomes of interest (e.g., disease incidence is measured by county, but face mask data is only available by state)[7,8]. Drawing inferences from this data necessitates assumptions about where an infection occurred, such as in the scenario above where researchers would be forced to aggregate disease incidence at the state level to understand the effect of mask wearing. This choice assumes that all counties within the state have consistent incidence and can obscure local heterogeneity due to geographic spillover (i.e., changes in one location due to changes in nearby locations). It can also result in the incorrect ascription of population level effect estimates to subunits, a phenomenon generally called the ecological fallacy or cross-level

bias but specifically referred to as the modifiable areal unit problem in the context of spatial aggregation. The resulting bias can be amplified in aerosolized infections such as tuberculosis and SARS-CoV-2 where high prevalence and opaque transmission events (i.e., not knowing exactly whom transmitted a disease to whom) frequently necessitate study at the population level[9–12] to understand localized risk.

This dissertation focuses on methodological approaches to improving estimates of respiratory infection surveillance parameters and disease relevant behavioral trends across three aims through the incorporating of high-resolution spatial and temporal data streams. In aim 1, we produce improved estimates of the reproductive number, a measure of disease contagiousness, for tuberculosis infections in Brazil. We utilize local census data, a fine-resolution spatial model, monthly infection data from a case surveillance system, and a cutting-edge reproductive number estimator to produce high quality estimates of the location of tuberculosis transmission hotspots. In aim 2, we improve estimates of the effect of mask mandates on mask wearing. To do so, we incorporate a digital health survey that has collected millions of geocoded responses daily over the course of the pandemic. We combine this data with a database of U.S. County mandates to estimate the effectiveness of mandates at a county-level, an improvement on previous efforts that have been limited to studying state-level effects. In aim 3, we produce improved estimates of who used at-home COVID-19 tests and when. We leverage the same large-scale digital health survey employed in aim 2 to examine whether these estimates of at-home test utilization could inform us about equity in the U.S. government's COVID response effort.

Across these three aims, this dissertation attempts to advance our knowledge of respiratory infection surveillance through improved measurement of disease patterns, human responses, and resource allocation. Ultimately, these findings can aid decision makers in their efforts to enhance public health response to respiratory viruses and guide future strategies that seek to control infectious diseases.

1.1 REFERENCES

1. Nelson KE, Williams CM. Infectious Disease Epidemiology: Theory and Practice. Jones & Bartlett Publishers; 2014. Accessed November 4, 2020. https://books.google.com/books/about/Infectious_Disease_Epidemiology.html?id=SnYGIlHpix0C
2. Bai Y, Yao L, Wei T, Tian F, Jin DY, Chen L, Wang M. Presumed Asymptomatic Carrier Transmission of COVID-19. JAMA: The Journal of the American Medical Association. 2020;323(14):1406–1407. doi:10.1001/jama.2020.2565
3. Long QX, Tang XJ, Shi QL, Li Q, Deng HJ, Yuan J, Hu JL, Xu W, Zhang Y, Lv FJ, Su K, Zhang F, Gong J, Wu B, Liu XM, Li JJ, Qiu JF, Chen J, Huang AL. Clinical and immunological assessment of asymptomatic SARS-CoV-2 infections. Nature Medicine. 2020;26(8):1200–1204. doi:10.1038/s41591-020-0965-6
4. Zhong NS, Zheng BJ, Li YM, Poon LLM, Xie ZH, Chan KH, Li PH, Tan SY, Chang Q, Xie JP, Liu XQ, Xu J, Li DX, Yuen KY, Peiris JSM, Guan Y. Epidemiology and cause of severe acute respiratory syndrome (SARS) in Guangdong, People's Republic of China, in February, 2003. Lancet. 2003;362(9393):1353–1358. doi:10.1016/S0140-6736(03)14630-2
5. Centers for Disease Control and Prevention. Principles of Epidemiology in Public Health Practice: An Introduction. U.S. Department of Health and Human Services; 2012.
6. Salathé M, Bengtsson L, Bodnar TJ, Brewer DD, Brownstein JS, Buckee C, Campbell EM, Cattuto C, Khandelwal S, Mabry PL, Vespignani A. Digital Epidemiology. Bourne PE, ed. PLoS Computational Biology. 2012;8(7):e1002616. doi:10.1371/journal.pcbi.1002616
7. Lee EC, Asher JM, Goldlust S, Kraemer JD, Lawson AB, Bansal S. Mind the scales: Harnessing spatial big data for infectious disease surveillance and inference. Journal of Infectious Diseases. 2016;214(S4):S409–S413. doi:10.1093/infdis/jiw344

8. Salkeld DJ, Antolin MF. Ecological Fallacy and Aggregated Data: A Case Study of Fried Chicken Restaurants, Obesity and Lyme Disease. EcoHealth. 2020;17(1):4–12. doi:10.1007/s10393-020-01472-1

9. Avendaño Carvajal L, Perret Pérez C. Epidemiology of Respiratory Infections. In: Pediatric Respiratory Diseases. Springer International Publishing; 2020:263–272. doi:10.1007/978-3-030-26961-6_28

10. Kutter JS, Spronken MI, Fraaij PL, Fouchier RA, Herfst S. Transmission routes of respiratory viruses among humans. Current Opinion in Virology. 2018;28:142–151. doi:10.1016/j.coviro.2018.01.001

11. Herfst S, Böhringer M, Karo B, Lawrence P, Lewis NS, Mina MJ, Russell CJ, Steel J, de Swart RL, Menge C. Drivers of airborne human-to-human pathogen transmission. Current Opinion in Virology. 2017;22:22–29. doi:10.1016/j.coviro.2016.11.006

12. Prather KA, Marr LC, Schooley RT, McDiarmid MA, Wilson ME, Milton DK. Airborne transmission of SARS-CoV-2. Science. 2020;370(6514):eabf0521. doi:10.1126/science.abf0521

2. TUBERCULOSIS TRANSMISSION IN GREATER VITÓRIA, BRAZIL

2.1 INTRODUCTION

Tuberculosis (TB) is a leading cause of morbidity and mortality, with the WHO estimating that the bacillus *Mycobacterium tuberculosis* causes over 10 million incident TB cases per year[1]. Despite TB's global prevalence, relative to other pathogenic infections there is limited information available on the epidemiologic parameters and properties of TB[2]. Disease transmission metrics such as the effective reproductive number (R_t), the parameter that describes the number of additional cases generated by each individual case, is an important measure of how a disease is spreading through a population and changes over time.

Quantifying R_t, such as instances of supercritical transmission ($R_t > 1$) where an epidemic is growing because each case, on average, generates more than one new case, is critical to directing public health interventions[3]. However, accurate measurements of R_t are difficult to quantify in TB for a variety of reasons including 1) the extended serial interval of TB can lead to substantial amounts of missing case information and downward bias R_t estimates when using traditional estimators and 2) localized measures of R_t can be problematic to pinpoint due to the fact that individuals may present as a case in a location other than where they were infected. Here we estimate the R_t of TB in four Brazilian municipalities while overcoming these two constraints by repurposing a routine TB surveillance system and employing a newly developed R_t estimator that is both less sensitive to missing future cases and allows us to account for potential movement from location of infection to location of case capture.

Estimation of TB transmission dynamics can be complicated by the difficulty of accurately measuring the serial interval (i.e., a measure of generation time based on the time between symptom onset of an infector and infected)[2,4,5]. There is often an extended (up to many years) latency period between infection and subsequent disease activation which can obscure future transmission caused by each infectious case[6]. Additionally, unbiased R_t estimation can be difficult without data covering the entire span of TB's extended serial interval distribution[3]. Traditional techniques of estimating R_t from right-censored datasets can result in substantial statistical uncertainty and parameter underestimation[2,3]. For example, Wallinga-Teunis (W-T) estimations of R_t are forward-looking and will attempt to evaluate the number of future infections to ascribe to current cases (i.e., the case reproductive number)[7]. In real-time estimation where future incidence is unknown, resulting W-T R_t estimates of current time periods are driven significantly downward due to the appearance of no subsequent infections. This bias is especially apparent in TB, when measuring R_t with W-T future case data is required over the multi-year serial interval to accurately measure current transmission. Alternative backward-looking approaches to estimating R_t such as the EpiEstim estimator (Cori, et al.[8]) can help prevent the underestimation of R_t due to right-censored case data. This approach uses data on past infections to measure the expected number of secondary infections occurring at the present (i.e., the instantaneous reproductive number) and therefore does not require future case data.

TB transmission patterns can show substantial spatial heterogeneity, suggesting results from subnational research are needed to understand local transmission risk[9]. This

lack of generalizability between regions also means locally-tailored interventions are necessary for proper disease control. However, limited research has been done to characterize TB across heterogenous risk environments and to date, localized movement between these environments has not been accounted for when measuring TB transmission in Brazil[10]. Previous work has shown this movement plays an important role in the transmission of infectious diseases in Brazil[11–13] and of TB in other settings[10,14]. Failure to account for host mobility can result in biased subnational R_t estimates and obscure regions of higher and lower transmission. Until recently, methods to estimate R_t while accounting for this spatial heterogeneity and potential spatial misclassification existed for W-T approaches[15] but not EpiEstim approaches. However, the newly developed R_t estimator from Zhou, et al.[16] is a spatial heterogeneity extension of the backward-looking EpiEstim approach and can be used to estimate local TB transmission metrics while overcoming the problems associated with right-censored datasets.

Due to the many previously described complications with direct R_t estimation, mathematical models and literature-based parameters of TB are often used to estimate R_t indirectly instead of case data[2]. However, routine laboratory and medical data from tuberculosis surveillance systems can be repurposed to create large longitudinal datasets and address this gap. These types of case notification systems have been shown to successfully proxy incidence to allow for unbiased measurements of R_t as well as uncover local disease dynamics, including shifts in spatial incidence and changes in drug resistance[17–19]. As a result, leveraging these monitoring systems is an important goal of the WHO Global Task Force on TB Impact Measurement[1].

Here, we utilize one of these regional TB case surveillance systems from Brazil's Greater Vitória metropolitan area in conjunction with the Zhou, et al. approach to estimating R_t to understand the heterogeneity of transmission across the region's four major municipalities from January 2003 to October 2018. We explicitly model spatial heterogeneity in TB transmission estimates by adjusting for movement imputed from a spatial radiation model in our R_t estimator and illustrate how the use of this methodology can elucidate regional TB dynamics in real-time and across space.

2.2 MATERIALS AND METHODS

2.2.1 Tuberculosis Case Surveillance Data

All microbiologically confirmed cases of tuberculosis within the four municipalities of the Greater Vitória metropolitan area (Vitória, Serra, Vila Velha and Cariacica) in the Brazilian state of Espírito Santo between January 2003 to October 2018 were captured in the internet-based TB Notes surveillance system[20,21]. Cases were aggregated into monthly counts. Confirmation was determined by ≥1 sputum specimen with acid-fast bacilli smear grade ≥2+ with subsequent MTB growth in culture. This data is collected for routine surveillance of TB infection in Greater Vitória. Case counts by municipality were cleaned at the Núcleo de Doenças Infecciosas (NDI) in Vitória, ES.

2.2.2 Estimates of Transmission

For each of the four municipalities, the instantaneous R_t was calculated monthly from the TB Notes surveillance database based on case data from January 2003 to October 2018. We use the Zhou, et. al, heterogeneous R_t estimator[16] that allows for the

reclassification of cases to their location of presumed transmission using information on human host mobility. We use a radiation movement model to estimate human mobility between municipalities and therefore how much spatial reclassification to model. To account for the extended serial interval of TB and variability of delay to diagnosis, we utilize a 36-month burn-in period and a 24-month smoothing window. Estimates are reported for the midpoint of each smoothing window[3]. The resulting R_t estimates are therefore available from January 2007 until October 2017. The serial interval (mean: 2.2 years, standard deviation: 1.8 years, median: 1.7 years) was described by a gamma distribution derived from data from a household contact study of TB in Brazil using survival modeling techniques[5].

2.2.3 R_t Estimator

The Zhou, et al.[16] heterogeneous instantaneous reproductive number (R_t) estimates the expected incidence k of infections at location j occurring at time t for each of the four municipalities*:*

$$m_j(t) \;=\; \sum_{i\,=\,1}^{j} \left[p_{ij} \sum_{\tau < t} \; R_i(t) k_i(t-\tau)\omega(\tau)\right].$$

The serial interval distribution is denoted as $\omega(\tau)$ where τ represents the generation time between the onset of symptoms between an infector and infectee. The estimator accounts for the fact individuals may have been infected in a location i other than the location j where they presented as a case by reclassifying incidence to the location of the presumed

transmission event. The probability (p_{ij}) of incident case reallocation (i.e., probability a case in location i was infected in location j) can be informed by a movement model (details below).

Summary statistics of R_t were computed and central tendency of multiple estimates was reported with the geometric mean. We chose the geometric mean instead of the arithmetic mean because R_t estimates can range from 0 (no new infections) to infinity (unbounded growth of infections), and a value of 1 indicates a stable epidemic. To illustrate this choice, take for example a population whose disease transmission rate alternated monthly between halving (R_t =0.5) and doubling (R_t =2). The arithmetic mean of R_t for this population (1.25) would misleadingly suggest growth over time. In contrast, the geometric mean (1) more accurately reflects a stable epidemic.

2.2.4 Spatial Reclassification of Cases

Case notification may occur in a municipality other than where the infection occurred. The likelihood that a case was spatially misclassified can be represented by an $J \times J$ dimensional matrix when considering J locations, where each cell represents the probability that a case who presented in location j was infected in location i where $i, j \in \{1, 2, \ldots, J\}$. For example, an identity matrix (Table 2.1a) implies that each secondary case arose from an index case within that same region (only autochthonous transmission). Alternatively, a matrix with equal constants in each entry implies that a case could have arisen from any municipality, including the source municipality, with equal probability.

In this study, we reallocate cases based on assumptions driven by three different reclassification schemes: autochthonous transmission (Table 2.1a), a matrix of flows

estimated from a human mobility model (Table 2.1b), and a matrix of flows estimated from a human mobility model that assumes individuals with TB are more likely to travel from home than the average individual[22] (Table 2.1c).

2.2.5 Human Movement Model

We estimate spatial case misclassification (i.e., the probability an individual was incorrectly identified as infected in one municipality when they were actually infected in a different municipality) using a human movement model. The underlying premise of this assumption is that the probability of case misclassification between places i and j is equivalent to the human-to-human movement between i and j.

Human movement estimates were modeled utilizing a nonparametric radiation model of mobility that attempts to model human movement from a region's population structure[23]. Briefly, the radiation model estimates the number of people that move between two locations based on the assumption that flows between two places are a function of both the number of work opportunities (here, assumed proportional with population count) in each location and the number of competing work opportunities available to the residents of each location. The term "work opportunities" here encompasses a wide range of elements, including the volume of available jobs in a particular area, the diversity of these jobs across different sectors and industries, the level of compensation, prospects for career advancement, etc. The model assumes that work opportunities are proportionate to the population count of the region (i.e., regions with more people have more work opportunities), and that individuals will travel and commute for work opportunities. It then posits that work travel and commuting flows are a proxy

for broader mobility between two locations. This estimate based on work opportunities has been shown to generalize to the relative movement of diverse processes including trade, yearly migrations, and inter-urban disease spread[23,24].

For example, if São Paulo is 400 kilometers from Rio de Janeiro, a radiation model estimates movement from São Paulo to Rio de Janeiro based on the population of São Paulo (i.e., work opportunities in São Paulo), the population of Rio de Janeiro (i.e., work opportunities in Rio de Janeiro), and the population within a 400-kilometer radius of São Paulo. The population within this radius represents all the alternative opportunities someone from São Paulo would have if they chose to go 400 kilometers in a direction other than Rio de Janeiro.

We implement the radiation model to estimate movement between each municipality pair p_{ij}:

$$p_{ij} = T_i \frac{m_i n_j}{(m_i + s_{ij})(m_i + n_j + s_{ij})},$$

so that flows are a function of the population counts within the boundaries of municipalities *i* and *j* ($m_i \; and \; n_j$). s_{ij} represents the total population count contained within a geometric circle centered at *i* with a radius of the distance between *i* and *j*, excluding the population counts $m_i \; and \; n_j$.

T_i represents the percentage of the population that travels a non-zero distance for work, a number estimated to be the same for all urban municipalities. The percentage of all individuals in each urban municipality who travel for work was estimated to be 21% from the 2010 Brazilian Population census (Table 3.18.2.4)[25]. Here, T_i was modeled as both 21% (general mobility) and 42% (TB-specific mobility) based on prior research that

individuals with TB are more likely to be commuters and/or commute significantly longer distances[21] than individuals who do not have TB.

These four municipalities were modeled as a closed system due to their geographic clustering and based on previous observations that movement between them was common, but substantial mobility outside the region was rare[21]. All population estimates were extracted from a 2015 gridded (1 km x 1 km) surface of the world's population[26] and municipal populations utilized admin level 2 (U.S. county equivalent) cartographic boundaries of Brazil[27].

2.3 RESULTS

The TB Notes Surveillance System recorded 9,144 cases of microbiologically confirmed tuberculosis between January 2003 and October 2018 in the four major municipalities of Greater Vitória, Brazil (Figure 2.1). On average, Vitória had the highest yearly incidence, 45.9 [SD: 5.1] per 100,000 residents, while Cariacica reported 36.4 [SD: 6.0] per 100,000, Vila Velha reported 34.7 [SD: 3.2] per 100,000, and Serra reported 30.7 [SD: 3.0] per 100,000. When aggregating all four regions, the most yearly cases (N=645) were reported during 2003 and the highest reported monthly total (N=75) was seen during March of that year.

The estimated instantaneous reproductive number of TB in the all-autochthonous transmission model (Figure 2.2) differs across each municipality studied and over time. There is a general trend of oscillation between supercritical transmission ($R_t > 1$) and subcritical transmission ($R_t < 1$) across the four municipalities for one-to-three-year

periods during varying timeframes, however there is substantial uncertainty in the continuous measurements (Figure 2.3). Under the assumption of all autochthonous transmission, the geometric mean reproductive number of all four municipalities is similar. Vitória (R_t=1.04, 95%CI: 1.02–1.05) and Serra (R_t=1.04, 95%CI: 1.03–1.05) had the highest overall estimated mean R_t across study period followed by Vila Velha (R_t=1.03, 95%CI: 1.01–1.04), and Cariacica (R_t=1.01, 95%CI: 0.99–1.02).

The radiation model estimated a mean of 4.6% (SD: 3.1%) inter-municipal flows (Table 2.1b) when modeling general population movement, meaning that of all the individuals living within one of these four municipalities, 4.6% regularly travel to one of the other three. Incorporating the assumption that individuals with TB are substantially more likely to travel, the radiation model estimated a mean of 9.1% (SD: 6.3%) inter-municipal flows. Across both models, Vila Velha (133,600 daily incoming individuals estimated in TB-specific model) and Vitória (174,165 daily incoming individuals estimated in TB-specific model) had the higher estimated incoming flows than Serra (41,036 daily incoming individuals estimated in TB-specific model) and Cariacica (85,739 daily incoming individuals estimated in TB-specific model) (Figure 2.4). Vila Velha and Vitória were also estimated to be the municipality pair with the highest mean percentage interaction while Vila Vela and Serra shared the least (Table 2.1).

R_t estimates incorporating these TB-specific mobility flows (Figure 2.2) had small effects on the relative trends and timing of TB transmission across the four municipalities. Shifts in the same direction were also observed when adjusted for general population movement, but larger differences were apparent when it was assumed that

individuals with TB commuted at a higher rate than others in their community. Under this TB-specific movement model, Vila Velha (R_t=1.05, 95%CI: 1.03–1.07) and Vitória (R_t=1.04, 95%CI: 1.02–1.06) both had slightly higher geometric mean transmission rates than under the all-autochthonous transmission model while Serra (R_t=1.03, 95%CI: 1.01–1.04) had slightly lower and Cariacica (R_t=0.95, 95%CI: 0.94–0.97) dropped significantly.

While the effects on the estimated R_t trends were minor, mobility incorporated estimates did dramatically change the number of months each municipality spent in a period of estimated supercritical transmission. When incorporating mobility, Vila Vela, Vitória, and Serra experienced both months that changed from the supercritical transmission to subcritical and vice versa (Figure 2.5). However, for Cariacica, the mobility adjusted estimates were all shifted downward and only resulted in months moving from supercritical transmission to subcritical.

Vila Velha and Vitória displayed a pattern where the months of the highest estimated transmission under an assumption of all-autochthonous transmission were even higher when adjusting for mobility (points above the diagonal slope in Figure 2.5) and R_t during months with the previously estimated lowest transmission were even lower (points below the diagonal slope in Figure 2.5). This pattern was not apparent in Serra. Interestingly, the two highly spatially coupled regions of Vila Velha and Vitória showed inversely correlated transmission patterns (Figure 2.2) under an assumption of all-autochthonous transmission. The incorporation of mobility adjusted R_t estimates led to more divergent estimates of transmission (Figure 2.6).

2.4 DISCUSSION

We show that the incorporation of a mobility-based model of spatial interaction into estimates of the time-varying reproductive number can illuminate important local patterns within TB case surveillance data. When analyzing crude reproductive number estimates in Greater Vitória, Brazil, we find TB transmission in all four regions to average above the supercritical transmission threshold. However, when incorporating flows estimated by a census-informed radiation model, we see that Vila Velha (the largest city in Greater Vitória) and Vitória (the state capital) emerge as regions of slightly higher transmission and the mean transmission in Cariacica falls below the critical value needed to sustain transmission. Vila Velha and Vitória account for the highest number of daily flows and may serve as a reservoir of disease for Cariacica, a more distant municipality that, in isolation, would be unable to support continued transmission.

While all four of the regions studied have similar population sizes, Vila Velha and Vitória have less land area and are much denser[25,27]. This pattern of higher TB transmission in densely populated urban locations is similar to what has been shown in Brazil nationally[28] and may be the result of these regions supporting more effective contacts[29] and sustaining longer chains of disease transmission[30]. TB control measures that focus on controlling urban transmission and rural importation may play a critical role in preventing the propagation of TB in the greater Vitória metropolitan region[31].

There are multiple limitations of the proposed R_t analysis, mobility estimates, and use of underlying case surveillance data. The requirement to use a long burn-in period and smoothing window highlights the difficulty of calculating R_t in a disease such as TB

with a long serial interval. Here we address the right censoring of the dataset by leveraging a newly developed method by Zhou et al. While the spatial heterogeneity is consistent between the spatially adjusted Zhou et al.[16] and Wallinga-Teunis[7] estimators, the former produces more stable contemporaneous estimates while the latter trends towards zero due to lack of future cases. Spatial interaction extensions of Parag's recursive Bayesian smoother (EpiFilter) should be developed, as they may be less sensitive to these edge effects[32].

The incorporation of a radiation-based mobility model to estimate R_t also has limitations. The modeled flow approximations assume that the distribution of work opportunities is reflective of the population distribution and that the estimated inter-municipality commutation flows are representative of their interaction more generally. If, for example, individuals from Serra are less likely to travel to Vitoria for daily activities (e.g., shopping) than work, our model may overestimate the incidence that was reclassified away from this location and lead us to incorrectly conclude it could not support TB transmission on its own. While radiation type models have been validated on subnational scales[23,24] and for short-term movement[33], empirical assessments of mobility (e.g., from mobile phone location data[34]) in Greater Vitória are necessary to support these assumptions locally. Further, it is difficult to confirm if measures of mobility directly translate to transmission risk.

While the present analysis can resolve questions about which municipalities have experienced heightened transmission during the period of study, the spatial coarseness of the data used does not account for heterogeneity of incidence within these municipalities.

Previous research has shown this may be nonuniform and dependent on socioeconomic status[35], and thus future studies are needed to understand this transmission stratified by more refined geography and socioeconomic status. Nevertheless, the integration of mobility data with the proposed spatial resolution is a notable improvement upon what is currently available to public health officials.

The TB notes surveillance system is a rich dataset that systemically captured all microbiologically confirmed cases of TB within Greater Vitória, however there are likely cases of active TB in the communities that have yet to present for laboratory confirmation. Our R_t estimates are robust to this gap provided this proportion is consistent across municipalities and time[36], but they may be biased if this gap is accompanied by differential care-seeking. Further, the TB notes surveillance system does not account for differential transmission that may manifest as varying burdens of latent TB. Additionally, the R_t heterogeneity estimator used here requires independence between infection probability due to spatial and temporal distance; an assumption that may be violated if there were different strains of TB with varying serial intervals that are circulating differentially in the four regions of Greater Vitória.

2.4.1 Conclusion

Understanding local dynamics of tuberculosis is essential for disease control. Here we show that incorporating modeled mobility flows and a backwards-looking R_t estimator can yield insights on the importation of TB between different municipalities within Greater Vitória, Brazil. We further highlight that routine TB case surveillance systems can be utilized in combination with these methods to identify and characterize

transmission parameters of hotspots that may be subsequently targeted for region-specific disease control interventions.

2.5 TABLES AND FIGURES

Table 2.1 Three interaction matrices used to account for spatial heterogeneity in the estimation of R_t: A. no interaction (all autochthonous transmission), B. a matrix of movement estimated from the radiation model, and C. a matrix of movement estimated from the radiation model that assumes individuals with TB travel more frequently than the general population. All movement estimates rounded to 2 decimal places. Interaction is used to model the opportunity for a TB case to present in a municipality other than where they were potentially infected. Cells represent the probability of a case having been misallocated.

A. All Autochthonous Transmission

		Incoming Movement		
Outgoing Movement	Cariacica	Serra	Vila Velha	Vitória
Cariacica	1	0	0	0
Serra	0	1	0	0
Vila Velha	0	0	1	0
Vitória	0	0	0	1

B. Radiation Model Estimates (General Population Mobility)

		Outgoing Movement*		
Incoming Movement	Cariacica	Serra	Vila Velha	Vitória
Cariacica	0.89	0.05	0.03	0.02
Serra	0.02	0.84	0.02	0.02
Vila Velha	0.04	0.03	0.87	0.12
Vitória	0.05	0.07	0.08	0.85

C. Radiation Model Estimates (TB Specific Mobility)

		Outgoing Movement*		
Incoming Movement	Cariacica	Serra	Vila Velha	Vitória
Cariacica	0.79	0.10	0.06	0.04
Serra	0.04	0.69	0.04	0.03
Vila Velha	0.08	0.07	0.74	0.24
Vitória	0.10	0.14	0.16	0.69

*All columns add to 1 and are rounded for presentation purposes

Figure 2.1 Tuberculosis Incidence Measured in Four Municipalities of Greater Vitória, Brazil

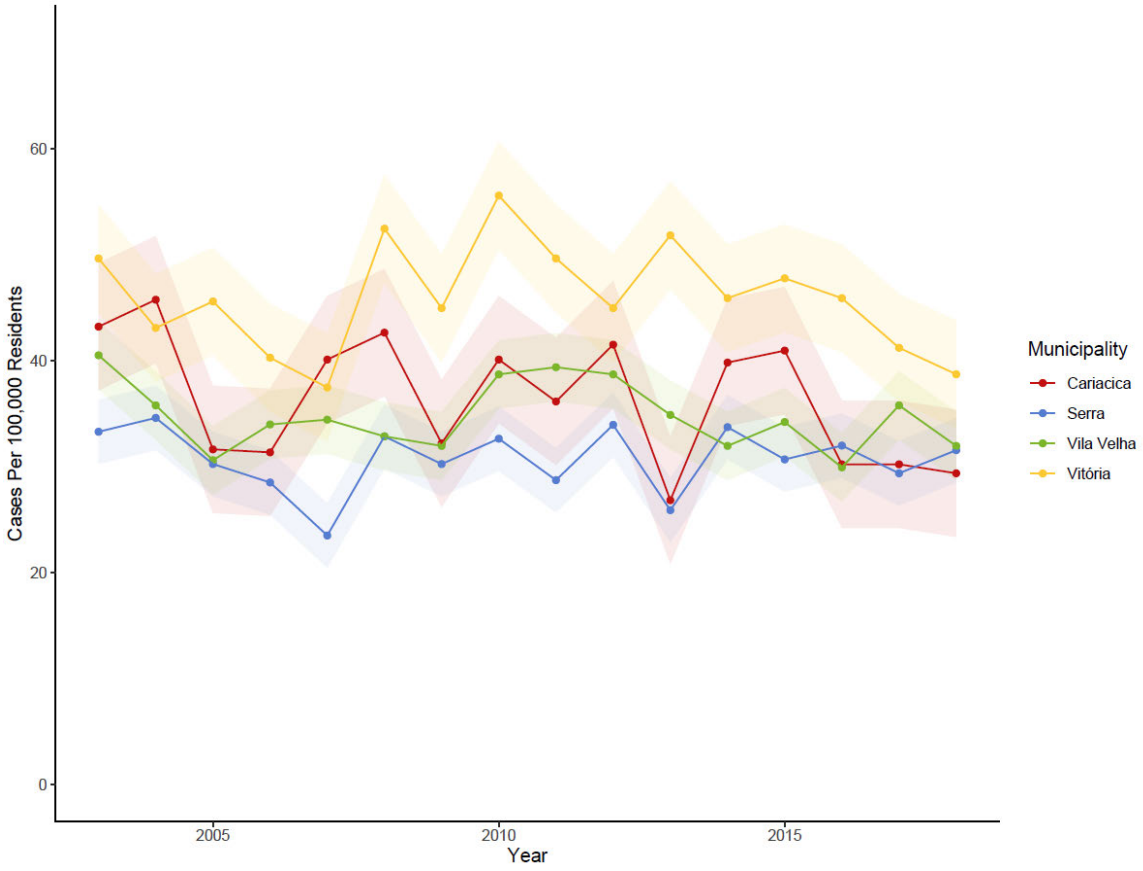

All cases of microbiologically confirmed tuberculosis in Greater Vitória between January 2003 and October 2018 were captured by the TB Notes Surveillance system at the Núcleo de Doenças Infecciosas in Vitória, Brazil. Cases here are presented for the four municipalities of the greater Vitoria metropolitan area, population-adjusted per 100,000 residents of each municipality. Color shaded bands represent the year-to-year standard deviation of cases in each municipality.

Figure 2.2 Mobility and the Time-Varying Reproductive Number of Tuberculosis in Greater Vitória

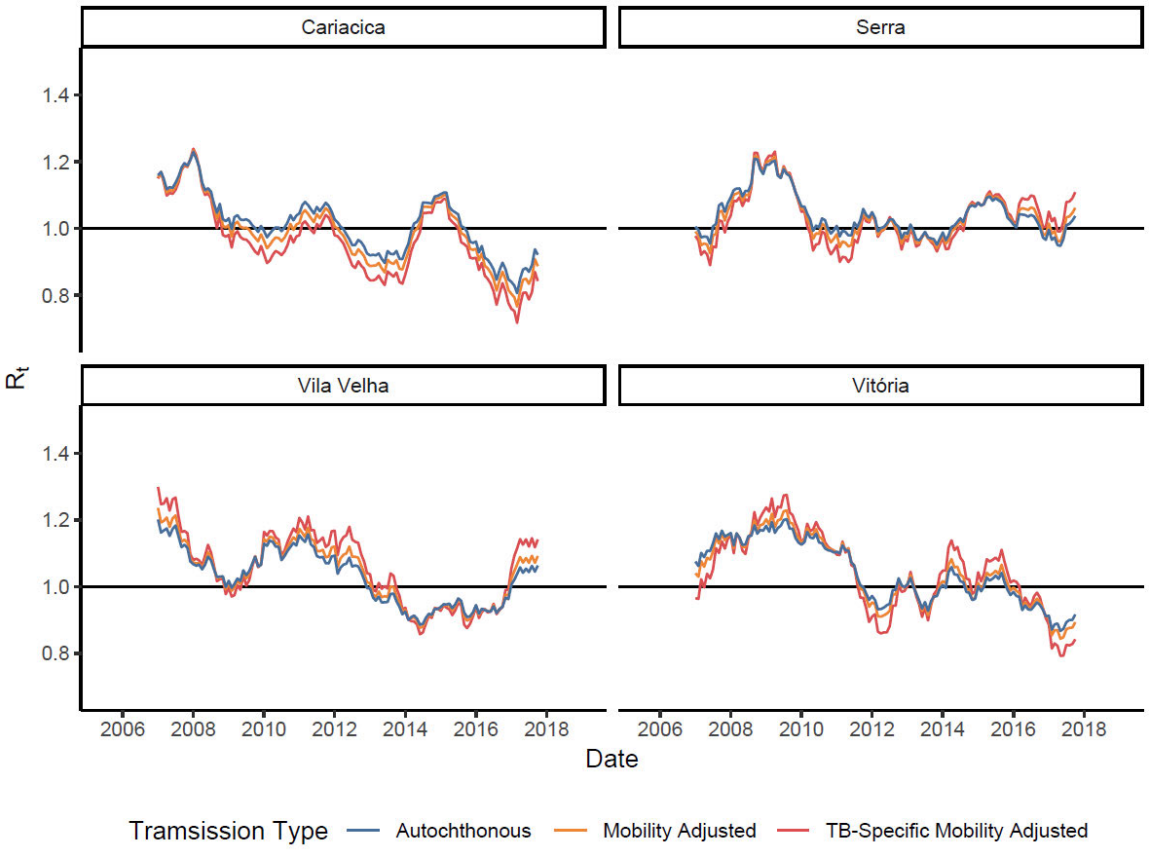

Estimates of the time-varying reproductive number of tuberculosis in four municipalities of Greater Vitória, Brazil between January 2007 and October 2017. The instantaneous reproductive number (R_t) was estimated utilizing three different assumptions of spatial interaction: only autochthonous transmission (blue), a matrix of flows estimated from a human mobility model (orange), and a matrix of flows estimated from a human mobility model that assumes individuals with TB have higher mobility than the average individual (red).

Figure 2.3 Variability and Uncertainty in the time-varying reproductive number (R_t) of tuberculosis in four municipalities of Greater Vitória, Brazil between January 2007 and October 2017

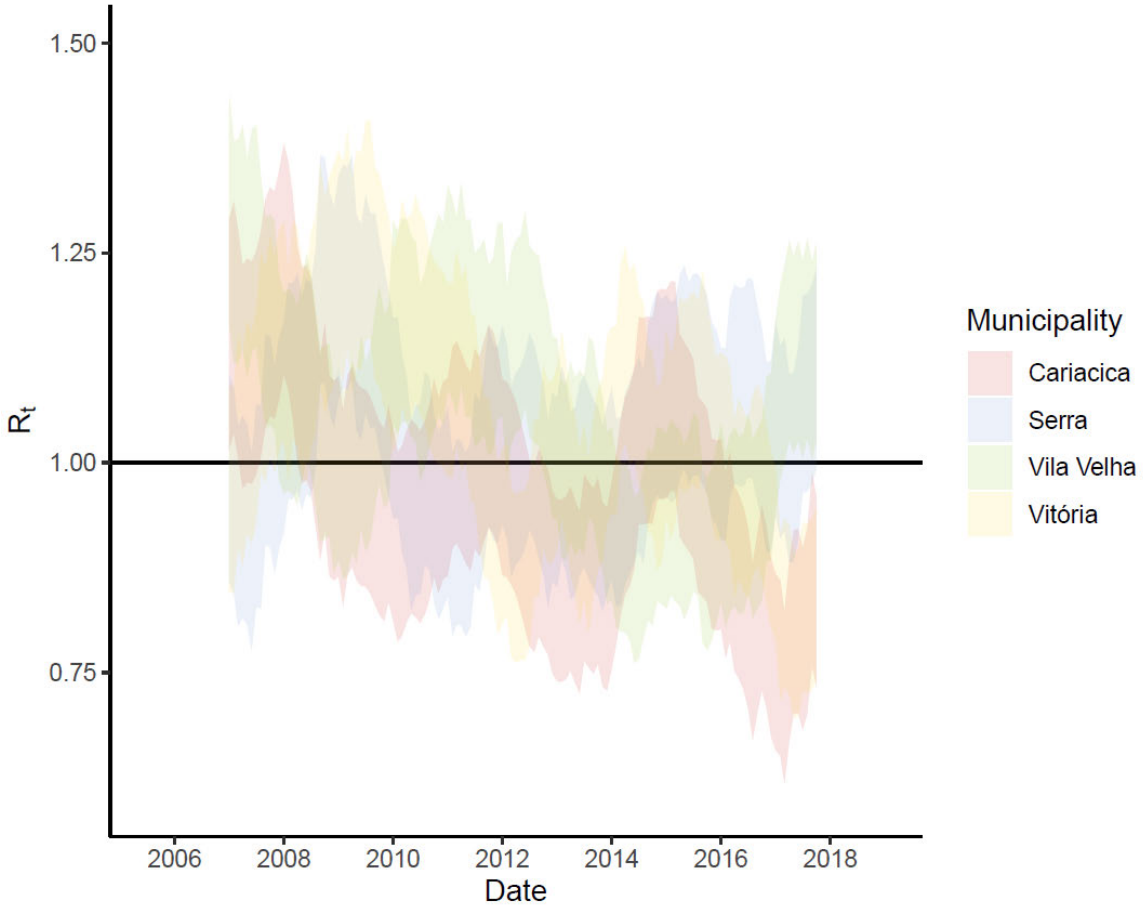

Estimates of the time-varying reproductive number of tuberculosis in four municipalities of Greater Vitória, Brazil between January 2007 and October 2017 assuming autochthonous transmission. Colored bands represent 95% simulation interval of time-varying reproductive number across the municipalities.

Figure 2.4 Estimated Mobility Between Four Municipalities of Greater Vitória, Brazil

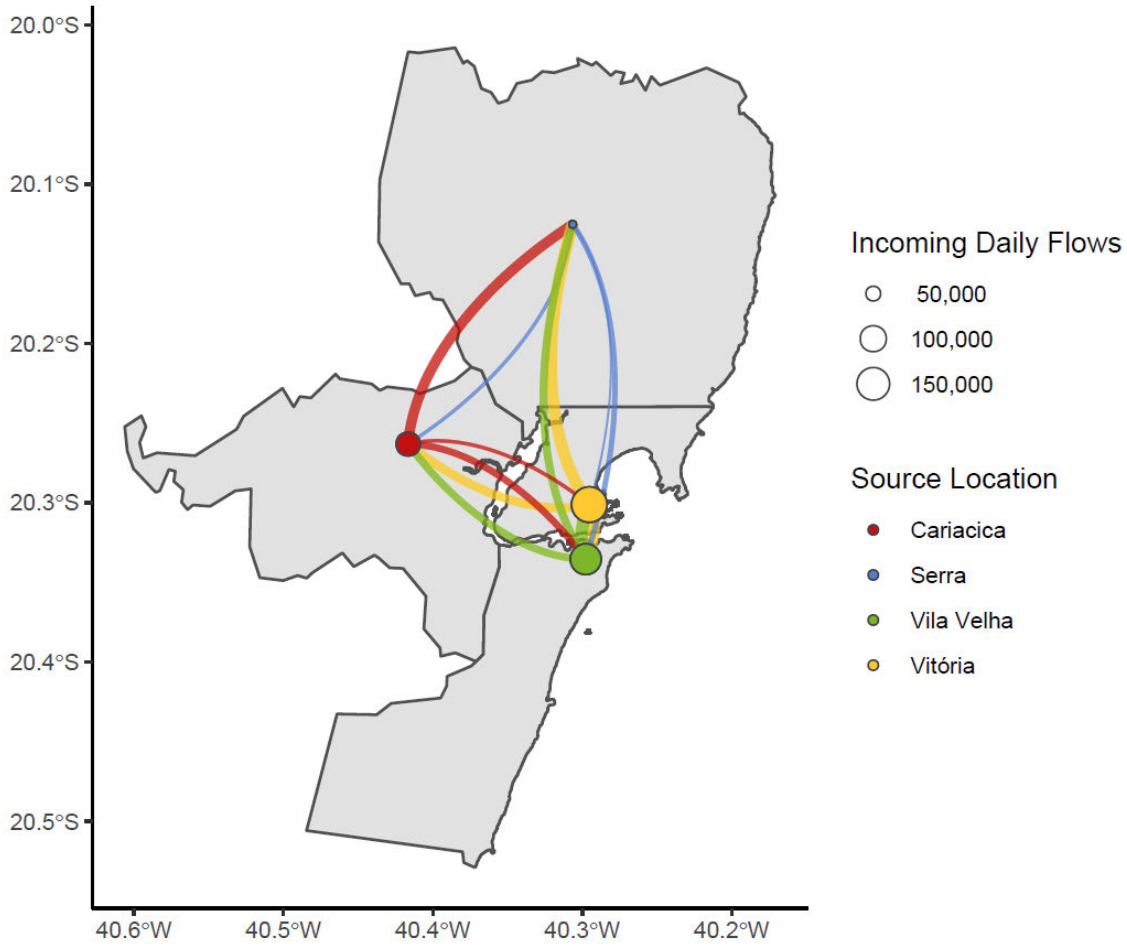

Inter-municipality flows from a radiation model estimating TB-specific movement in four municipalities in Greater Vitória, Brazil. Colored lines represent movement from one municipality to the city with the same color point. Line thickness and point size represent the volume of estimated mobility flows.

Figure 2.5 Estimated R_t of TB in four municipalities of Greater Vitória, Brazil comparing assumptions of autochthonous transmission to estimates that incorporate inter-municipality interactions

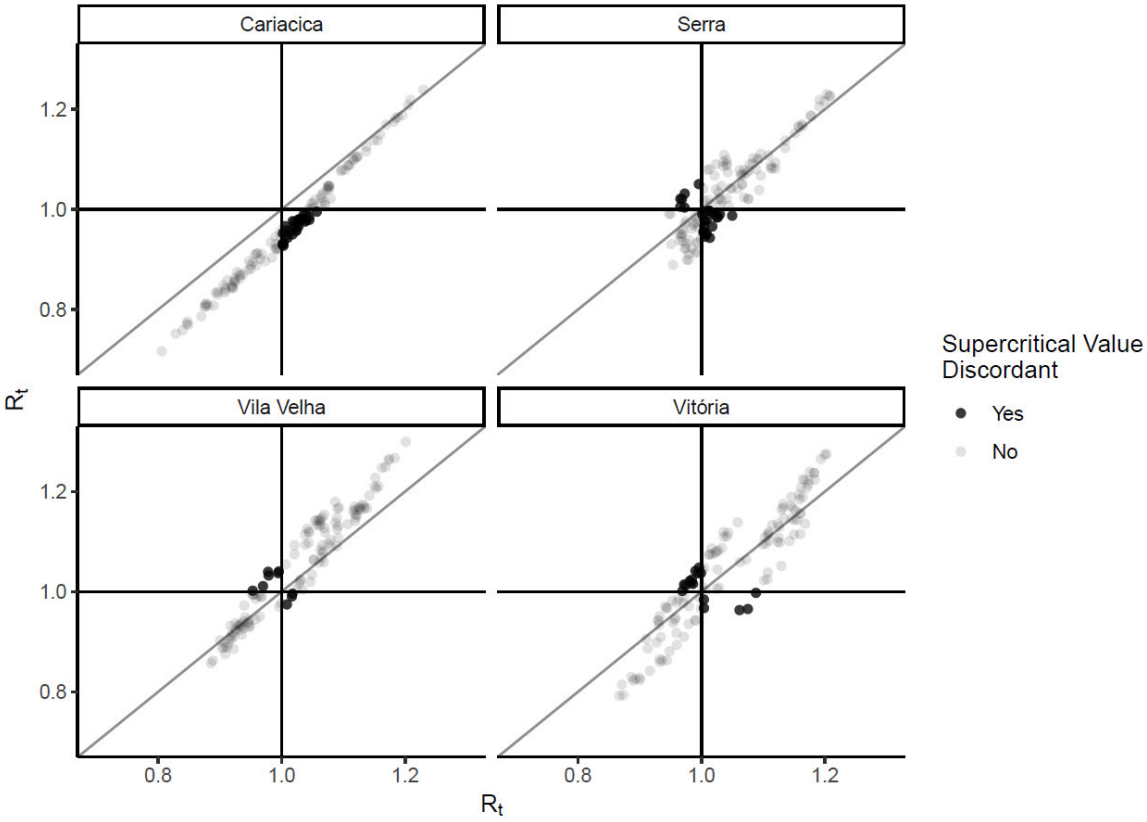

Estimated R_t in the four municipalities of greater Vitoria metropolitan area in Greater Vitória, Brazil. X-axis R_t values are estimated from a model that assumes each of the four regions are independent with respect to TB transmission. Y-axis R_t values are estimated from a model that incorporates estimates of human movement from a radiation mobility model, assumes cases who presented in each region may have been infected in another region, and assumes that individuals with TB may be more likely to travel than individuals who do not have TB. Supercritical values are discordant when R_t is estimated to be the value of supercritical transmission ($R_t > 1$) in one model, but not the other

Figure 2.6 Longitudinal ratio of estimated R_t accounting for inter-municipality interaction over R_t assuming autochthonous transmission in two highly connected municipalities of Greater Vitória, Brazil

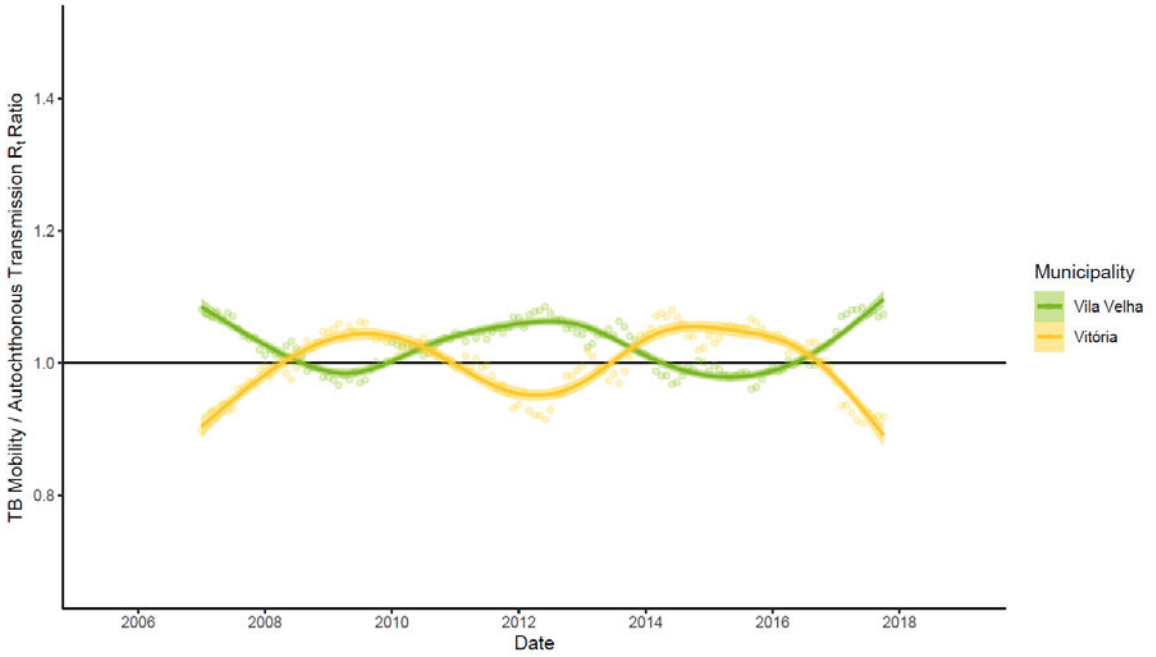

Estimated R_t in the two highly spatially connected municipalities of greater Vitoria metropolitan area in Greater Vitória, Brazil over time. Y-axis represents R_t estimated from a model accounting for spatial interaction divided by R_t estimated from the model that assumed all transmission was autochthonous. Fitted values from generalized additive models fit to R_t estimates from Vila Velha (green) and Vitoria (yellow) with 95% confidence interval (shaded area) are shown for visualization of trend.

2.6 REFERENCES

1. WHO. *Global Tuberculosis Report 2019*. World Health Organization; 2019:7. Accessed October 6, 2020. http://www.who.int/tb/publications/global_report/en/

2. Ma Y, Horsburgh CR, White LF, Jenkins HE. Quantifying TB transmission: A systematic review of reproduction number and serial interval estimates for tuberculosis. *Epidemiology and Infection*. 2018;146(12):1478–1494. doi:10.1017/S0950268818001760

3. Gostic KM, McGough L, Baskerville EB, Abbott S, Joshi K, Tedijanto C, Kahn R, Niehus R, Hay JA, De Salazar PM, Hellewell J, Meakin S, Munday JD, Bosse NI, Sherrat K, Thompson RN, White LF, Huisman JS, Scire J, Bonhoeffer S, Stadler T, Wallinga J, Funk S, Lipsitch M, Cobey S. Practical considerations for measuring the effective reproductive number, Rt. Pitzer VE, ed. *PLOS Computational Biology*. 2020;16(12):e1008409. doi:10.1371/journal.pcbi.1008409

4. Lehtinen S, Ashcroft P, Bonhoeffer S. On the relationship between serial interval, infectiousness profile and generation time. *Journal of The Royal Society Interface*. 2021;18(174):20200756. doi:10.1098/rsif.2020.0756

5. Ma Y, Jenkins HE, Sebastiani P, Ellner JJ, Jones-López EC, Dietze R, Horsburgh, Jr. CR, White LF. Using Cure Models to Estimate the Serial Interval of Tuberculosis With Limited Follow-up. *American Journal of Epidemiology*. 2020;189(11):1421–1426. doi:10.1093/aje/kwaa090

6. Lillebaek T, Dirksen A, Baess I, Strunge B, Thomsen V, Andersen ÅB. Molecular evidence of endogenous reactivation of Mycobacterium tuberculosis after 33 years of latent infection. *Journal of Infectious Diseases*. 2002;185(3):401–404. doi:10.1086/338342

7. Wallinga J, Teunis P. Different epidemic curves for severe acute respiratory syndrome reveal similar impacts of control measures. *American Journal of Epidemiology*. 2004;160(6):509–516. doi:10.1093/aje/kwh255

8. Cori A, Ferguson NM, Fraser C, Cauchemez S. A New Framework and Software to Estimate Time-Varying Reproduction Numbers During Epidemics. *American Journal of Epidemiology*. 2013;178(9):1505–1512. doi:10.1093/aje/kwt133

9. Theron G, Jenkins HE, Cobelens F, Abubakar I, Khan AJ, Cohen T, Dowdy DW. Data for action: Collection and use of local data to end tuberculosis. *The Lancet*. 2015;386(10010):2324–2333. doi:10.1016/S0140-6736(15)00321-9

10. Moreno V, Espinoza B, Barley K, Paredes M, Bichara D, Mubayi A, Castillo-Chavez C. The role of mobility and health disparities on the transmission dynamics of

Tuberculosis. *Theoretical Biology and Medical Modelling*. 2017;14(1):1–17. doi:10.1186/s12976-017-0049-6

11. Zinszer K, Morrison K, Brownstein JS, Marinho F, Santos AF, Nsoesie EO. Reconstruction of zika virus introduction in Brazil. *Emerging Infectious Diseases*. 2017;23(1):92–94. doi:10.3201/eid2301.161274

12. Nunes MRT, Faria NR, de Vasconcelos JM, Golding N, Kraemer MUG, de Oliveira LF, da Silva Azevedo R do S, da Silva DEA, da Silva EVP, da Silva SP, Carvalho VL, Coelho GE, Cruz ACR, Rodrigues SG, da Silva Gonçalves Vianez JL, Nunes BTD, Cardoso JF, Tesh RB, Hay SI, Pybus OG, da Costa Vasconcelos PF. Emergence and potential for spread of Chikungunya virus in Brazil. *BMC Medicine*. 2015;13(1):102. doi:10.1186/s12916-015-0348-x

13. Angelo JR, Katsuragawa TH, Sabroza PC, de Carvalho LAS, Silva LHP da, Nobre CA. The role of spatial mobility in malaria transmission in the Brazilian Amazon: The case of Porto Velho municipality, Rondônia, Brazil (2010–2012). Mertens F, ed. *PLOS ONE*. 2017;12(2):e0172330. doi:10.1371/journal.pone.0172330

14. Robsky KO, Isooba D, Nakasolya O, Mukiibi J, Nalutaaya A, Kitonsa PJ, Kamoga C, Baik Y, Kendall EA, Katamba A, Dowdy DW. Characterization of geographic mobility among participants in facility- and community-based tuberculosis case finding in urban Uganda. Lebina L, ed. *PLOS ONE*. 2021;16(5):e0251806. doi:10.1371/journal.pone.0251806

15. White LF, Archer B, Pagano M. Estimating the reproductive number in the presence of spatial heterogeneity of transmission patterns. *International Journal of Health Geographics*. 2013;12(1):1–10. doi:10.1186/1476-072x-12-35

16. Zhou Z, Kolaczyk E, Thompson R, White L. *Estimation of Heterogeneous Instantaneous Reproduction Numbers with Application to Characterize SARS-CoV-2 Transmission in Massachusetts Counties*. Infectious Diseases (except HIV/AIDS); 2021. doi:10.1101/2021.12.02.21267164

17. McIntosh AI, Jenkins HE, White LF, Barnard M, Thomson DR, Dolby T, Simpson J, Streicher EM, Kleinman MB, Ragan EJ, van Helden PD, Murray MB, Warren RM, Jacobson KR. Using routinely collected laboratory data to identify high rifampicin-resistant tuberculosis burden communities in the Western Cape Province, South Africa: A retrospective spatiotemporal analysis. Suthar AB, ed. *PLOS Medicine*. 2018;15(8):e1002638. doi:10.1371/journal.pmed.1002638

18. Leavitt SV, Lee RS, Sebastiani P, Horsburgh CR, Jenkins HE, White LF. Estimating the relative probability of direct transmission between infectious disease patients. *International journal of epidemiology*. 2020;49(3):764–775. doi:10.1093/ije/dyaa031

19. White LF, Moser CB, Thompson RN, Pagano M. Statistical Estimation of the Reproductive Number From Case Notification Data. *American Journal of Epidemiology*. 2021;190(4):611–620. doi:10.1093/aje/kwaa211

20. Vieira RDCA, Fregona G, Palaci M, Dietze R, Maciel ELN. Epidemiological profile of multidrug-resistant tuberculosis cases in Espírito Santo. *Revista Brasileira de Epidemiologia*. 2007;10(1):56–65. doi:10.1590/s1415-790x2007000100007

21. Vinhas SA, Jones-López EC, Ribeiro Rodrigues R, Gaeddert M, Peres RL, Marques-Rodrigues P, de Aguiar PPL, White LF, Alland D, Salgame P, Hom D, Ellner JJ, Dietze R, Collins LF, Shashkina E, Kreiswirth B, Palaci M. Strains of Mycobacterium tuberculosis transmitting infection in Brazilian households and those associated with community transmission of tuberculosis. *Tuberculosis*. 2017;104:79–86. doi:10.1016/j.tube.2017.03.003

22. Zamudio C, Krapp F, Choi HW, Shah L, Ciampi A, Gotuzzo E, Heymann J, Seas C, Brewer TF. Public Transportation and Tuberculosis Transmission in a High Incidence Setting. Mokrousov I, ed. *PLOS ONE*. 2015;10(2):e0115230. doi:10.1371/journal.pone.0115230

23. Simini F, González MC, Maritan A, Barabási AL. A universal model for mobility and migration patterns. *Nature*. 2012;484(7392):96–100. doi:10.1038/nature10856

24. Wen TH, Hsu CS, Hu MC. Evaluating neighborhood structures for modeling intercity diffusion of large-scale dengue epidemics. *International Journal of Health Geographics*. 2018;17(1):9. doi:10.1186/s12942-018-0131-2

25. *Sinopse Do Censo Demográfico: 2010*. Brazilian Institute of Geography and Statistics; 2011.

26. Doxsey-Whitfield E, MacManus K, Adamo SB, Pistolesi L, Squires J, Borkovska O, Baptista SR. Taking Advantage of the Improved Availability of Census Data: A First Look at the Gridded Population of the World, Version 4. *Papers in Applied Geography*. 2015;1(3):226–234. doi:10.1080/23754931.2015.1014272

27. Global Administrative Areas. GADM database of Global Administrative Areas. Published 2020. Accessed October 6, 2020. https://gadm.org/

28. Harling G, Castro MC. A spatial analysis of social and economic determinants of tuberculosis in Brazil. *Health and Place*. 2014;25:56–67. doi:10.1016/j.healthplace.2013.10.008

29. Maas J, van Dillen SME, Verheij RA, Groenewegen PP. Social contacts as a possible mechanism behind the relation between green space and health. *Health and Place*. 2009;15(2):586–595. doi:10.1016/j.healthplace.2008.09.006

30. Rader B, Scarpino SV, Nande A, Hill AL, Adlam B, Reiner RC, Pigott DM, Gutierrez B, Zarebski AE, Shrestha M, Brownstein JS, Castro MC, Dye C, Tian H, Pybus OG, Kraemer MUG. Crowding and the shape of COVID-19 epidemics. *Nature Medicine*. Published online October 5, 2020:1–6. doi:10.1038/s41591-020-1104-0

31. Dowdy DW, Golub JE, Chaisson RE, Saraceni V. Heterogeneity in tuberculosis transmission and the role of geographic hotspots in propagating epidemics. *Proceedings of the National Academy of Sciences of the United States of America*. 2012;109(24):9557–9562. doi:10.1073/pnas.1203517109

32. Parag KV. Improved estimation of time-varying reproduction numbers at low case incidence and between epidemic waves. Kosakovsky Pond SL, ed. *PLOS Computational Biology*. 2021;17(9):e1009347. doi:10.1371/journal.pcbi.1009347

33. Tuite AR, Thomas-Bachli A, Acosta H, Bhatia D, Huber C, Petrasek K, Watts A, Yong JHE, Bogoch II, Khan K. Infectious disease implications of large-scale migration of Venezuelan nationals. *Journal of travel medicine*. 2018;25(1):1–8. doi:10.1093/jtm/tay077

34. Wesolowski A, Buckee CO, Engø-Monsen K, Metcalf CJE. Connecting mobility to infectious diseases: The promise and limits of mobile phone data. *Journal of Infectious Diseases*. 2016;214(Suppl 4):S414–S420. doi:10.1093/infdis/jiw273

35. Maciel ELN, Pan W, Dietze R, Peres RL, Vinhas SA, Ribeiro FK, Palaci M, Rodrigues RR, Zandonade E, Golub JE. Spatial patterns of pulmonary tuberculosis incidence and their relationship to socio-economic status in Vitoria, Brazil. *International Journal of Tuberculosis and Lung Disease*. 2010;14(11):1395–1402.

36. White LF, Pagano M. Reporting errors in infectious disease outbreaks, with an application to Pandemic Influenza A/H1N1. *Epidemiologic Perspectives and Innovations*. 2010;7(1). doi:10.1186/1742-5573-7-12

3. MASK MANDATES AND MASKING DURING THE COVID-19 PANDEMIC

3.1 INTRODUCTION

Although the usage of face masks has become a common practice across the U.S. during the COVID-19 pandemic[1], their effectiveness in reducing transmission events remains a topic of debate[2,3]. An important source of conflict over their usage stems from binding mask mandates often accompanying masking recommendations, perceived by many as an infringement on civil liberties[3,4]. While there is robust evidence that masks can reduce respiratory disease spread[5–8], the impact of mask mandates on this reduction is less clear[5,9–14]. This disconnect may be attributed to a variety of factors, including variable adherence to mandates[5,13], the occurrence of substantial disease spread in private settings — despite public mandate compliance[15], aggregation bias obscuring that masking is protective in some settings and not in others, and the inherent difficulty of accurately measuring the effects of complex government policies[16]. These divergent findings can also be considered within the historical context of inconsistent compliance to public health mandates[17], despite clear evidence of the effectiveness of the mandated behavior (e.g., seatbelt wearing)[18].

Accurately measuring the effect of mask mandates on disease outcomes presents several challenges, including confounding by indication. Mask mandates, typically introduced in response to a surge in COVID-19 incidence, often trigger other mitigation measures and behavioral changes that can confound the isolation of the mandates' effects. Consequently, studies employing pre-post designs might capture trends in alternative behavioral responses to disease dynamics (e.g., social isolation) rather than the effect of

the mandates on outcomes mediated through the desired masking behavior. This potential confounding may also explain why some studies have found no added benefit of mask mandates when accompanied by other non-pharmaceutical interventions[10], while others found a reduction in COVID-19 mortality implausibly just one week following their issuance[11].

In addition to the complexities of establishing a causal link between mandates and disease outcomes, another possible reason for the inconsistent results between the impacts of masking and mandates might stem from the variability in mask adherence due to mandates. Policies spanning multiple jurisdictions and the potential for geographic spillover effects can substantially influence this variability. Mandates have been implemented at different levels of government and geography, with some local mandates being issued before broader statewide ones (e.g., Cuyahoga County, Ohio, the location of Cleveland, implemented a mandate approximately two weeks prior to Ohio State)[19]. Early county-level mandates may effectively increase adherence but obscure the impact of later statewide ones because they had already caused the population proportion masking to peak. Additionally, geographic spillover effects can occur when neighboring regions respond to mandates in adjacent localities (e.g., Akron, Ohio masking levels being influenced by Cleveland's mask mandate[20]) before being formally required to do so. Previous studies measuring the effect of mask mandates on adherence to masking have primarily focused on statewide mandates and mask usage aggregated at the state level, which may be downwardly biased by these geographic spillover effects and obscure important heterogeneities in the intervention's impact. This hypothesis is

supported by a U.S. study that found increased mask-wearing reduced COVID-19 transmission, but statewide mask mandates did not alter mask-wearing[5].

To better understand the disease mitigation benefits of masking and mask mandates, we sought to answer a fundamental question: do mask mandates modify masking behavior? Importantly, because mask usage forms a critical link in the causal chain from mandates to disease mitigation, if mandates do not alter mask-wearing behavior, they are unlikely to influence the control of disease transmission. To mitigate the issues arising from multi-jurisdictional mandates and geographic spillover effects, we conduct our analysis at the county level. Using data from the first year of the COVID-19 pandemic, we estimate how much initial implementations of county-level government mask mandates changed masking behavior using an interrupted time series (ITS) analysis across the U.S. By examining the effect of mask mandates through a more local lens, we aim to understand the heterogeneity of the intervention's effectiveness across different communities which is crucial for informing future infectious disease mitigation strategies.

3.2 METHODS AND MATERIALS

First, we measured the effect of county-level mask mandates on self-reported masking behavior during the initial phase of the COVID-19 pandemic using an ITS stacked design. Next, we ran subgroup analyses stratified by geography, urbanicity, and population proportion masking prior to the issuance of mandates. Finally, we employ a pooled ITS design to ensure our results are robust to model specification.

3.2.1 County Mask Mandate (Exposure)

We extracted dates of county mandates from "Tracking Mask Mandates During the Covid-19 Pandemic," a database of county- and state-level mask interventions[19] previously used to understand adherence to mask mandates at the state level[14]. All U.S. counties (n=624 counties in 14 U.S. states) that issued a county-level mask mandate after June 17, 2020 (14 days after the start of mask adherence data, described below) preceding, concurrent with, or in the absence of respective state mandate are included for analysis.

3.2.2 Self-Reported Mask Adherence (Outcome)

Individual self-reports of mask-wearing in public and private settings were collected between June 2, 2020 and January 1, 2021 by the OutbreaksNearMe anonymous serial cross-sectional web survey (N > 3,000,000) in the United States.[5,21] Survey respondents were asked multiple demographic and behavioral questions, including their home location and how likely they were to wear a mask "while grocery shopping" (masking in public settings) or "while visiting with family or friends in their homes" (masking in private settings) on a four-point scale. Individuals are considered masked if they respond that they are very likely to wear a mask and not masked if they report they are somewhat likely, not so likely to mask or not likely at all. A sensitivity analysis was performed where individuals who responded that they were very likely and somewhat likely to wear a mask were considered masked.

For each county in the dataset, masking was measured for each of the 14-days pre- and post- the issuance of mandates to assess the short-term effect of mask mandates.

Measuring masking for fourteen days post-mandate was chosen because this time period was within two-to-three generation intervals of early COVID-19 variants (i.e., within the window of time necessary to acutely modify a circulating wave's dynamics)[22].

The OutbreaksNearMe survey is a collaboration between Boston Children's Hospital and Momentive.ai. The survey employs a non-probability sampling method known as river sampling to gain a diverse representation of U.S. adult respondents. The potential participant pool, or the sampling frame, includes all adults in the U.S. who are using the SurveyMonkey platform for alternative activities. When these individuals have completed their other activities on the platform, they are then randomly invited to participate in the OutbreaksNearMe Survey (approximately 11% presented with the option to take the survey to complete it). As the SurveyMonkey user base is highly diverse, this method results in a varied sample for the OutbreaksNearMe survey. Additionally, inverse probability weights derived from the 2019 U.S. Census demographics (age, race, sex, education, and geography) are applied to generalize the survey to the broader U.S. This weighting scheme generates a pseudo-population, henceforth referred to as the sample population. Respondents were not incentivized to complete the survey and individuals younger than 13 years old or older than 100 years old were excluded. Previous validation efforts have shown the OutbreaksNearMe population to be of similar composition to the U.S. according to Census demographics and CDC disease estimates[21].

The OutbreaksNearMe survey was approved by the Boston Children's Hospital IRB and received a waiver of informed consent.

3.2.3 Analysis

We used an ITS stacked design[23] to estimate changes in masking in the 14-day period following a county-level mandate compared to the 14-days preceding the mandate. This design utilized individual-level masking observations, i, as rows (i.e., a panel design) within a single regression framework. When estimating the effects of mandates in the entire population, the dataset for analysis consisted of the entire study sample. The dataset for analysis was then filtered down to smaller samples (e.g., only individuals living in urban areas) when estimating the heterogeneity of the effect (more details in *Analysis of heterogeneity* below). The stacked ITS model was based on a modified Poisson regression model with a log link function and robust error variance[24] and was fit to assess if there is a change in slope and intercept of masking in s setting (public [measured by grocery shopping masking behavior] versus private [measured by masking behavior with family/friends]) following the introduction of a mandate:

$$ln\left[p(Masking)_{s,i}\right] = \beta_0 + \beta_1 Time_i + \beta_2 Mandate_i + \beta_3 TimeSinceMandate_i + \varepsilon_i ,$$

where $Masking$ is a binary variable indicating if the individual self-reported masking, $Time$ is an ordinal variable measured in days from 0 (first day of observation) to 28 (last day of observation), $Mandate$ is an indicator variable representing the presence of a mask mandate at the time of observation, and $TimeSinceMandate$ is an ordinal variable with a value of 0 for the pre-mandate period and the first day of a mandate after which it increases up to 14 for each day a mandate is in place.

The ITS analysis estimates if a change in the presence of a mandate is associated with an immediate shift in masking levels (β_2, known as a pulse effect or one-time change in masking) and/or change in slope (β_3, known as a ramp effect or a change in masking trends). The model assumes that each individual's choice to mask is binary, makes no distinction in the type of masks individuals are wearing, and assumes that the 14-day period prior to the mandate was sufficiently long to characterize it[16]. The counterfactual that the effect is compared against assumes that the pre-intervention trend continued and that there were no exogenous influences on the measured outcome.

Robust standard errors were calculated with the *sandwich* (v3.0-2) and *lmtest* (v0.9-40) R packages. From the results of the ITS analysis, we computed the marginal effects[24] of mask-wearing to estimate the average increase in mask-wearing in counties that implemented a mandate.

3.2.4 Poisson Model to Estimate Relative Risk

A modified Poisson regression with robust error variance was chosen as a primary model for our binary masking data. This decision was driven by our intent to report relative risk, which is more interpretable in the context of common outcomes such as mask-wearing[25]. Logistic regression models yield odds ratios, which can be inflated over risk ratios for common outcomes. This inflation may lead to an overestimated perception of risk, particularly when the actual effects are small. However, Poisson models do not constrain the data between 0 and 1, and estimates at the extremes should be interpreted with caution. Log-binomial models are an alternative method to report relative risk with estimates constrained between 0 and 1; however they often suffer from convergence

issues as was the case when attempted here.

3.2.5 Analysis of Heterogeneity

Analyses were conducted to assess the heterogeneous effect of mask mandates on mask-wearing. We focused on differences in the effect of mandates based on the counties they were implemented in. To do so, we stratified by county features: U.S. Census Region geography (Northeast, Midwest, South, West), urbanicity (metropolitan, micropolitan, and nonmetropolitan, defined by the National Center for Health Statistics Urban-Rural classification scheme), tertile of the previous degree of mask-wearing (measured by computing the tertile of each county based on the mean percentage of the population reporting masking in grocery stores and with family/friends pooled across the 14-days prior to mandate implementation), and calendar time of mandate implementation (June vs. July 2020). These analyses were executed by filtering the dataset for analysis, d, down to the relevant counties and then recalculating the combined parameter coefficients for each stratum (e.g., the effect of mandates in the Northeast U.S.).

3.2.6 Sensitivity Analysis of Model Specification

To ensure our results were robust to model specification and ITS parameterization, we conducted a sensitivity analysis utilizing a pooled design ITS model. The pooled design fits separate ITS models for each county ($j = 1, 2, .., k$) and pools parameter estimates to measure the effect of mandates. While the pooled design is well suited to capture the effect of mandates across many counties, it produces unstable parameter estimates in counties with just a few survey observations, a problem the

stacked design is less vulnerable to[26]. The pooled ITS design also utilized a Poisson regression model with a log link function and robust error variance:

$$ln\,[p(Masking)_{s,j}] = \beta_0 + \beta_1 Time_j + \beta_2 Mandate_j + \beta_3 TimeSinceMandate_j + \varepsilon_j.$$

To estimate the general effect of mask mandates across all counties, pooled parameter estimates were calculated by an inverse variance weighted average of each of the individual model parameter coefficients ($n = 1,2,3$)[26]:

$$\beta_{n,pooled} = \frac{\sum_{j=1}^{k} w_{n,j}\beta_{n,j}}{\sum_{j=1}^{k} w_{n,j}},$$

where $w_{n,j} = \frac{1}{(Standard\ Error[\beta_{n,j}])^2}$ and the pooled variance is: $var(\beta_{n,pooled}) = \frac{1}{\sum_{j=1}^{k} w_{n,j}}$. Wald-based confidence intervals are then constructed for each parameter $\beta_{n,pooled} \pm 1.96\sqrt{var(\beta_{n,pooled})}$.

3.2.7 Model Selection Over Alternatives

The ITS methods used here can be contrasted with a difference-in-differences (DiD) approach, a common technique for measuring the causal effect of a policy. The ITS method is preferred over DiD in the current study because DiD can be strongly affected by geographical spillover for masking. For a DiD approach to study the effect of mask mandates on masking, we would ideally compare a county that implemented mask

mandates with a similar county that did not. However, if people travel between these counties to grocery shop, have family/friends across county lines, consume media from adjacent counties, etc., the effects of the mandate on individuals' masking behavior are likely to spill over from the surrounding region, muddying the comparison. For example, Middlesex County, MA might be the best counterfactual for Suffolk County, MA, but someone in Middlesex County is also the most likely to change their behavior due to a mask mandate being implemented in Suffolk County, rendering it a poor counterfactual. The only suitable stand-ins are counties that are demographically and compositionally similar but are unlikely to have their resident's behavior influenced by the other's policy, a somewhat paradoxical relationship that heavily limits the availability of counterfactual locations.

3.3 RESULTS

3.3.1 Study Respondents

From June 2, 2020, to January 1, 2021, 34,106 unique respondents submitted self-reports of their masking behavior (Table 3.1). Respondents were 53.7% female, 45.1% male, and 1.2% transgender or non-binary, compared to the 2019 U.S. American Community Survey which estimates the U.S. to be 50.8% female and 49.2% male[27]. Self-reported household income in the lowest (<$30,000) and highest (≥$150,000) yearly categories contained 23.8% and 10.2% of the respondents compared to 23.6% and 14.4% estimated by the U.S. Census, respectively. Self-reports of masking were not evenly distributed across demographics (Table 3.1).

3.3.2 Sample of U.S. Counties

Of the 624 counties eligible for analysis, 555 had at least one self-reported observation on mask-wearing both before and after their issuance of a mandate. Most mandates were implemented in July 2020 (n=423 counties) compared to June 2020 (n=132 counties). Of the 69 counties without sufficient reports, 20% were metropolitan compared to 47% of the included ones. The counties included were not evenly distributed geographically across the U.S. (Figure 3.1). Of the counties in the sample, the majority (n=471) issued mandates on the same day as statewide mandates. In the 84 counties that issued mandates prior to statewide ones, the county mandates were issued a mean of 11.0 (SD: 6.5) days earlier. These counties were spread across 11 states, though the majority were in Ohio (n=21), Indiana (n=14), Alabama (n=12), and Minnesota (n=12).

3.3.3 Masking in U.S. Counties

The median number of completed surveys on masking per county was 18 [IQR: 8–51] surveys or 4.1 [IQR: 3.0–5.5] surveys per 10,000 residents of each included county. The total number of completed surveys (N=16,569) prior to mandates was smaller than the number of completed surveys (N=17,537) following mandates. Over time, there was a general trend of increased self-reported masking in public and private settings. County-adjusted likelihood to report masking in grocery stores went from 73.7% in the two-weeks prior to mandates to 83.5% in the two-weeks following their issuance. Reports of masking with family/friends went from 32.8% to 37.5% from the two-weeks prior to mandates compared to the two-weeks after.

3.3.4 Effect on Mask Wearing in Private Settings

Stacked ITS analysis (Figure 3.2) of mask-wearing with family/friends found a very small pulse effect (RR: 1.03 [95% CI: 0.95–1.12]), and no ramp effect (RR: 1.00 [95% CI:0.99–1.01]). This indicates that there may have been a minor one-time increase in masking but no change in private-setting masking behavior trends. The marginal estimates from this model suggest that, across all counties during the study period, the mean observed mask-wearing with family/friends was 1.1 percentage points [95% CI: -1.7–3.9]) higher than what would have been expected if no mandates were in place. Similar findings for pulse (RR: 1.05 [95% CI: 0.96–1.15]) and ramp (RR: 1.01 [95% CI: 0.99–1.02]) effects were observed on pooled ITS sensitivity analysis.

3.3.5 Effect on Mask Wearing in Public Settings

Stacked ITS analysis (Figure 3.2) found a small pulse effect (RR: 1.04 [95% CI: 1.01–1.08]) and no ramp effect (RR: 1.00 [95% CI:1.00–1.00]) of mask-wearing in grocery stores following mandates. The marginal estimates from this model suggest that, across all counties during the study period, the mean observed mask-wearing in grocery stores was 3.4 percentage points [95% CI: 0.8–6.0]) higher than what would have been expected if no mandates were in place. A sensitivity analysis utilizing a pooled ITS design and incorporating the effect of counties found similar pulse (RR: 1.03 [95% CI: 1.02–1.04]) and ramp (RR: 1.00 [95% CI:1.00–1.00]) effects.

3.3.6 County Heterogeneity in the Effect of Mask Mandates

The effects of mandates on mask-wearing varied substantially across different counties (Table 3.2). In an analysis where counties were stratified by masking levels prior to mandate implementation (Figure 3.3), the absolute effect of mandates was greatest in counties with the lowest prior masking levels and lowest in counties with high prior masking. In an analysis of geography, the absolute effect of mandates was greatest in counties in the U.S. West census region and lowest in counties in the Northeast region. In an analysis of urbanicity, the absolute effect of mandates was greatest in micropolitan and non-metropolitan counties and lowest in metropolitan counties. In an analysis of the calendar time of when the mandates were issued, minimal difference was observed between counties that issued mandates in June compared to those issued in July.

3.3.7 Sensitivity of Outcome Definition

In a sensitivity analysis that considered an individual masked if they were somewhat or very likely to mask, we find similar results to when the outcome was defined more narrowly as only those very likely to mask. When measuring the effect of mandates on masking with family/friends, stacked ITS analysis found a very small pulse (RR: 1.02 [95% CI:0.97–1.07]) effect and no ramp (RR: 1.00 [95% CI:1.00–1.00]) effect. When measuring the effect of mandates on masking at the grocery store, stacked ITS analysis found a small pulse (RR: 1.03 [95% CI:1.00–1.05]) effect and no ramp (RR: 1.00 [95% CI:1.00–1.00]) effect. A similar heterogeneity of estimates was seen (Table 3.3), however, mandates having a greater effect in counties with low prior masking levels compared to high prior masking levels was seen only in public setting masking.

Additionally, a calendar time effect was seen that suggested June mandates had a greater impact on masking increases than July ones.

3.4 DISCUSSION

In this interrupted time series estimating the effect of U.S county-level mask mandates on self-reported mask-wearing, we find that mandates led to a small (approximately 1%–3%) increase on masking in public and private settings. However, the effect of mandates on masking varied substantially (from approximately -4 to 8 percentage points) by geography, urbanicity, and prior masking levels.

The findings from our study help to clarify the effectiveness of mask mandates and to reconcile this with previous literature reporting mixed effectiveness. Our analysis suggests that mandates tended to have a slightly larger impact on masking in public compared to private settings and a substantially larger impact in areas with low levels of mask usage prior to masking implementation. When mandates were implemented in these areas, the post-mandate levels of mask usage in were elevated to levels that were comparable to those seen in counties with higher mask usage before the mandates were put into effect. Given the heterogeneity of mandates in the U.S., previous results suggesting mandates did not reduce transmission may be attributed to mandates being enacted in areas with already elevated masking behavior and a subsequently limited pool of unmasked individuals amenable to mandate-related behavioral changes. For example, we show here that in Northeast U.S. counties, where pre-mandate masking behavior were highest, masking may have only increased approximately 1–3 percentile points in the two

weeks following mandates and our model ascribes almost none of this gain to the mandates themselves.

Prior estimates in the literature have found the effect of statewide mandates on masking behavior ranging from 23 percentage points to no change[14]. Our estimates fall within this range and may be short of the largest estimated effect due to the fact three (Iowa, North Dakota, and New Hampshire) of the four (three previously mentioned in addition to Hawaii) states in that analysis are largely rural and experienced a flat pre-treatment masking trend, something not seen in this county-level data. Studies that found no evidence of masking increases following mandates have aggregated data from states with large effects and null effects. They may also be subject to geographic spillover due to the fact some county mandates preceded statewide ones. Importantly, the counties involved in this study — those that issued mandates either prior to, in tandem with, or independent of their respective state mandates after June 17, 2020, and for which mask usage data was available — represent only a small portion of the total counties in the United States. Given the substantial variability observed in the impact of mandates, these findings do not offer a definitive or comprehensive understanding of the effects of mandates broadly. However, the diversity of the counties included in this analysis does shed light on why previous studies may have yielded conflicting results. Specifically, we find the effect of mask mandates on masking is not uniformly consistent and supports the hypothesis that there is effect measure modification by important county-specific factors such as the theoretical population pool of those willing to mask.

There are several additional limitations to the current analysis. Although the

survey data has shown a high correlation with other sources, it is still reliant on anonymous self-reports that may reflect social incentives related to masking and the systematic exclusion of those with limited internet access. It is possible we are overestimating the effect of mandates because individuals believe they should be wearing masks during mandated periods and therefore are more likely to report masking. Self-reports can also induce selection bias (e.g., only those adhering to the law will want to report post-mandate) that would bias estimates of mandate effectiveness away from the null. Additionally, by utilizing counties, this analysis minimized urban/rural confounding found in statewide analyses but is still susceptible to bias created by other municipal mandates (e.g., citywide ones) and spillover from changes introduced in nearby jurisdictions. Lastly, our model assumes that there were no exogenous influences on masking behavior in the two weeks prior to the issuance of a mandate, which is unlikely to be true. Increases in masking may respond to the same disease pressures as mandates (e.g., increases in cases). This confounding would cause our effect estimates to overreport the effect mandates would have on masking in isolation. However, this study still improves upon prior attempts as it directly measures the effect of mandates on masking and not mandates on disease outcomes, the latter of which is causally circular with pressures exerted by the disease itself, and therefore more susceptible to this bias.

Notably, irrespective of the broad population effects of mandates on adherence, mandates may be an important tool to enable individual-level risk reduction and for especially vulnerable workers to protect themselves from infection (e.g., citing mandates to enforce masking within a particular establishment). Mandates may also be an

important tool to prevent long-term decreases in masking. This analysis can only draw a link between mandates and self-reported adherence in the short term and provides no direct evidence of the link between mandates and disease transmission and outcomes, nor the sustainability of the behavioral change acutely affected by a mandate. However, we have demonstrated an effect modification by important demographic characteristics in the effect of mandates on masking behavior which may explain the conflicting effects of mandates on disease-related outcomes reported in the literature and provide helpful insight as to which regions may experience the greatest benefit of a mask mandate.

3.4.1 Conclusion

Masking is an important tool to reduce respiratory disease transmission. Throughout 2020, mask mandates were introduced across U.S. states and counties to increase mask-wearing and combat the coronavirus pandemic. In this analysis, we showed that the effects of these mandates were substantially varied, and they only altered masking behavior in select contexts, such as when implemented when the current proportion of the population masking was low. Future pandemic response will need to consider that broad mandates induce mixed effects and that crafting tailored and hyperlocal interventions may be a more efficient way to increase masking and reduce disease transmission.

3.5 TABLES AND FIGURES

Table 3.1 Self-reported demographics and masking behavior from U.S. adults (n=34,106) who lived in U.S. counties (n=555) that issued mask mandates preceding, concurrent with, or in the absence of respective state mandates

Characteristic	Weighted survey respondents Total: 34,106 n (%)	Survey respondents who were very likely to mask with family/friends Total: 12,586 (36.8%) n (%)	Survey respondents who were very likely to mask while grocery shopping Total: 28,362 (83.2%) n (%)
Race			
White	26066.5 (76.4)	7662.3 (64.3)	19800.8 (74.2)
Black	4346.0 (12.7)	2682.7 (22.5)	3819.2 (14.3)
Hispanic	981.3 (2.9)	465.7 (3.9)	866.0 (3.2)
Other	1869.2 (5.5)	790.8 (6.6)	1585.4 (5.9)
Missing	843.1 (2.5)	316.4 (2.7)	611.0 (2.3)
Gender			
Female	18312.8 (53.7)	6879.5 (57.7)	15033.7 (56.3)
Male	15383.2 (45.1)	4877.5 (40.9)	11353.3 (42.5)
Transgender or Nonbinary	410.1 (1.2)	160.9 (1.4)	295.4 (1.1)
Education			
High School or Less	13385.1 (39.2)	4732.3 (39.7)	9709.2 (36.4)
Some College	10493.3 (30.8)	3476.2 (29.2)	8152.6 (30.6)
College or More	6446.8 (18.9)	2145.3 (18.0)	5404.0 (20.3)
Post Graduate Degree	3780.9 (11.1)	1564.2 (13.1)	3416.6 (12.8)
Age			
18–29 years	6140.2 (18.0)	1849.9 (15.5)	4446.5 (16.7)
30–39 years	5732.1 (16.8)	1823.3 (15.3)	4138.8 (15.5)
40–49 years	5633.8 (16.5)	1714.5 (14.4)	4151.3 (15.6)
50–64 years	9190.4 (26.9)	3399.3 (28.5)	7409.2 (27.8)
65–74 years	5580.8 (16.4)	2348.6 (19.7)	4912.4 (18.4)
75+ years	1828.7 (5.4)	782.3 (6.6)	1624.2 (6.1)
Household Income			
Less than $30,000	8112.1 (23.8)	3410.6 (28.6)	6204.8 (23.3)
$30,000–49,999	5439.7 (15.9)	1974.0 (16.6)	4261.6 (16.0)
$50,000–$74,999	5745.2 (16.8)	1848.0 (15.5)	4399.9 (16.5)
75,000–$99,999	4403.0 (12.9)	1367.4 (11.5)	3437.5 (12.9)
$100,000–$149,999	4871.8 (14.3)	1397.4 (11.7)	3803.2 (14.3)
$150,000 and Over	3476.9 (10.2)	1064.1 (8.9)	2834.0 (10.6)
Did Not Respond	2057.3 (6.0)	856.5 (7.2)	1741.5 (6.5)
U.S. Census Division			
Northeast	7320.1 (21.5)	2611.9 (21.9)	6257.3 (23.5)
Midwest	9616.2 (28.2)	3111.3 (26.1)	7336.1 (27.5)
South	11993.1 (35.2)	4404.8 (37.0)	9012.5 (33.8)
West	5176.6 (15.2)	1789.9 (15.0)	4076.6 (15.3)

Table 3.2 Results from stacked interrupted time series fit to self-reported masking levels pre- and post-mask mandate in U.S. counties (n=555) across county characteristic and masking setting with masking defined as those very likely to mask

Mask Wearing Setting	County Characteristic	Variable	Mean Very Likely to Mask Pre-Mandate (%)	Mean Very Likely to Mask Post-Mandate (%)	Estimated Percentile Increase of Individuals Likely Masking Attributed to Mandate (95% CI)
Grocery Store	Prior Masking	Lowest	50.2	67.0	8.0 (-0.6–16.5)
		Moderate	69.2	79.4	3.3 (-1.6–8.2)
		Highest	82.3	89.6	2.3 (-0.6–5.1)
	U.S. Census Region	South	69.4	81.1	3.5 (-1.1–8.0)
		West	72.4	86.0	7.5 (1.6–13.4)
		Midwest	70.6	82.3	2.2 (-2.6–7.0)
		Northeast	84.7	87.8	1.3 (-3.8–6.5)
	Mandate Month	July	74.7	84.1	3.1 (0.1–6.1)
		June	71.2	81.9	3.4 (-1.5–8.4)
	Urbanicity	Metro	76.0	85.0	3.0 (0.3–5.7)
		Nonmetro	58.7	71.4	5.6 (-9.0–20.3)
		Micropolitan	60.5	75.9	7.0 (-2.0–16.0)
With Family and Friends	Prior Masking	Lowest	16.9	22.9	8.0 (0.7–15.3)
		Moderate	27.9	32.0	1.8 (-3.0–6.6)
		Highest	39.7	43.9	-1.0 (-4.9–2.8)
	U.S. Census Region	South	34.1	39.7	4.4 (-0.3– 9.1)
		West	31.8	37.7	1.6 (-5.0–8.2)
		Midwest	29.4	35.5	0.3 (-4.8–5.4)
		Northeast	35.6	36.3	-4.0 (-10.8–2.7)
	Mandate Month	July	32.8	36.9	0.6 (-2.8–3.9)
		June	32.9	38.8	2.8 (-2.3–7.9)
	Urbanicity	Metro	33.8	38.8	0.9 (-2.1–4.0)
		Nonmetro	28.5	29.0	4.2 (-8.8–17.3)
		Micropolitan	26.2	29.7	2.0 (-6.4–10.3)

Table 3.3 Results from stacked interrupted time series sensitivity analysis fit to self-reported masking levels pre- and post-mask mandate in U.S. counties (n=555) across county characteristic and masking setting with masking defined as those very or somewhat likely to mask

Mask Wearing Setting	County Characteristic	Variable	Mean Very or Somewhat Likely to Mask Pre-Mandate (%)	Mean Very or Somewhat Likely to Mask Post-Mandate (%)	Estimated Percentile Increase of Individuals Likely Masking Attributed to Mandate (95% CI)
Grocery Store	Prior Masking	Lowest	69.2	82.1	4.2 (-3.3–11.7)
		Moderate	84.1	92	1.6 (-1.7–4.9)
		Highest	91.4	95.3	1.4 (-0.7–3.6)
	U.S. Census Region	South	84.1	90.9	0.9 (-2.5–4.3)
		West	84.3	93.1	6.0 (1.4–10.6)
		Midwest	81.7	91.9	2.4 (-1.6–6.3)
		Northeast	92	95	1.8 (-2.0–5.5)
	Mandate Month	June	84.3	91.3	4.6 (0.8–8.5)
		July	85.8	92.8	1.3 (-1.0–3.6)
	Urbanicity	Metro	86.8	93.1	2.4 (0.4–0.5)
		Nonmetro	78.5	87.4	2.6 (-9.4–14.6)
		Micropolitan	76	87.9	2.1 (-5.4– .6)
With Family and Friends	Prior Masking	Lowest	35.9	39.4	-0.8 (-8.6–7.0)
		Moderate	49.5	55.7	1.7 (-3.2–6.6)
		Highest	63.8	67.4	-0.4 (-4.4–3.5)
	U.S. Census Region	South	56.1	61.1	3.1 (-1.7–8.0)
		West	52.5	61	5.9 (-1.1–13.0)
		Midwest	52.2	57.8	-2.2 (-7.6–3.2)
		Northeast	55.7	57.9	-2.0 (-9.0–4.9)
	Mandate Month	June	54.6	61	4.7 (-0.6–10.1)
		July	54.4	58.8	-0.4 (-3.9–3.1)
	Urbanicity	Metro	55.7	61.1	1.1 (-2.0–4.2)
		Nonmetro	47.4	49.8	2.5 (-13.4–18.3)
		Micropolitan	46.4	49.7	-0.5 (-9.8–8.8)

Figure 3.1 Map of masking reports from U.S. counties that issued mask mandates preceding, concurrent with, or in the absence of respective state mandate

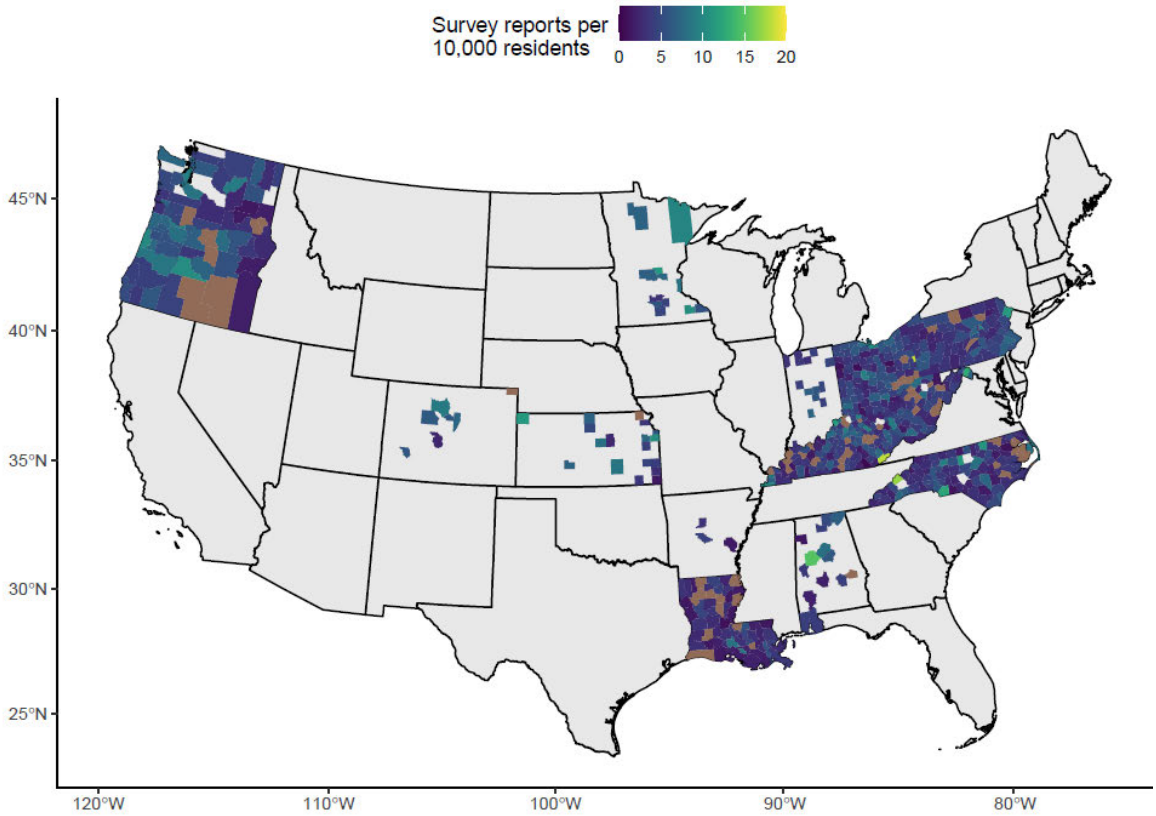

U.S. respondents completed a web survey on their masking behavior between June 2, 2020 and January 1, 2021. Self-reports from the U.S. adults (n=34,106) who lived in U.S. counties (n=555) that issued mask mandates preceding, concurrent with, or in the absence of respective state mandates were included for analysis. Sixty-nine additional counties (*brown*) met the inclusion criteria for analysis but did not contribute masking self-reports in the 14 days pre- and/or post-mandate issuance and were therefore excluded. County-level mandate information was extracted from the "Tracking Mask Mandates During the Covid-19 Pandemic" database.

Figure 3.2 Self-reported masking in public and private settings pre- and post-mask mandate

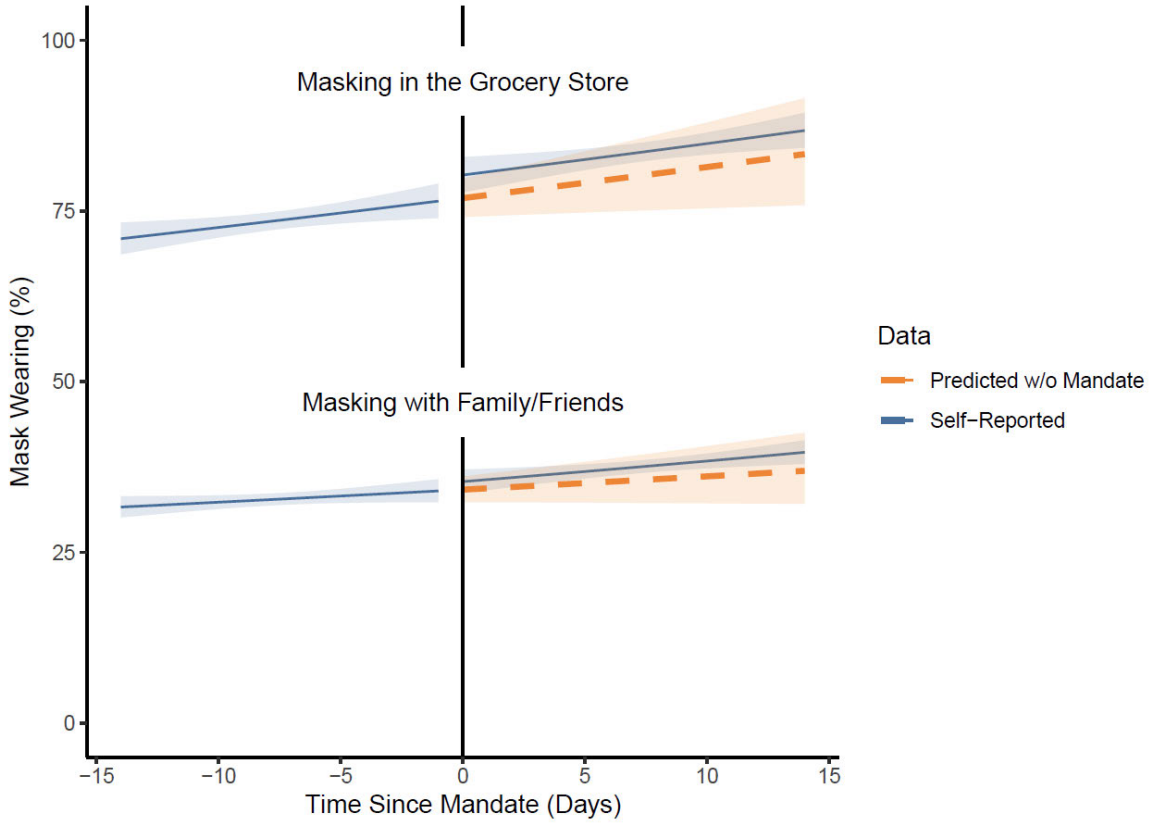

U.S. respondents completed a web survey on their masking behavior between June 2, 2020 and January 1, 2021. Self-reports from the U.S. adults (n=34,106) who lived in U.S. counties (n=555) that issued mask mandates preceding, concurrent with, or in the absence of respective state mandates were included for analysis. Individuals were considered masked if they reported they were very likely to wear a mask "while grocery shopping" (masking in public settings) or "while visiting with family or friends in their homes" (masking in private settings). Stacked interrupted time series models were fit to self-reported masking (*blue*). Masking levels in the absence of a mandate (*orange*) were predicted from the models.

Figure 3.3 Self-reported masking in public and private settings pre- and post-mask mandate by county tertile of reported pre-mandate masking

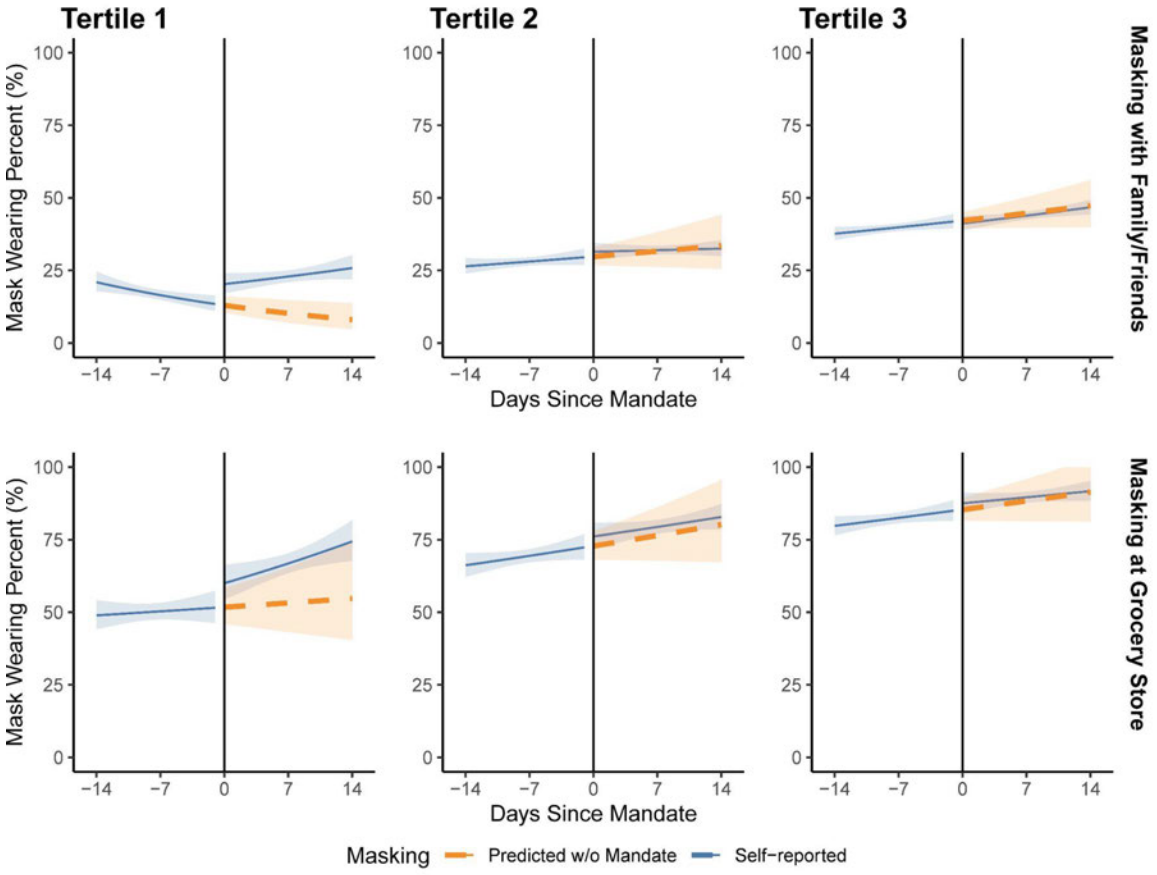

U.S. respondents completed a web survey on their masking behavior between June 2, 2020 and January 1, 2021. Self-reports from the U.S. adults (n=34,106) who lived in U.S. counties (n=555) that issued mask mandates preceding, concurrent with, or in the absence of respective state mandates were included for analysis. Individuals were considered masked if they reported they were very likely to wear a mask "while grocery shopping" (masking in public settings) or "while visiting with family or friends in their homes" (masking in private settings). Separate stacked interrupted time series models were fit to self-reported masking (*blue*) for counties based on the tertile of reported pre-mandate masking levels. Masking levels in the absence of a mandate (*orange*) were predicted from the models. When computing the confidence intervals three upper bound estimates exceeded 1. These estimates were adjusted to 1 to reflect valid probabilities.

3.6 REFERENCES

1. Katz J, Sanger-Katz M, Quealy K. A Detailed Map of Who Is Wearing a Mask in the U.S. The New York Times. Published 2020. Accessed August 5, 2020. https://www.nytimes.com/interactive/2020/07/17/upshot/coronavirus-face-mask-map.html
2. Jefferson T, Dooley L, Ferroni E, Al-Ansary LA, Van Driel ML, Bawazeer GA, Jones MA, Hoffmann TC, Clark J, Beller EM, Glasziou PP, Conly JM. Physical interventions to interrupt or reduce the spread of respiratory viruses. Cochrane Acute Respiratory Infections Group, ed. *Cochrane Database of Systematic Reviews*. 2023;2023(4). doi:10.1002/14651858.CD006207.pub6
3. Clinton J, Cohen J, Lapinski J, Trussler M. Partisan pandemic: How partisanship and public health concerns affect individuals' social mobility during COVID-19. *Science Advances*. 2021;7(2):eabd7204. doi:10.1126/sciadv.abd7204
4. McKelvey T. Coronavirus: Why are Americans so angry about masks? *BBC News*. https://www.bbc.com/news/world-us-canada-53477121. Published July 20, 2020. Accessed May 3, 2021.
5. Rader B, White LF, Burns MR, Chen J, Brilliant J, Cohen J, Shaman J, Brilliant L, Kraemer MUG, Hawkins JB, Scarpino SV, Astley CM, Brownstein JS. Mask-wearing and control of SARS-CoV-2 transmission in the USA: a cross-sectional study. *The Lancet Digital Health*. 2021;3(3):e148–e157. doi:10.1016/S2589-7500(20)30293-4
6. Cowling BJ, Zhou Y, Ip DKM, Leung GM, Aiello AE. Face masks to prevent transmission of influenza virus: a systematic review. *Epidemiology and Infection*. 2010;138(4):449–456. doi:10.1017/S0950268809991658
7. Hendrix MJ, Walde C, Findley K, Trotman R. Absence of Apparent Transmission of SARS-CoV-2 from Two Stylists After Exposure at a Hair Salon with a Universal Face Covering Policy — Springfield, Missouri, May 2020. *MMWR Morbidity and Mortality Weekly Report*. 2020;69(28):930–932. doi:10.15585/mmwr.mm6928e2
8. Wang X, Ferro EG, Zhou G, Hashimoto D, Bhatt DL. Association Between Universal Masking in a Health Care System and SARS-CoV-2 Positivity Among Health Care Workers. *JAMA*. Published online July 14, 2020. doi:10.1001/jama.2020.12897
9. Leech G, Rogers-Smith C, Monrad JT, Sandbrink JB, Snodin B, Zinkov R, Rader B, Brownstein JS, Gal Y, Bhatt S, Sharma M, Mindermann S, Brauner JM, Aitchison L. Mask wearing in community settings reduces SARS-CoV-2 transmission. *Proceedings of the National Academy of Sciences*. 2022;119(23):e2119266119. doi:10.1073/pnas.2119266119
10. Brauner JM, Mindermann S, Sharma M, Johnston D, Salvatier J, Gavenčiak T, Stephenson AB, Leech G, Altman G, Mikulik V, Norman AJ, Monrad JT, Besiroglu

T, Ge H, Hartwick MA, Teh YW, Chindelevitch L, Gal Y, Kulveit J. Inferring the effectiveness of government interventions against COVID-19. *Science*. 2021;371(6531):eabd9338. doi:10.1126/science.abd9338

11. Guy GP, Lee FC, Sunshine G, McCord R, Howard-Williams M, Kompaniyets L, Dunphy C, Gakh M, Weber R, Sauber-Schatz E, Omura JD, Massetti GM, Bailey M, Brown A, Cramer R, Clodfelter C, Davison R, Dugmeoglu S, Fitts A, Gilchrist S, Hulkower R, Limeres A, Pepin D, Popoola A, Schroeder M, Tynan MA, Ukoha C, Williams M, Whitson CD, Jeong G, Landsman L, Moreland A, Shelburne J. Association of State-Issued Mask Mandates and Allowing On-Premises Restaurant Dining with County-Level COVID-19 Case and Death Growth Rates — United States, March 1–December 31, 2020. *MMWR Morbidity and Mortality Weekly Report*. 2021;70(10):350–354. doi:10.15585/mmwr.mm7010e3
12. Cowger TL, Murray EJ, Clarke J, Bassett MT, Ojikutu BO, Sánchez SM, Linos N, Hall KT. Lifting Universal Masking in Schools — Covid-19 Incidence among Students and Staff. *New England Journal of Medicine*. 2022;387(21):1935–1946. doi:10.1056/NEJMoa2211029
13. Fischer CB, Adrien N, Silguero JJ, Hopper JJ, Chowdhury AI, Werler MM. Mask adherence and rate of COVID-19 across the United States. Tu WJ, ed. *PLOS ONE*. 2021;16(4):e0249891. doi:10.1371/journal.pone.0249891
14. Adjodah D, Dinakar K, Chinazzi M, Fraiberger SP, Pentland A, Bates S, Staller K, Vespignani A, Bhatt DL. *Association between COVID-19 Outcomes and Mask Mandates, Adherence, and Attitudes*. Cold Spring Harbor Laboratory Press; 2021:2021.01.19.21250132. doi:10.1101/2021.01.19.21250132
15. Whaley CM, Cantor J, Pera M, Jena AB. Assessing the Association Between Social Gatherings and COVID-19 Risk Using Birthdays. *JAMA Internal Medicine*. 2021;181(8):1090. doi:10.1001/jamainternmed.2021.2915
16. Haber NA, Clarke-Deelder E, Salomon JA, Feller A, Stuart EA. *COVID-19 Policy Impact Evaluation: A Guide to Common Design Issues*.
17. Hedlund J, Gilbert SH, Ledingham K, Preusser D. *How States Achieve High Seat Belt Use Rates*. National Highway Traffic Safety Administration; 2008:1–170. Accessed May 17, 2021. https://crashstats.nhtsa.dot.gov/Api/Public/ViewPublication/810962
18. Cohen A, Einav L. The effects of mandatory seat belt laws on driving behavior and traffic fatalities. *Review of Economics and Statistics*. 2003;85(4):828–843. doi:10.1162/003465303772815754
19. Wright AL, Chawla G, Chen L, Farmer A. Tracking Mask Mandates During the Covid-19 Pandemic. *SSRN Electronic Journal*. Published online August 7, 2020. doi:10.2139/ssrn.3667149
20. Randy Ludlow. Coronavirus in Ohio: DeWine requires masks in seven counties, including Cuyahoga. *Akron Beacon Journal*.

https://www.beaconjournal.com/story/news/coronavirus/2020/07/07/coronavirus-in-ohio-dewine-requires-masks-in-seven-counties-including-cuyahoga/113367044/. Published July 7, 2020.

21. Rader B, Gertz A, Iuliano AD, Gilmer M, Wronski L, Astley CM, Sewalk K, Varrelman TJ, Cohen J, Parikh R, Reese HE, Reed C, Brownstein JS. Use of At-Home COVID-19 Tests — United States, August 23, 2021–March 12, 2022. *MMWR Morbidity and Mortality Weekly Report*. 2022;71(13):489–494. doi:10.15585/mmwr.mm7113e1
22. Hart WS, Miller E, Andrews NJ, Waight P, Maini PK, Funk S, Thompson RN. Generation time of the alpha and delta SARS-CoV-2 variants: an epidemiological analysis. *The Lancet Infectious Diseases*. 2022;22(5):603–610. doi:10.1016/S1473-3099(22)00001-9
23. Wagner AK, Soumerai SB, Zhang F, Ross-Degnan D. Segmented regression analysis of interrupted time series studies in medication use research. *Journal of Clinical Pharmacy and Therapeutics*. 2002;27(4):299–309. doi:10.1046/j.1365-2710.2002.00430.x
24. Lüdecke D. ggeffects: Tidy Data Frames of Marginal Effects from Regression Models. *Journal of Open Source Software*. 2018;3(26):772. doi:10.21105/joss.00772
25. Zou G. A Modified Poisson Regression Approach to Prospective Studies with Binary Data. *American Journal of Epidemiology*. 2004;159(7):702–706. doi:10.1093/aje/kwh090
26. Gebski V, Ellingson K, Edwards J, Jernigan J, Kleinbaum D. Modelling interrupted time series to evaluate prevention and control of infection in healthcare. *Epidemiology and Infection*. 2012;140(12):2131–2141. doi:10.1017/S0950268812000179
27. U.S. Census Bureau. *2015–2019 American Community Survey*. U.S. Census Bureau; 2021.

4. AT-HOME COVID-19 TESTING EQUITY IN THE UNITED STATES

4.1 INTRODUCTION

In response to the COVID-19 pandemic, United States (U.S.) federal and local jurisdictions have implemented epidemiologic surveillance programs aimed at quantifying the disease's burden, many of which rely on systematic reporting of confirmed COVID-19 infections[1,2]. Nucleic Acid Amplification Tests (NAATs) such as polymerase chain reaction tests, the gold standard for diagnosing SARS-CoV-2 infection, were adopted at the start of the pandemic and form the foundation of traditional COVID-19 case surveillance[3]. Following the initial waves of disease transmission, at-home COVID-19 rapid antigen tests (at-home COVID-19 tests), which provided several advantages over NAATs, were developed and made available to the U.S. public[4,5].

NAAT testing can be resource-intensive and access throughout the pandemic has not been equally distributed among all individuals in the U.S. Disparities in access to NAATs have been well documented and tend to favor more affluent, insured, and white populations[6,7]. Heterogeneous access to NAATs has also had substantial impacts on U.S. communities' ability to track disease transmission and on the validity of epidemiological parameter estimates such as prevalent and incident case counts which often rely on case definitions including a positive NAAT[8,9]. On the other hand, at-home tests are typically cheaper, more convenient, and more accessible than NAATs as they can be ordered online and shipped directly to the home, eliminating the common requirement that individuals physically visit a NAAT testing site, and potentially lowering the disease severity threshold for undertaking testing. This is particularly beneficial for individuals

who live in areas with limited geographic access to testing, individuals who may not have the flexibility in their schedule or economic resources required to travel for NAAT testing, or when a variant may cause mild symptoms in some and more severe in others[6]. Previous research has shown that, despite these advantages and rapid U.S. adoption of at-home tests, usage patterns exhibit some of the same disparities seen in NAAT utilization[10]. At-home test utilization has been shown to be lower among persons who self-identify as Black, are aged ≥75 years, have lower incomes, are more likely to be uninsured, and have lower education levels.

To address the ongoing need for COVID-19 testing and give the public easy access to tools that facilitate self-management of exposure and infection, the federal government launched Covidtests.gov in January 2022. The program provides free at-home COVID-19 tests that could be ordered online and sent directly to people's homes via the United States Postal Service[11,12]. A key goal of the program was to help mitigate at-home COVID-19 test access barriers and it included several measures designed to increase equity, such as prioritizing delivery to communities that had experienced a disproportionate share of COVID-19 cases and offering bilingual telephone ordering assistance[11]. According to the White House, Covidtests.gov shipped hundreds of millions of tests to greater than two-thirds of U.S. households over the course of the program[13]. Despite the clear logistic success of Covidtests.gov at delivering tests across the U.S., there has been no systematic evaluation of whether the stated equity goals were achieved during this ambitious initiative. Covidtests.gov was suspended in mid-2022 and then reinstated in December of the same year[14,15].The purpose of this study is to use the

implementation, suspension, and reinstatement of the federal government's COVID-19 at-home testing program to evaluate changes in overall patterns of test utilization and whether equity of at-home test utilization was measurably different during periods of Covidtests.gov operation.

In a 2021 study, researchers at Washington University in St. Louis, discovered evidence of racial inequity in the distribution of COVID-19 NAAT tests across Missouri counties[16]. The study revealed notable disparities in test usage and COVID-19 burden among various racial groups, showing that the likelihood of receiving a COVID-19 test was not proportionate to the risk of hospitalization across all races. To explore this issue, the researchers used the Gini coefficient, a common economic metric for assessing income inequality, and adapted it to examine the equitable distribution of COVID-19 tests. This research focused on the relationship between NAAT test allocation and COVID-19 impact measurements at the county level, using hospitalizations as the primary indicator of COVID-19 burden, yet those with NAAT-generated test results and hospitalizations represent only a fraction of all COVID-19 infections.

In the current study, we sought to evaluate testing equity for at-home tests among those with a clear symptomatic indication for testing – that is, Covid-like illness. We adopted a similar methodology as Mody et al., levering economic distribution metrics to evaluate COVID-19 test equity. However, we made three key innovations to improve estimates and mitigate aggregation bias: 1) measuring at-home tests instead of NAATs, 2) examining testing at the individual, not county, level, and 3) broadening the COVID-19 burden definition to include the risk of experiencing any Covid-like illness. We

generated two measures to examine at-home test distribution equity in the U.S. between September 13, 2021, to March 4, 2023, one overall (the Gini coefficient) and one longitudinal (Theil's T). The Gini coefficient was used to quantify the proportionality of at-home test utilization to COVID-19 burden over the entire study period. Theil's T, a measure of multigroup entropy (i.e., randomness/disorder in the testing proportion across multiple subgroups), was calculated weekly to track the changes in test utilization equity over time. Both measures were calculated to assess proportionality in test utilization compared to Covid-like illness and general population share, as well as across multiple demographic categories including race/ethnicity, age, geography, and household income. Further, we used a regression model with autoregressive integrated moving average (ARIMA) errors to assess if Covidtests.gov was associated with Theil's T for any of these demographic strata during its period of distribution.

4.2 MATERIALS AND METHODS

4.2.1 Cross-Sectional Health Survey Data

We utilized digital health survey data from the OutbreaksNearMe-SurveyMonkey Survey approved by the Boston Children's Hospital Institutional Review Board (P00023700). The survey is a retrospective and ongoing, geographically nationally representative, cross-sectional online survey developed by Boston Children's Hospital researchers and administered through the SurveyMonkey platform since September 2020. The survey collects data on demographics, respiratory illness symptoms, and health practices. The survey is continuously administered and collects responses from over

5,000 participants across the United States every week. To achieve demographic diversity in respondents, the survey utilizes river sampling, a non-probability technique that recruits participants to the survey when they are finished engaging in other online activities. The sampling frame encompasses all U.S. adults already on the SurveyMonkey platform, which are then recruited to the OutbreaksNearMe-SurveyMonkey Survey, yielding a diverse sample due to the wide array of SurveyMonkey users. Additionally, inverse probability weights derived from 2019 U.S. Census demographics (age, race, sex, education, and geography) are applied to generalize the survey to the broader U.S. This weighting scheme generates a pseudo-population, henceforth referred to as the sample population. The survey has been previously used by the Centers for Disease Control and Prevention (CDC) to measure disparities in at-home COVID-19 test usage across demographic subgroups and its sample population has been shown to approximate the demographics of the U.S.[10]. The study period includes September 13, 2021, to March 4, 2023.

4.2.2 Survey Covariates and Variable Definitions

Self-reported demographic measures included age (18–99 years old), race/ethnicity, annual household income ($/yr), education, and state of current residence (mapped to U.S. Census Division). Respondents (n=53,478) who did not complete answers to age, race, education, and geographic residence questions, which were necessary to generate inverse probability weights, and household income, a key demographic of interest, were excluded from this study. Respondents were also asked how they were feeling and to report individual medical symptoms from a pre-populated

list. Covid-like illness was defined as those reporting symptoms consistent with the CDC's broad syndromic surveillance definition[10] (one of [loss of taste/smell, cough, gasping for air, shortness of breath] and/or two or more of [fever, chills, aches, headache, sore throat, nausea, vomiting, diarrhea, fatigue, running nose]). The outcome of interest was self-reported utilization of at-home COVID-19 tests. Respondents were asked if they tested for COVID-19 in the preceding 30 days, and, if yes, the type of test used (e.g., at-home, PCR, etc.).

4.2.3 Federal COVID Test Dissemination Policy Exposure Periods

The exposure of interest was periods of time when Covidtest.gov was operational and distributing at-home COVID-19 tests. The program opened January 18, 2022 and was ongoing as of March 4, 2023. The program was temporarily suspended from September 2, 2022 to December 15, 2022. Periods of government test dissemination were defined by five days after each initial ordering period from covidtest.gov opened and 35 days after each one closed. The five-day lag represents the time from ordering to receiving tests and the 35 days represents that lag in addition to a 30-day period of expected utilization. This rule was applied for each period Covidtests.gov was open.

4.2.4 Overall Measure of Equity in At-Home Test Utilization

Equity in COVID-19 at-home test utilization across demographic subgroups was estimated over the study period (September 13, 2021, to March 4, 2023) using the Gini coefficient as a static measure of resource distribution. First, a Lorenz Curve was generated to visualize the distribution of at-home test usage across demographic

subgroups, including annual household income, geography, age, and race. The Lorenz Curve is a graphical representation of resource distribution that plots the cumulative proportion of a variable (in this case, population with Covid-like illness) against the cumulative proportion of resource usage (here, at-home test). Each point on the plot represents these numerical values for each demographic subgroup. The diagonal line of equality represents equity (i.e., proportional share of utilization matching proportional burden), while the difference between the Lorenz Curve and the line of equality graphically illustrates a departure from equitable distribution.

The Gini coefficient is a summary statistic to estimate inequity of resource distribution across all population strata from the Lorenz Curve[17]. It is commonly used in economics to evaluate the distribution of income in a population but can be adapted to study the distribution of any resource. The Gini coefficient is calculated as the area between Lorenz Curve and line of equality over the total area under line of equality.

For each demographic, the Gini coefficient measures if observed within-stratum at-home COVID-19 test utilization differs from the utilization expected based on symptom-based need[16,18]. A Gini coefficient of 0 represents numeric equity and suggests that utilization of at-home tests was proportionate to population burden. A Gini coefficient of 1 represents a single group utilizing all tests. For reference, the Gini coefficient in 2021 for income in the United States was approximately 0.49[19]. While the Gini coefficient does not specify where within a distribution inequality exists, a coefficient of 0.49 might equate to 50% of the population having only 1% of the income.

The Gini coefficient calculation assumes that we would expect all individuals

reporting Covid-like illness symptoms to equally test for COVID-19. The basis for this assumption is that any person who met CDC criteria for Covid-like illness was indicated for testing[20]. Additionally, successful approaches for disease mitigation should focus on testing not only the most severe cases at risk of hospitalization but any cases that may contribute to continued disease spread or benefit from intervention.[16]

4.2.5 Longitudinal Measure of Equity in At-Home Test Utilization

Theil's T is a multigroup entropy measure of resource inequities[21,22] here employed to quantify if at-home COVID-19 test utilization within each stratum was proportional to COVID-19 burden over time. In contrast to the Gini coefficient, Theil's T is a summary statistic that can only be used to compare each demographic to itself over time (e.g., at-home testing proportional to income in September compared to October), and not across groups (e.g., at-home testing balanced on income vs. race). The study sample was split by each demographic separately and then Theil's T was calculated (e.g., the sample was split according to income, and then Theil's T was calculated for income). Theil's T at time T under condition c is defined as:

$$T_{T,c} = \frac{1}{n_c} \sum_{i=1}^{n_c} \frac{x_i}{\bar{x}} ln \left(\frac{x_i}{\bar{x}}\right),$$

where x_i is at-home test usage of group i (e.g., at-home test usage among individuals with household incomes ≤$49,999), $\bar{x}$ is the population mean at-home test usage, and n_c is the sample size under condition c. Theil's T was calculated for each demographic group under two conditions, once with n_c as the entire study population and once limited

to those reporting Covid-like illness.

Theil's T is bounded by 0 (perfect equity) and ∞ and heavily positively skewed, so the central tendency and variance is reported with the geometric mean and geometric standard deviation. Spearman correlations were also performed between Theil's T metrics and Covid-like illness to evaluate if there was a correlation between increased disparities and increased population COVID-19 burden.

4.2.6 Simulation of System Level Entropy

In this study, we used a simulation approach to understand the potential noise in the Gini coefficient and Theil's T that could naturally arise from a dataset that includes both randomness and week-to-week fluctuations in sample size, the number of people reporting COVID-19 at-home testing, and Covid-like illness (e.g., we would expect increased entropy when the survey sample drops). Along with self-reported demographics, each individual in the dataset was also randomly assigned membership to one of seven groups: A, B, C, D, E, F, or G. The Gini coefficient and Theil's T were calculated for this random group membership. High magnitudes and fluctuations in the Gini coefficient and/or Theil's T calculated across random group membership would suggest additional caution is necessary in interpreting high magnitudes and fluctuations in the Gini coefficient and/or Theil's T calculated across demographic variables (i.e., it would suggest the metrics are inflated due to randomness and system-wide noise).

4.2.7 Regression Analysis

We computed an interrupted time series regression with autoregressive integrated moving average (ARIMA) errors to test if periods when Covidtests.gov was operational were associated with changes in Theil's T for each demographic category[23]. A binary step function (1 when Covidtests.gov was operating per 30-day rule outlined above, and 0 when program was not operational) was included in the model:

$$Log(Theil's\ T_t) = \beta_0 + \beta_1 \cdot Covidtests.gov\ Operational_t + \beta_2 \cdot\ USA\ Percentage\ of\ COVID\ like\ illness_t\ + \epsilon_t,$$

where ϵ_t is an ARIMA (p, d, q) error fit using the *auto.arima* (forecast package) function in R. This approach assumes that the effect on Theil's T during the two distinct phases of Covidtests.gov operation is equivalent. Additionally, it is only designed to measure equity through the lens of test utilization proportional to burden — and does not account for the possibility that improved at-home test supply improved utilization across all demographics. Higher test utilization among groups with previously low utilization may have public health benefit, but if subgroup differences remain, than inequity also remains.

4.2.8 Peak Demand Analysis

To measure at-home test utilization equity during periods of high COVID-19 burden, when presumably demand for at-home tests was at the highest, we performed a comparative analysis during weeks in the highest 20th percentile of reported Covid-like

illness across the entire population (weeks of peak illness). Theil's T during weeks of peak illness was compared across Covidtest.gov operational status using a Mann-Whitney U test.

4.3 RESULTS

4.3.1 Study Respondents

From September 13, 2021, to March 4, 2023, 795,722 respondents completed the survey (Table 4.1), of which 53,478 (6.7%) were excluded for not completing demographic questions (study N/pseudopopulation: 742,244). The final study population was 50.7% female, 47.7% male, and 1.5% transgender or non-binary compared to the 2019 U.S. American Community Survey which estimates the U.S. population as binary, at 50.8% female, 49.2% male[24]. Our lowest (<$30,000) and highest (≥$150,000) yearly household income values were 27.1% and 13.1% of our population compared to 23.6% and 14.4% respectively estimated by the U.S. Census. Excluded participants that reported at least one piece of demographic information were more likely to be female (56.6% compared to 50.7%), have earned a high school degree or less (39.3% compared to 38.3%), and have a higher mean age (51.4 compared to 47.0) than the study population. Excluded participants were also slightly less likely to report at-home test usage (7.0% compared to 7.6%).

4.3.2 Covid-like Illness in the Study Sample

Across the entire study period, 4.8% (95% CI: 4.7–4.9) of responses reported experiencing acute symptoms consistent with Covid-like illness. The median (IQR) monthly percentage of people reporting Covid-like illness was 4.6% (4.1%–5.2%) with the highest percentage (7.7%) be reported in January 2022 and the lowest (3.2%) in March 2023.

4.3.3 At-Home Test Usage

Across the entire study period, 7.6% (95% CI: 7.5–7.7) of individuals in the study population and 24.4% (95% CI: 23.8–25.0) of individuals with Covid-like illness reported utilization of an at-home test. During the periods when Covidtests.org was active, 32.2% (95% CI: 31.4–33.0) of individuals with Covid-like illness reported at-home tests compared to 15.2% (95% CI: 14.5–16.0) when the program was not active. Higher utilization of at-home tests during periods of Covidtests.org operation was seen across all demographic groups analyzed.

4.3.4 Disparities in At-Home Test Usage

During the study period, there were disparities in at-home COVID-19 test usage across household income, age, race, and geography both when comparing test use to overall U.S. population share and COVID-19 burden. Individuals in households with incomes ≤$30,000, individuals aged 18–29 years, Black individuals, and individuals living in the South Atlantic, had the lowest reported testing relative to their U.S. population share. Individuals from households with incomes ≤$30,000 made up 18.4% of

those reporting at-home test utilization, but 33.0% of the total population and 27.0% of those reporting symptoms consistent with Covid-like illness. Individuals aged 18–29 made up 17.1% of those reporting at-home test utilization, but 19.8% of the total population and 16.6% of those reporting symptoms consistent with Covid-like illness. Black individuals made up 8.5% of those reporting at-home test utilization, but 13.3% of the total population and 6.9% of those reporting symptoms consistent with Covid-like illness. Individuals living in the South Atlantic made up 16.2% of those reporting at-home test utilization, but 19.2% of the total population and 17.0% of those reporting symptoms consistent with Covid-like illness.

For all demographics measures, the Gini coefficient was greater than zero, indicating that the at-home test utilization was not perfectly equitable (Figures 4.1–4.2). With values further from zero and closer to one indicating higher levels of inequity, we found Gini coefficients of 0.22 and 0.12 for income and geography, respectively, and 0.03 for age and race. There are many different population distributions that could lead to these numbers; however, in a simple example, a Gini coefficient of 0.22 could mean that 50% of people utilized 72% of tests or 28% of people utilized 50% of tests, while a Gini coefficient of 0.03 could mean that 50% of people utilized 53% of tests or 47% of people utilized 50% of tests. A Gini coefficient of ≤0.01 (i.e., near equity) was computed for the random 7-option variable meant to proxy the appearance of disparities due to system-level noise, suggesting the indicated demographic disparities were larger than those measured from random variation alone.

4.3.5 Disparities in At-Home Test Usage Over Time

Disparities in at-home COVID-19 testing across household income, age, and race also varied with time (Figure 4.3). Theil's T comparing the expected utilization of at-home testing based on observed Covid-like illness burden varied for household income (geometric mean: 1.94 and [geometric standard deviation: 1.78], age (0.49 [GSD: 2.30]), race (6.68 [GSD: 3.72]), and geography (2.79 [GSD:2.24]). Theil's T comparing the expected utilization of at-home testing based on population share also varied for household income (0.07 [GSD: 1.89], age (0.02 [GSD: 1.95]), race (0.08 [GSD: 2.02]), and geography (0.13 [GSD:2.57])(Figure 4.4).

Spearman correlations were performed to evaluate the correlation of Theil's T with the measured disparities and population Covid-like illness (i.e., were disparities higher when COVID-19 was circulating). Overall, there were moderate correlations between Theil's T and Covid-like illness for household income (spearman's ρ: 0.50), race (spearman's ρ: 0.50), and geography (spearman's ρ: 0.38), and a small correlation for age (spearman's ρ: 0.14), when measuring Theil's T as expected utilization of at-home testing proportional to population share. There are no meaningful (i.e, spearman's $\rho < 0.01$) correlations between Theil's T and Covid-like illness when measuring Theil's T comparing expected utilization of at-home testing proportional to Covid-like illness burden (i.e., we did not find increased disparities measuring whether at-home tests were equitably utilized among people with Covid-like illness, during periods of high Covid-like illness) except by geography (spearman's ρ: 0.23).

4.3.6 Estimating Impact of Policy on At-Home Test Usage Disparities

An interrupted time series regression model found an association between Theil's T and the periods that Covidtests.gov was operational (Figures 4.5–4.8) when measuring whether at-home tests utilization was proportional to Covid-like illness burden (Table 4.2) across race, household income, and geography. These regression results suggest that disparities measured via Theil's T was 53% (95%CI: 6%–121%) higher for household income, 214% (95%CI: 86%–429%) higher for race, and 90% (95%CI: 23%–193%) higher for geography during Covidtest.gov dissemination periods. Said differently, this finding indicates lower levels of racial, income, and geographic equity in at-home testing utilization during periods when Covidtest.gov was operational versus periods when it was not. Further, there was no association between Theil's T when measuring equity in random group membership and Covidtest.gov periods, suggesting the indicated associations between race, income, and geographic disparities and Covidtests.gov were larger than associations that we might expect from random group assignment alone.

4.3.7 Estimating Impact of Policy During Weeks of Peak Illness

Sixteen weeks comprised the top 20th percentile of COVID-19 burden during the study period. Five of these weeks occurred during periods of Covidtest.gov operation and 11 occurred outside the program's operation. The distribution of Theil's T for income, race, age, geographic, and random group membership was compared across the two periods (Figures 4.9–4.13). During periods of Covidtest.gov operation compared to periods when it was not operating, the median [interquartile range] of Theil's T was higher for income (2.3 [2.1–2.5] compared to 1.2 [0.9–2.7]), race (8.7 [6.2–10.2]

compared to 4.9 [2.0–9.4]), and geography (4.7 [3.8–5.5] compared to 3.6 [1.6–6.3]). Theil's T was lower during periods of operation compared to periods of non-operation for age (0.3 [0.2–0.4] compared to 0.5 [0.4–0.8]) and random group membership (0.4 [0.4–0.4] compared to 0.5 [0.2–0.5]). None of these differences were statistically significant when comparing the distributions using a Mann-Whitney U test.

4.4 DISCUSSION

Using a nationally representative digital health survey and two measures of equitable resource distribution, we quantify disparities in access to at-home testing across household income, age, and race/ethnic demographic groups. Importantly, we show that income and race-based disparities in at-home test utilization were heightened during periods when the Covidtest.gov scheme was active.

In general, we found disparities in at-home testing across household income, age, and race both when comparing expected test utilization based on overall population share and share of COVID-19 burden. While disparities in at-home testing were evident across the study period and the implementation of the Covidtests.gov program led to an increase in some of these disparities, it is worth noting that overall testing rates were higher during the program's active periods for all demographic groups. This finding suggests that although the Covidtests.gov program was successful in its goal of increasing testing, the benefits were not distributed equally for everyone in the U.S.

The largest inequities in at-home testing occurred across household income, with respondents from more wealthy households disproportionately reporting at-home testing

with Covid-like illness and in general. When measuring inequities in at-home testing across race, we find that Black individuals were disproportionately more likely to test with Covid-like illness but disproportionately less likely to test in general. This pattern suggests that among some demographic groups, at-home testing may be favored as a diagnostic tool, while among others it may be favored when not indicated by symptoms alone (e.g., prior to an event or post-exposure).

Disparities in testing by age were smaller than those by geography and income. The relationship between age and testing was not monotonically associated with increased COVID-19 risk profiles (i.e., older individuals were not substantially more likely to test than younger ones) and was not shown to increase with broad population Covid-like illness. This pattern provides further evidence that individuals are not just using at-home COVID-19 tests to evaluate symptoms or as indication for treatment, as we would then expect to see an increase in age-related testing disparities during COVID-19 waves given the strong association between age and symptoms/necessity for treatment[25,26]. Alternatively, older individuals may tend to proceed with other means of Covid-like illness evaluation, such as NAAT or hospitalization.

We find a correlation between Covid-like illness and Theil's T measuring race- and income- based disparities, suggesting that there are greater inequities in at-home test use during periods of increased need for testing. An analysis of weeks when COVID-19 burden was high suggests that, while test distribution increased across all groups, this problem of inequitable distribution was mildly exacerbated during periods of Covidtests.gov operation. Interestingly, the identified increase in inequity during periods

of increased need only exists when measuring expected at-home test utilization based on population share, and not expected based on Covid-like illness burden. Through the lens of income disparities, this indicates that when Covid-like illness increases, individuals in wealthier households utilize a disproportionately larger share of at-home tests for reasons other than them having a higher burden of COVID illness. This data does not indicate whether this is a function of wealthy individuals having a lower barrier for use of a test (i.e., more likely to test when with mild symptoms), differences in diagnostic vs. alternative use as previously noted, or easier access to home testing during periods of scarcity.

The dataset and analyses employed have several limitations. At-home tests can be stored for later use, and at-home testing is retrospectively reported over a 30-day period. The period in late 2022 where Covidtest.gov was dormant was only 104 days, and individuals likely used tests from the program during that time. We mitigated this concern by utilizing a 30-day delay period in our models; however, if Covidtests.gov truly increased inequities, we likely underestimated it due to misclassification of individuals using government provided tests during times they were not actively disseminated. Additionally, our survey measured at-home test use as a binary (i.e., did test vs did not test), and did not query the number of tests used nor whether individuals sought other evaluation. If some individuals were more likely to use at-home tests, it is likely that the same individuals used more than one test (especially if they used them for prophylactic exposures which are likely to occur more than once) and that the inequities we report here are underestimations. Lastly, our test utilized self-reports of demographic

exposure and disease outcome data which may lead to misclassification; however, the survey instrument was designed as anonymous to mitigate this issue. Additionally, the use of a web survey is likely susceptible to selection bias in who initiates and who completes the questionnaire, which may bias our results in either direction. The survey sample also underrepresents individuals without access to the internet; however, this also likely positions it as an appropriate sample for evaluating Covidtests.gov — an internet-based program.

4.4.1 Conclusion

Our findings suggest that, while increasing at-home testing rates across all demographic groups, the introduction of a government program to freely disseminate at-home tests may have led to larger income-, racial-, and geographic-based at-home testing disparities. Purposeful design of an equity-driven public health policy is not enough to ensure equity goals are met. Continued efforts to ensure equitable access to COVID-19 testing are needed.

4.5 TABLES AND FIGURES

Table 4.1 Description of the weighted study sample (pseudopopulation) overall and among those with Covid-like illness

Characteristic	**Survey Pseudopopulation, N (%)**	**Survey Pseudopopulation With Covid-like Illness, N (%)**
Race		
American Indian or Alaska Native	5861.1 (0.8)	308.4 (0.9)
Asian	39187.6 (5.3)	1211.0 (3.4)
Black or African American	99156.7 (13.3)	2437.8 (6.9)
Hispanic or Latino/a	106742.2 (14.3)	3979.6 (11.2)
Native Hawaiian or Pacific Islander	3640.1 (0.5)	144.4 (0.4)
White	468735.5 (62.9)	26322.5 (74.2)
Multi-Racial	7728.6 (1.0)	418.4 (1.2)
Single Other Race	13842.0 (1.9)	652.7 (1.8)
Gender		
Female	378015.4 (50.7)	22345.0 (63.0)
Male	355541.5 (47.7)	11733.7 (33.1)
Transgender or Nonbinary	11336.9 (1.5)	1396.2 (3.9)
Education		
High School or Less	285290.1 (38.3)	11708.9 (33.0)
Some College	232126.8 (31.2)	12059.6 (34.0)
College or More	143605.7 (19.3)	7247.0 (20.4)
Post Graduate Degree	83871.3 (11.3)	4459.4 (12.6)
Age		
18–29 years	147345.9 (19.8)	5873.4 (16.6)
30–39 years	134062.9 (18.0)	6970.7 (19.6)
40–49 years	123364.5 (16.6)	6470.4 (18.2)
50–64 years	193639.5 (26.0)	9644.2 (27.2)
65–74 years	108329.3 (14.5)	4775.8 (13.5)
75+ years	38151.8 (5.1)	1740.4 (4.9)
Household Income		
Less than $30,000	201757.4 (27.1)	11708.1 (33.0)
$30,000–49,999	125855.2 (16.9)	5585.4 (15.7)
$50,000–$74,999	122737.0 (16.5)	5264.1 (14.8)
75,000–$99,999	92056.2 (12.4)	3880.4 (10.9)
$100,000–$149,999	105122.1 (14.1)	4720.0 (13.3)
$150,000 and Over	97366.0 (13.1)	4317.0 (12.2)

U.S. Census Division		
New England	36222.0 (4.9)	2062.2 (5.8)
Middle Atlantic	98026.0 (13.2)	4155.6 (11.7)
East North Central	98845.3 (13.3)	5052.1 (14.2)
West North Central	55190.5 (7.4)	2982.1 (8.4)
East South Central	42527.0 (5.7)	2305.2 (6.5)
West South Central	98869.5 (13.3)	4442.4 (12.5)
South Atlantic	143142.2 (19.2)	6021.1 (17.0)
Pacific	110455.0 (14.8)	5282.3 (14.9)
Mountain	61616.4 (8.3)	3171.9 (8.9)

Table 4.2 Results from a regression model with autoregressive integrated moving average (ARIMA) errors to assess the association between Covidtests.gov operational periods in the United States and equitable utilization of at-home COVID-19 tests measured via Theil's T

	Estimated effect of Covidtests.gov on Theil's T measuring at-home COVID-19 testing proportional to:	
Theil's T Measured Across:	**Covid-like illness Burden**	**Population Share**
Household Income	1.53 (1.06–2.21)	1.24 (0.85–1.83)
Age	1.12 (0.79–1.58)	1.16 (0.79–1.69)
Race	3.14 (1.86–5.29)	1.18 (0.88–1.57)
U.S. Census Division	1.9 (1.23–2.93)	0.86 (0.46–1.59)
Random Grouping	1.17 (0.78–1.76)	1.01 (0.69–1.47)

Figure 4.1 Lorenz curves measuring the proportionality between self-reported at-home COVID-19 test utilization and COVID-19 burden in the United States across income, race, age, and geography

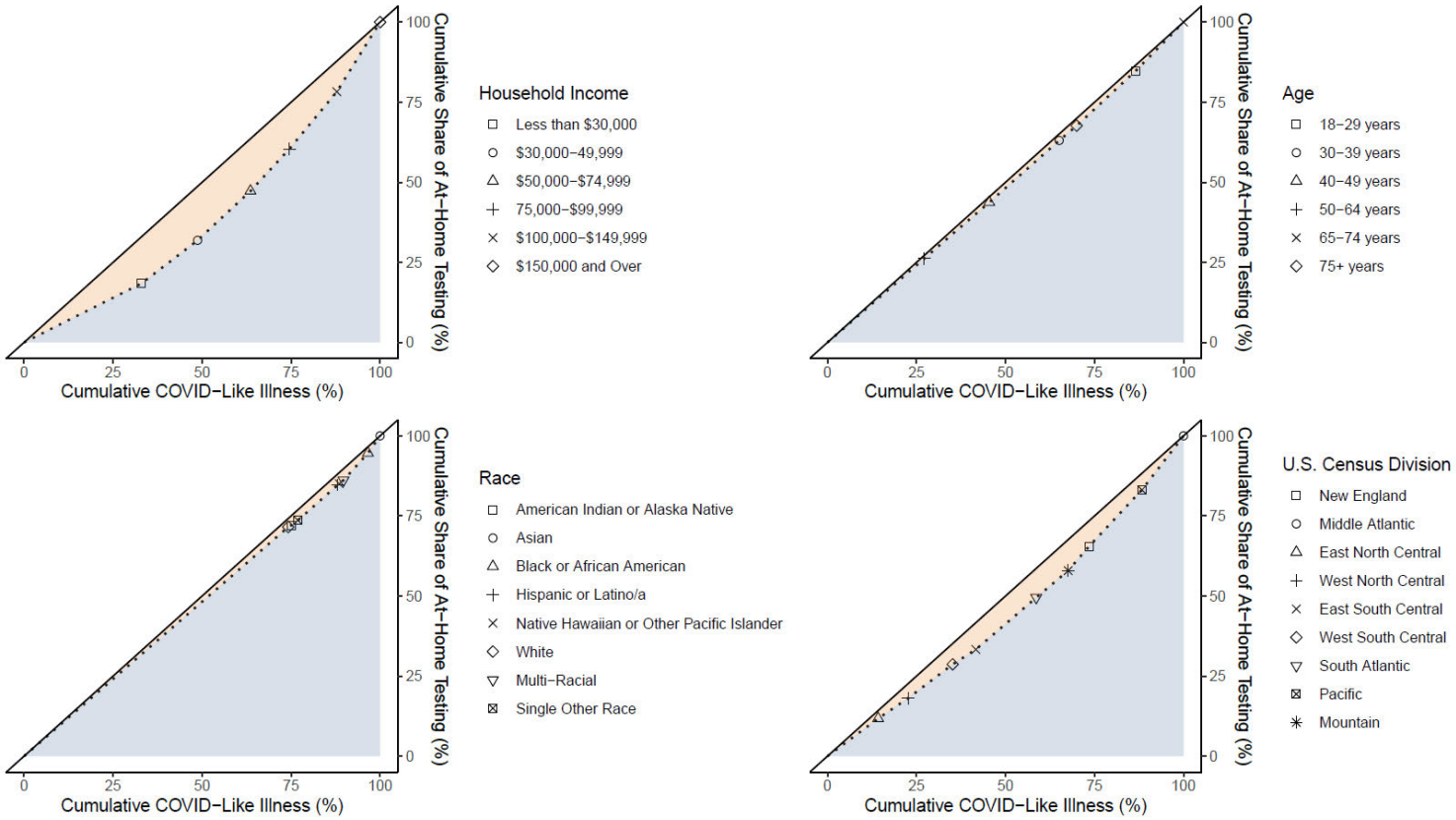

United States adults (N=742,244) self-reported utilization of at-home COVID-19 test and acute experiences of medical symptoms via an online survey. Cumulative at-home testing is plotted against the cumulative burden of medical symptoms consistent with COVID-19 (Covid-like illness [Covid-like illness]) by population substrata in four separate Lorenz curves. Note, legend values are presented in alphanumeric order, while points are plotted from left to right by order of least amount of observed test utilization compared to expected. Diagonal line in each plot represents proportional equity between at-home testing and COVID-19 burden. Increasing convexity of curves suggests increasing departures from proportional equity. Gini coefficients are calculated as the orange area (expected – observed) divided by the sum of the orange and blue areas (expected). Gini coefficients were calculated for income (0.22), geography (0.12), age (0.03) and race (0.03).

Figure 4.2 Lorenz curves measuring the proportionality between self-reported at-home COVID-19 utilization and population share in the United States across income, race, age, and geography

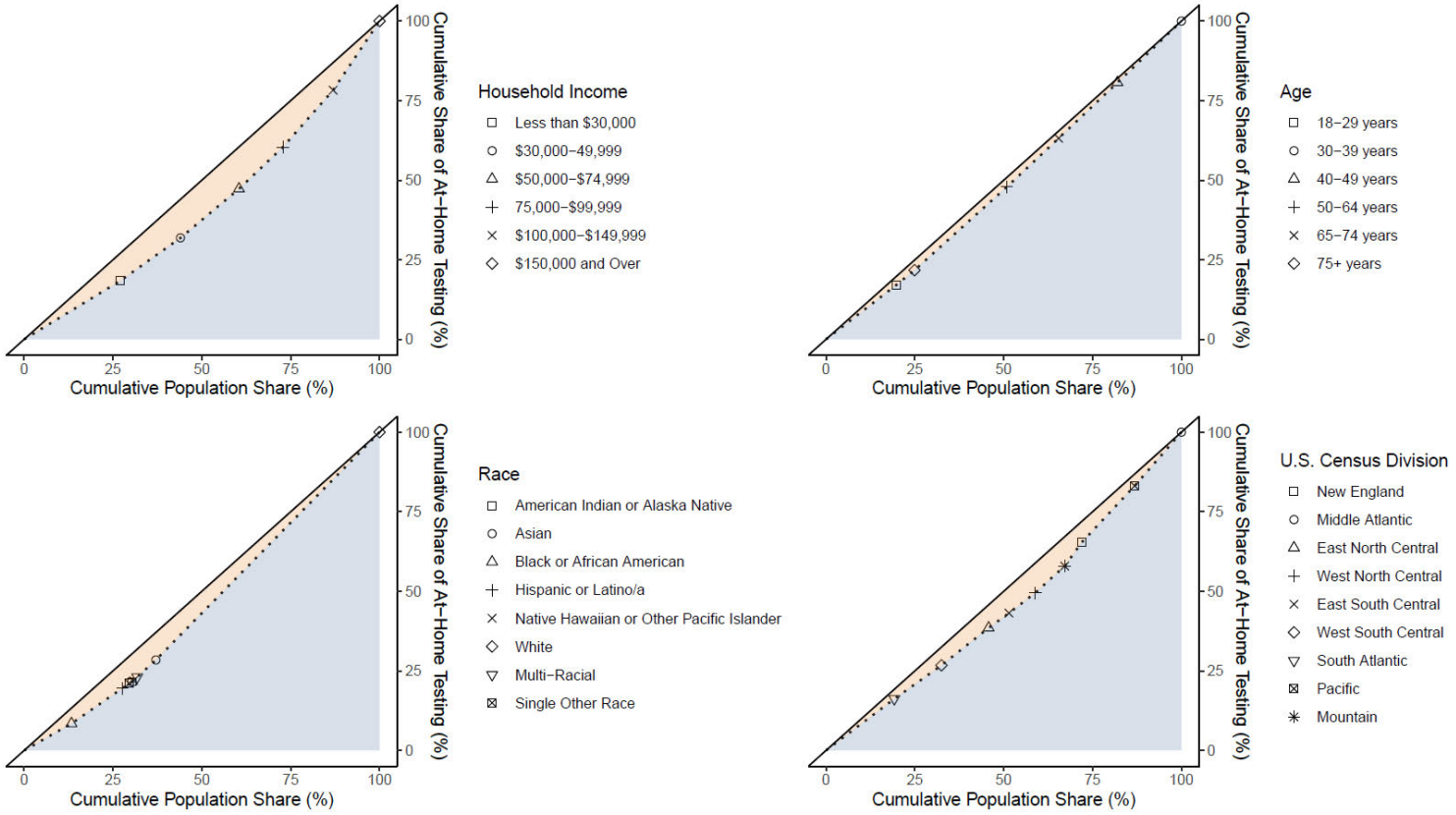

United States adults (N=742,244) self-reported utilization of at-home COVID-19 test. Cumulative at-home testing is plotted against the cumulative proportion of the survey sample population by substrata in four separate Lorenz curves. Note, legend values are presented in alphanumeric order, while points are plotted from left to right by order of least amount of observed test utilization compared to expected. Diagonal line in each plot represents proportional equity between at-home testing and population share. Increasing convexity of curves suggests increasing departures from proportional equity. Gini coefficients are calculated as the orange area divided by the sum of the orange and blue areas. Gini coefficients were calculated for income (0.17), geography (0.10), age (0.04) and race (0.10).

Figure 4.3 Self-reports of at-home COVID-19 testing measured via web survey by demographic subgroup in the United States, September 13, 2021, to March 4, 2023

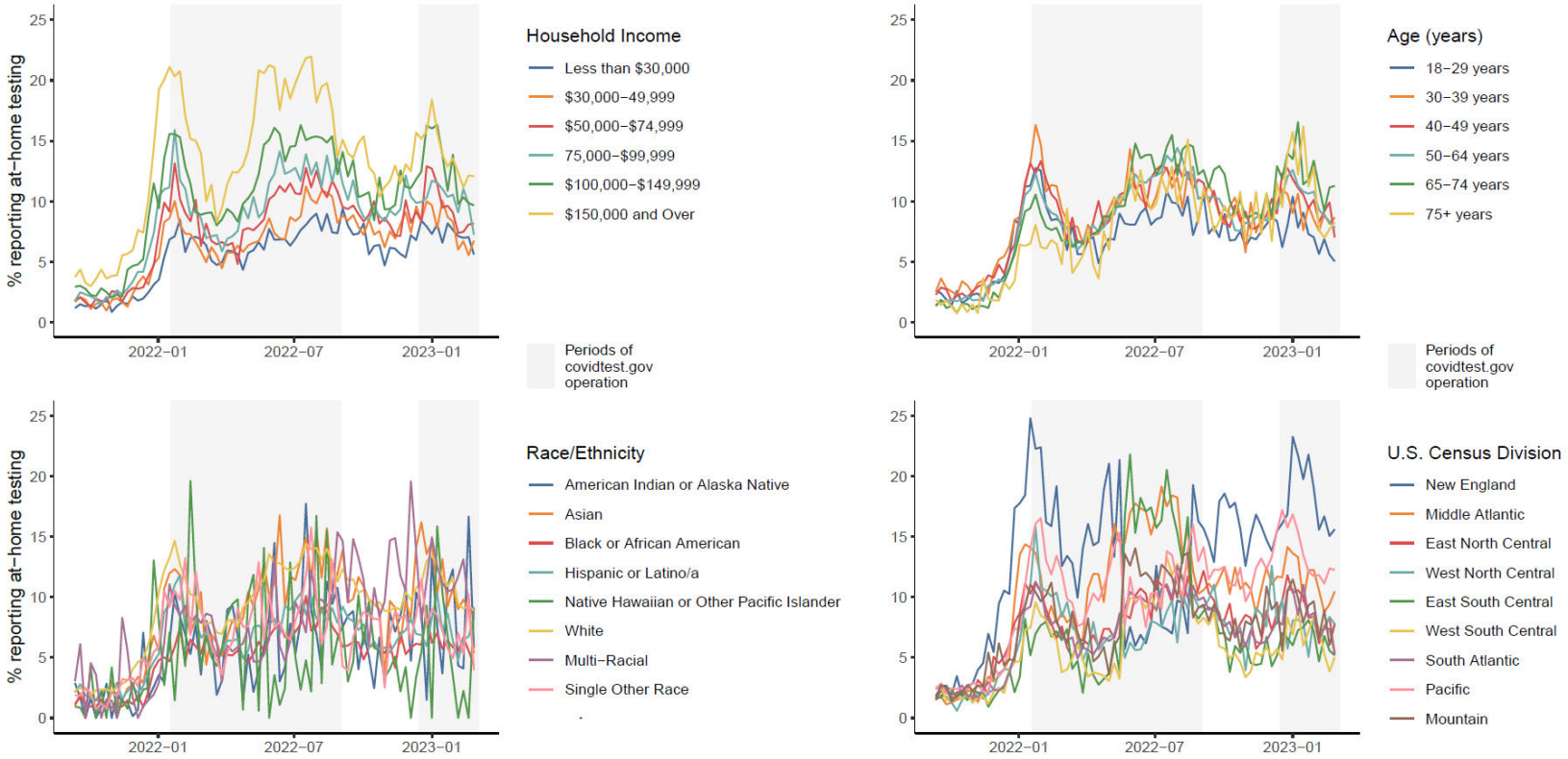

United States adults (N=742,244) self-reported utilization of at-home COVID-19 test by self-reported demographic between September 12, 2021 and February 26, 2023. Gray shading represents periods when Covidtests.gov was operational.

Figure 4.4 Theil's T quantification of at-home COVID testing equity over time by demographic group in the United States, September 13, 2021, to March 4, 2023

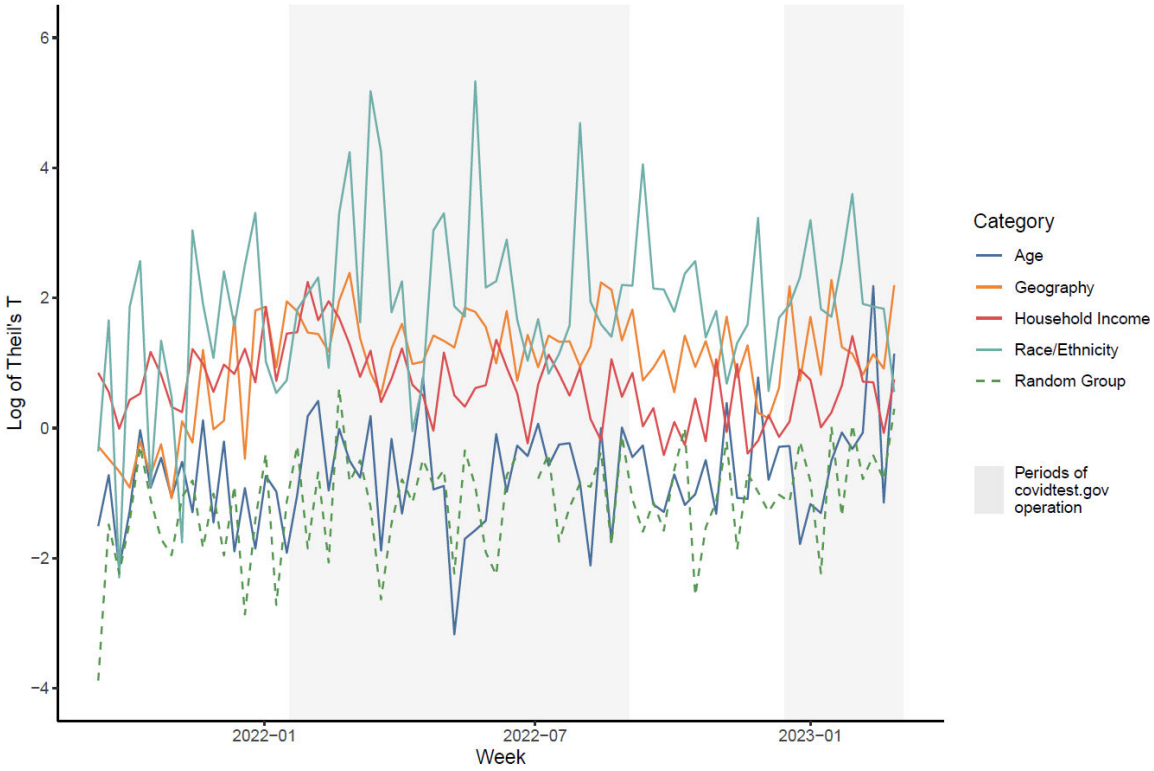

United States adults (N=742,244) self-reported utilization of at-home COVID-19 testing and acute experiences of medical symptoms via an online survey. Proportionality between at-home testing and burden of medical symptoms consistent with COVID-19 (Covid-like illness) was measured by Theil's T. Higher values of Theil's T represent more entropy (i.e., less proportionality in testing) among the strata of each subgroup. A 0 value of Theil's T would suggest all strata (e.g., people living in every census division) tested for COVID-19 exactly proportional to their COVID-19 burden. Gray shading represents periods when Covidtests.gov was operational.

Figure 4.5 Observed and predicted income equity in at-home COVID-19 test utilization by Covidtest.gov operational status in the United States, September 13, 2021, to March 4, 2023

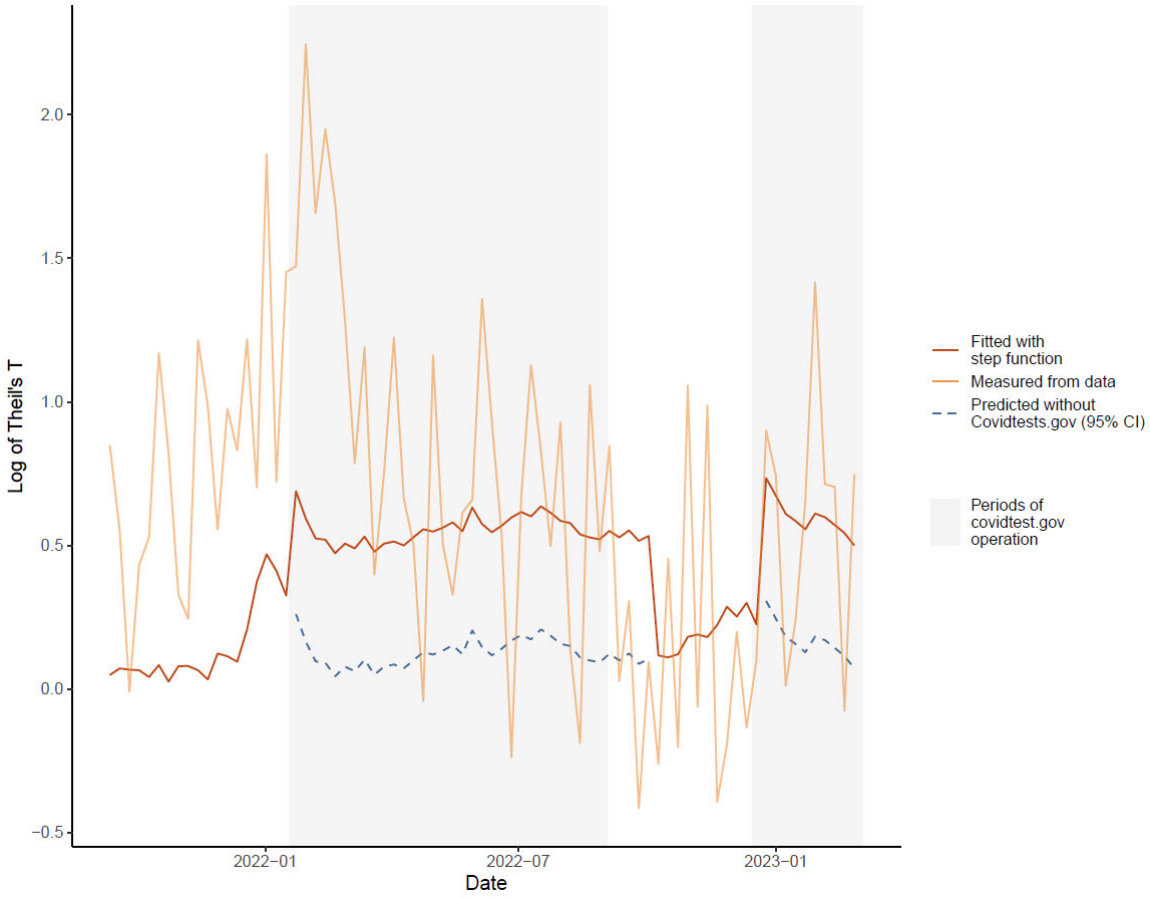

United States adults (N=742,244) self-reported utilization of at-home COVID-19 testing and acute experiences of medical symptoms via an online survey. Proportionality between at-home testing and burden of medical symptoms consistent with COVID-19 (Covid-like illness) was measured by Theil's T across income. A regression model with autoregressive integrated moving average (ARIMA) errors and a binary indicator for dates when Covidtests.gov was operational (including a lag to allow for shipping and use) was fit to the log of Theil's T. Plot displays actual data (light orange), regression fitted data (dark orange), and the regression predicted Theil's T if Covidtests.gov was not in operation. Gray shading represents periods when Covidtests.gov was operational.

Figure 4.6 Observed and predicted racial equity in at-home COVID-19 test utilization by Covidtest.gov operational status in the United States, September 13, 2021, to March 4, 2023

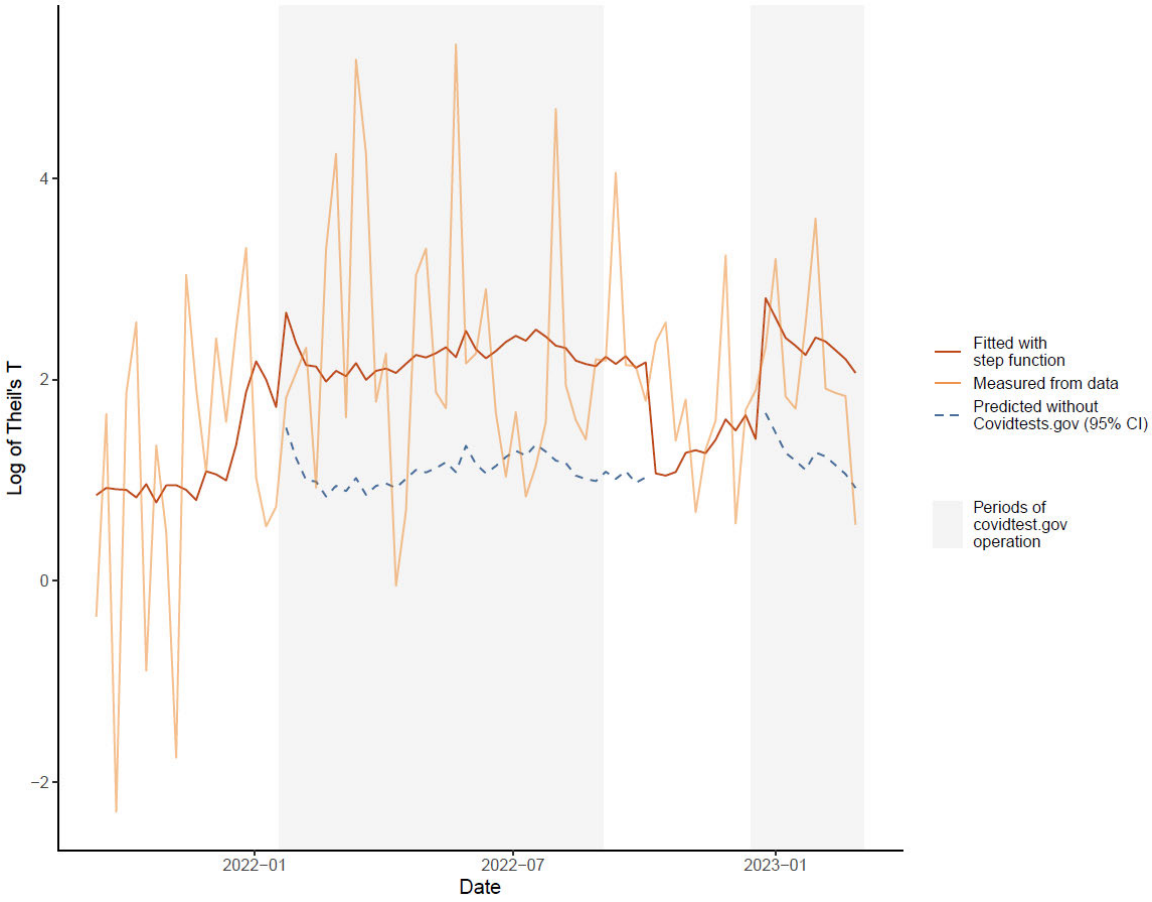

United States adults (N=742,244) self-reported utilization of at-home COVID-19 testing and acute experiences of medical symptoms via an online survey. Proportionality between at-home testing and burden of medical symptoms consistent with COVID-19 (Covid-like illness) across race was measured by Theil's T. A regression model with autoregressive integrated moving average (ARIMA) errors and a binary indicator for dates when Covidtests.gov was operational (including a lag to allow for shipping and use) was fit to the log of Theil's T. Plot displays actual data (light orange), regression fitted data (dark orange), and the regression predicted Theil's T if Covidtests.gov was not in operation. Gray shading represents periods when Covidtests.gov was operational.

Figure 4.7 Observed and predicted age equity in at-home COVID-19 test utilization by Covidtest.gov operational status in the United States, September 13, 2021, to March 4, **2023**

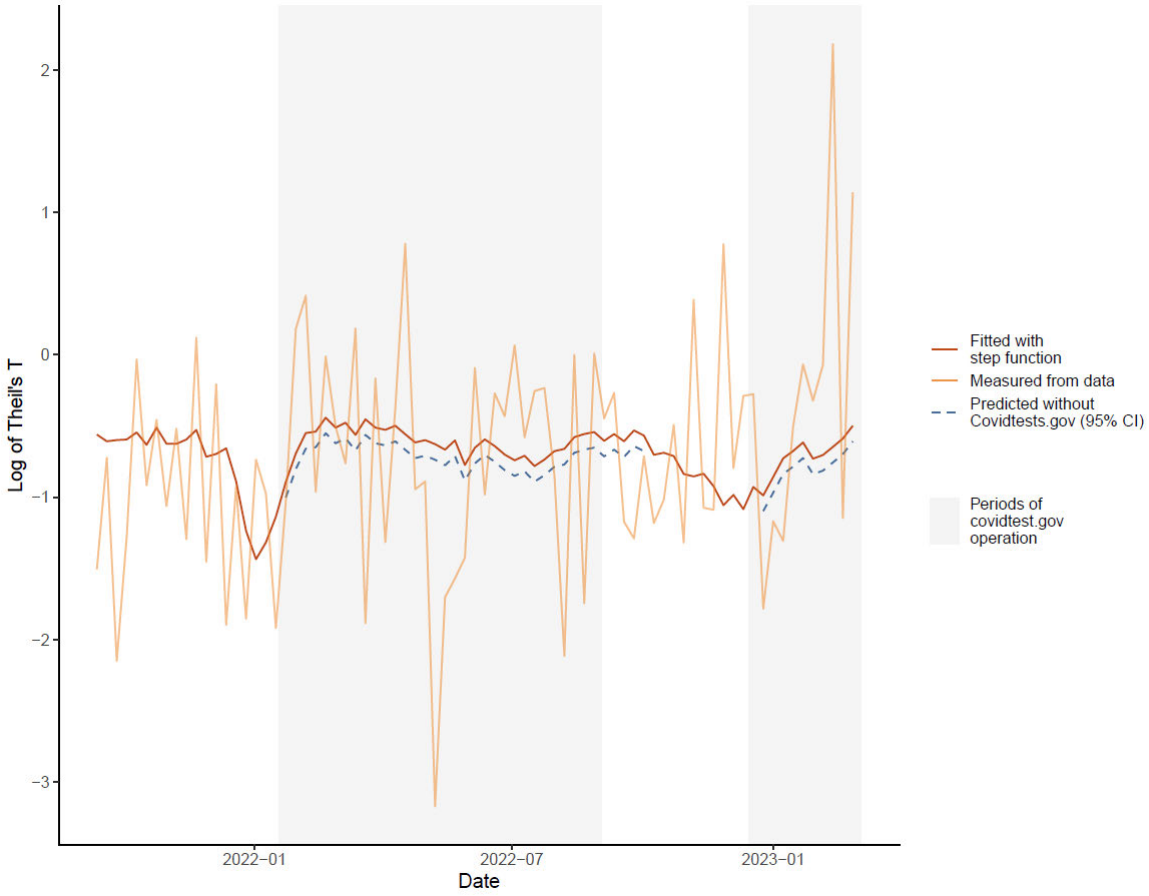

United States adults (N=742,244) self-reported utilization of at-home COVID-19 testing and acute experiences of medical symptoms via an online survey. Proportionality between at-home testing and burden of medical symptoms consistent with COVID-19 (Covid-like illness) across age was measured by Theil's T. A regression model with autoregressive integrated moving average (ARIMA) errors and a binary indicator for dates when Covidtests.gov was operational (including a lag to allow for shipping and use) was fit to the log of Theil's T. Plot displays actual data (light orange), regression fitted data (dark orange), and the regression predicted Theil's T if Covidtests.gov was not in operation. Gray shading represents periods when Covidtests.gov was operational.

Figure 4.8 Observed and predicted geographic equity in at-home COVID-19 test utilization by Covidtest.gov operational status in the United States, September 13, 2021, to March 4, 2023

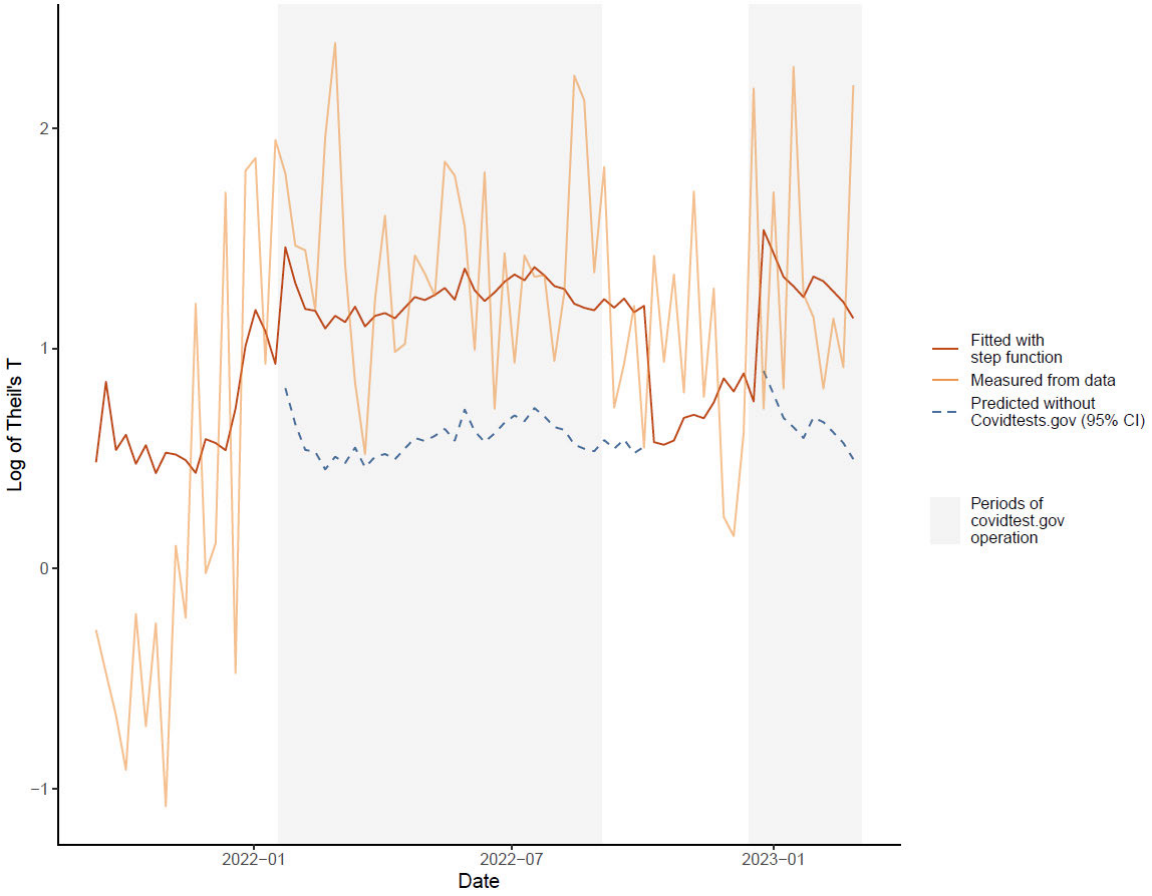

United States adults (N=742,244) self-reported utilization of at-home COVID-19 testing and acute experiences of medical symptoms via an online survey. Proportionality between at-home testing and burden of medical symptoms consistent with COVID-19 (Covid-like illness) across U.S. Census division was measured by Theil's T. A regression model with autoregressive integrated moving average (ARIMA) errors and a binary indicator for dates when Covidtests.gov was operational (including a lag to allow for shipping and use) was fit to the log of Theil's T. Plot displays actual data (light orange), regression fitted data (dark orange), and the regression predicted Theil's T if Covidtests.gov was not in operation. Gray shading represents periods when Covidtests.gov was operational.

Figure 4.9 At-home test utilization income equity during periods of peak COVID-19 burden by operational status of Covidtests.gov in the United States, September 13, 2021, to March 4, 2023

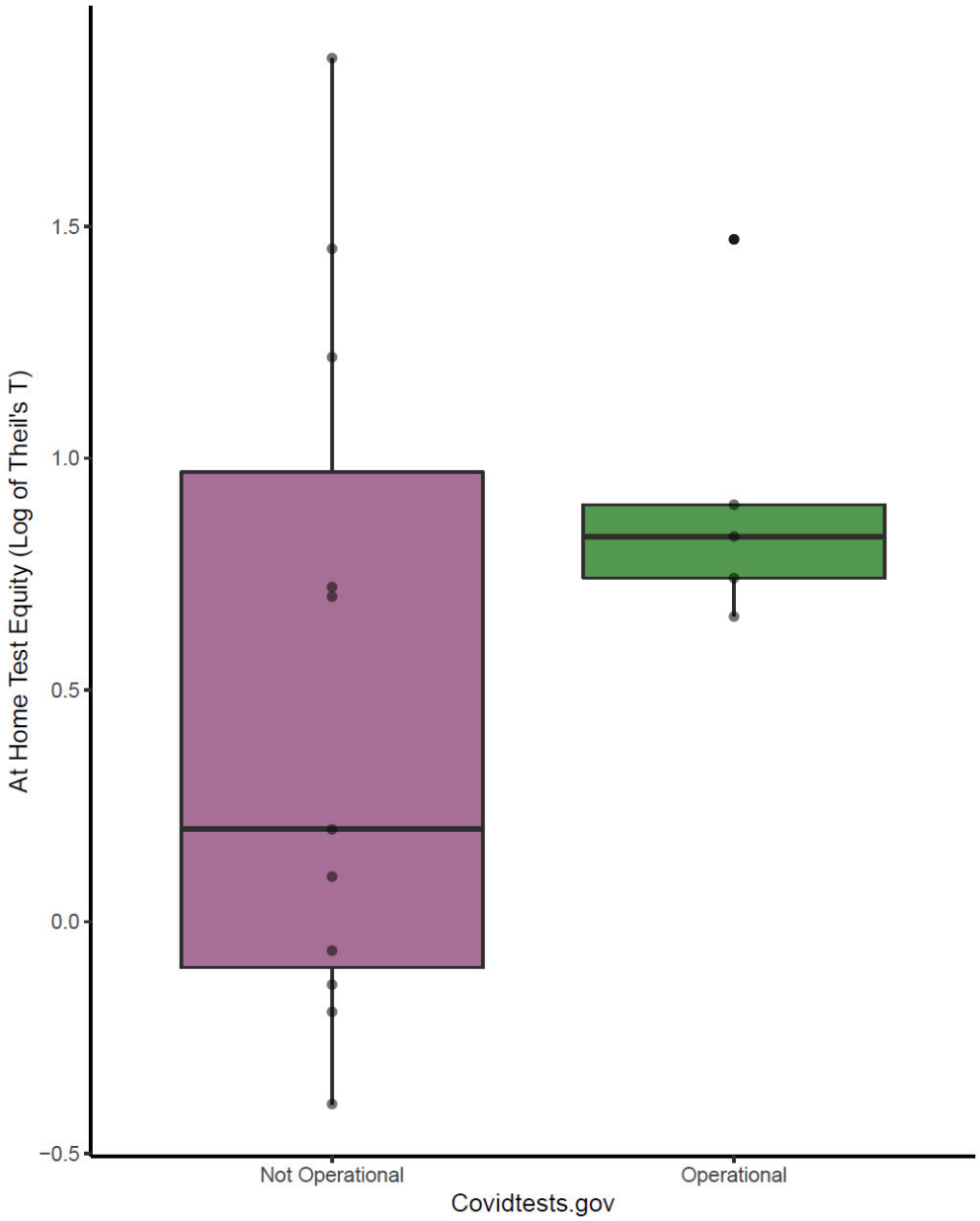

United States adults (N=742,244) self-reported utilization of at-home COVID-19 testing and acute experiences of medical symptoms via an online survey. Proportionality between at-home testing and burden of medical symptoms consistent with COVID-19 (Covid-like illness) across household income was measured by Theil's T. Sixteen of the weeks of the study period were identified (top 20th percentile) as weeks of peak COVID-19 burden. Distribution of Theil's T during the five of these weeks occurring during periods of Covidtest.gov operation were compared to the 11 that occurred outside programs operation. Higher Theil's T value suggests reduced equity.

Figure 4.10 At-home test utilization racial equity during periods of peak COVID-19 burden by operational status of Covidtests.gov in the United States, September 13, 2021, to March 4, 2023

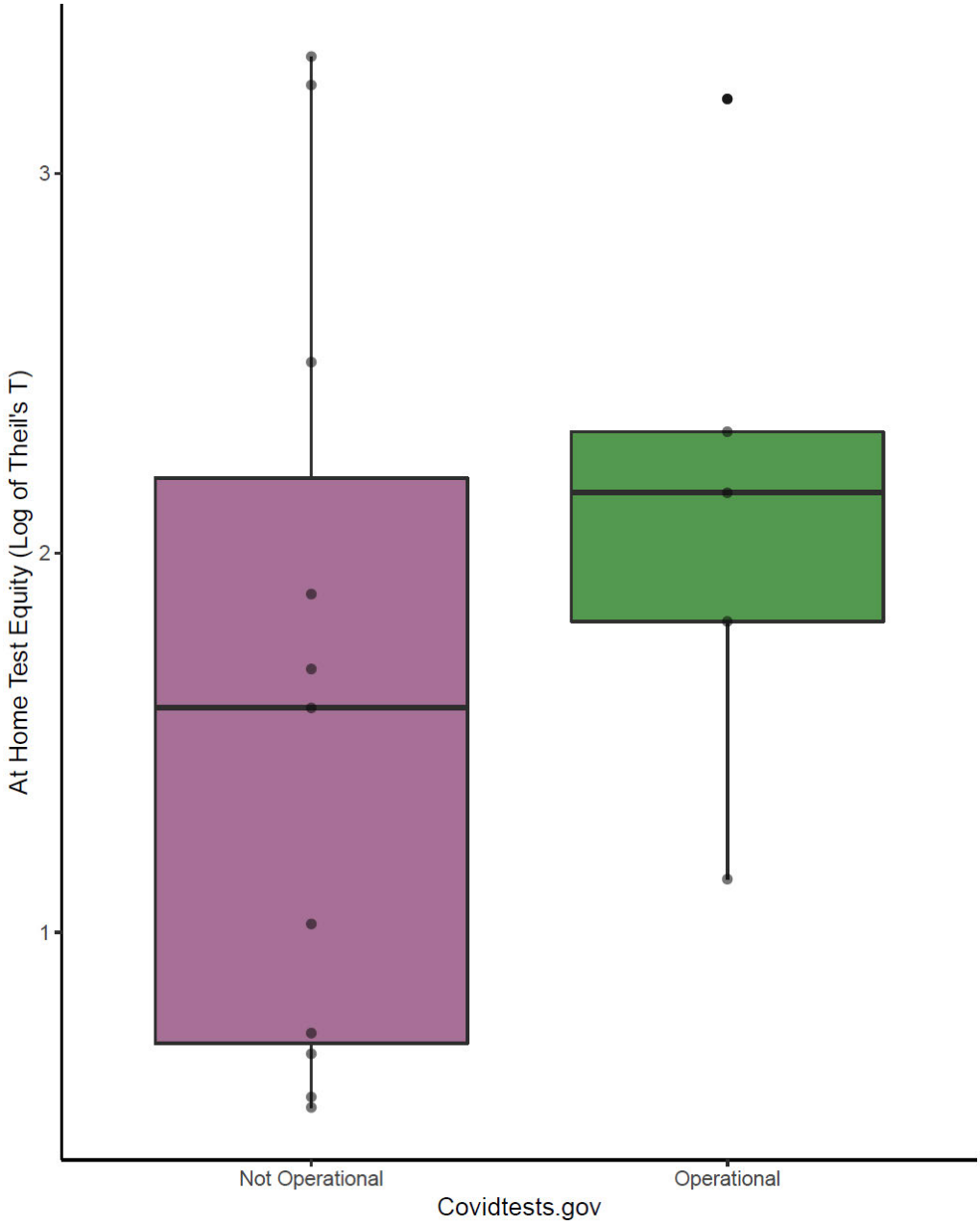

United States adults (N=742,244) self-reported utilization of at-home COVID-19 testing and acute experiences of medical symptoms via an online survey. Proportionality between at-home testing and burden of medical symptoms consistent with COVID-19 (Covid-like illness) across race was measured by Theil's T. Sixteen of the weeks of the study period were identified (top 20th percentile) as weeks of peak COVID-19 burden. Distribution of Theil's T during the five of these weeks occurring during periods of Covidtest.gov operation were compared to the 11 that occurred outside programs operation. Higher Theil's T value suggests reduced equity.

Figure 4.11 At-home test utilization age equity during periods of peak COVID-19 burden by operational status of Covidtests.gov in the United States, September 13, 2021, to March 4, 2023

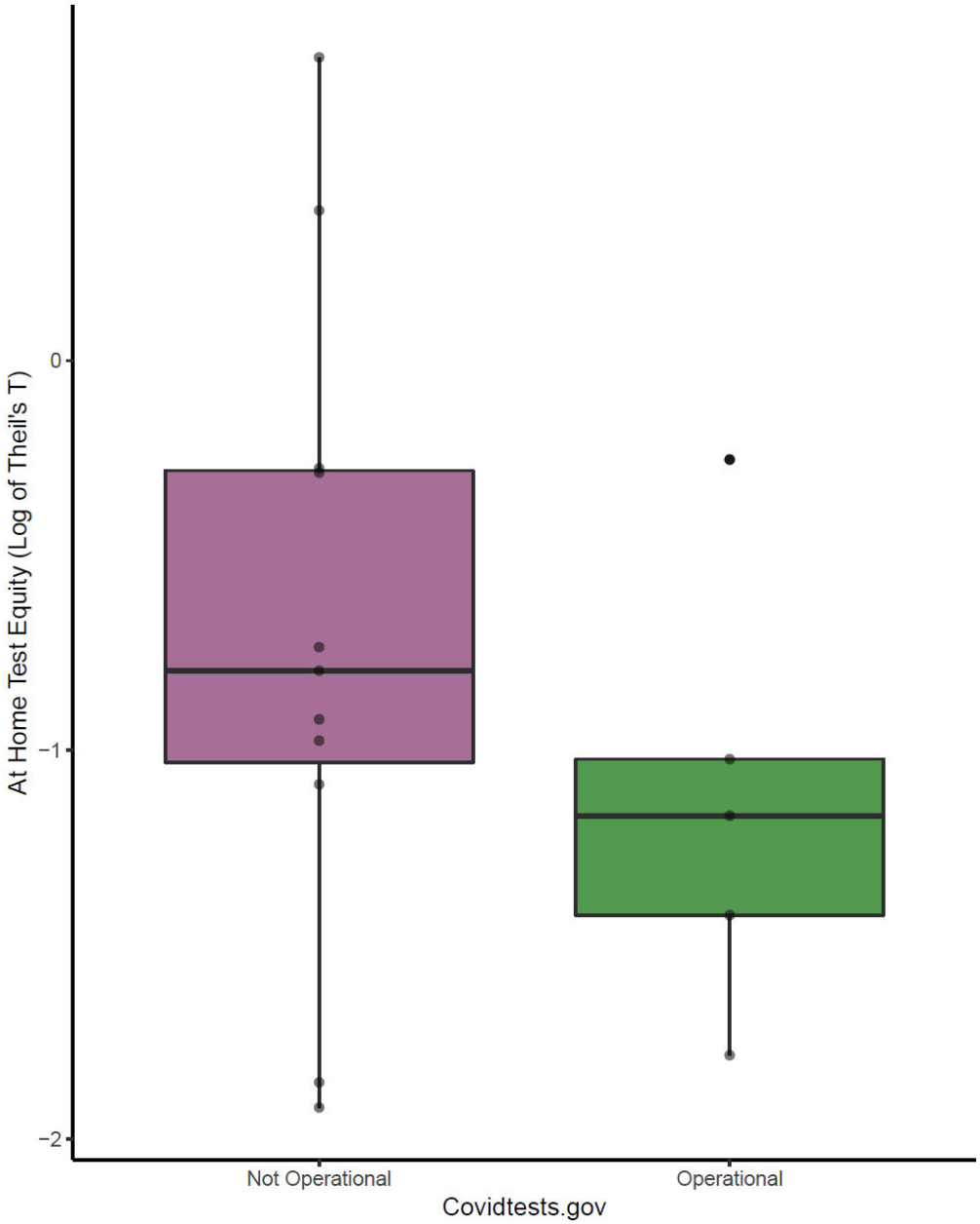

United States adults (N=742,244) self-reported utilization of at-home COVID-19 testing and acute experiences of medical symptoms via an online survey. Proportionality between at-home testing and burden of medical symptoms consistent with COVID-19 (Covid-like illness) across age was measured by Theil's T. Sixteen of the weeks of the study period were identified (top 20th percentile) as weeks of peak COVID-19 burden. Distribution of Theil's T during the five of these weeks occurring during periods of Covidtest.gov operation were compared to the 11 that occurred outside programs operation. Higher Theil's T value suggests reduced equity.

Figure 4.12 At-home test utilization geographic equity during periods of peak COVID-19 burden by operational status of Covidtests.gov in the United States, September 13, 2021, to March 4, 2023

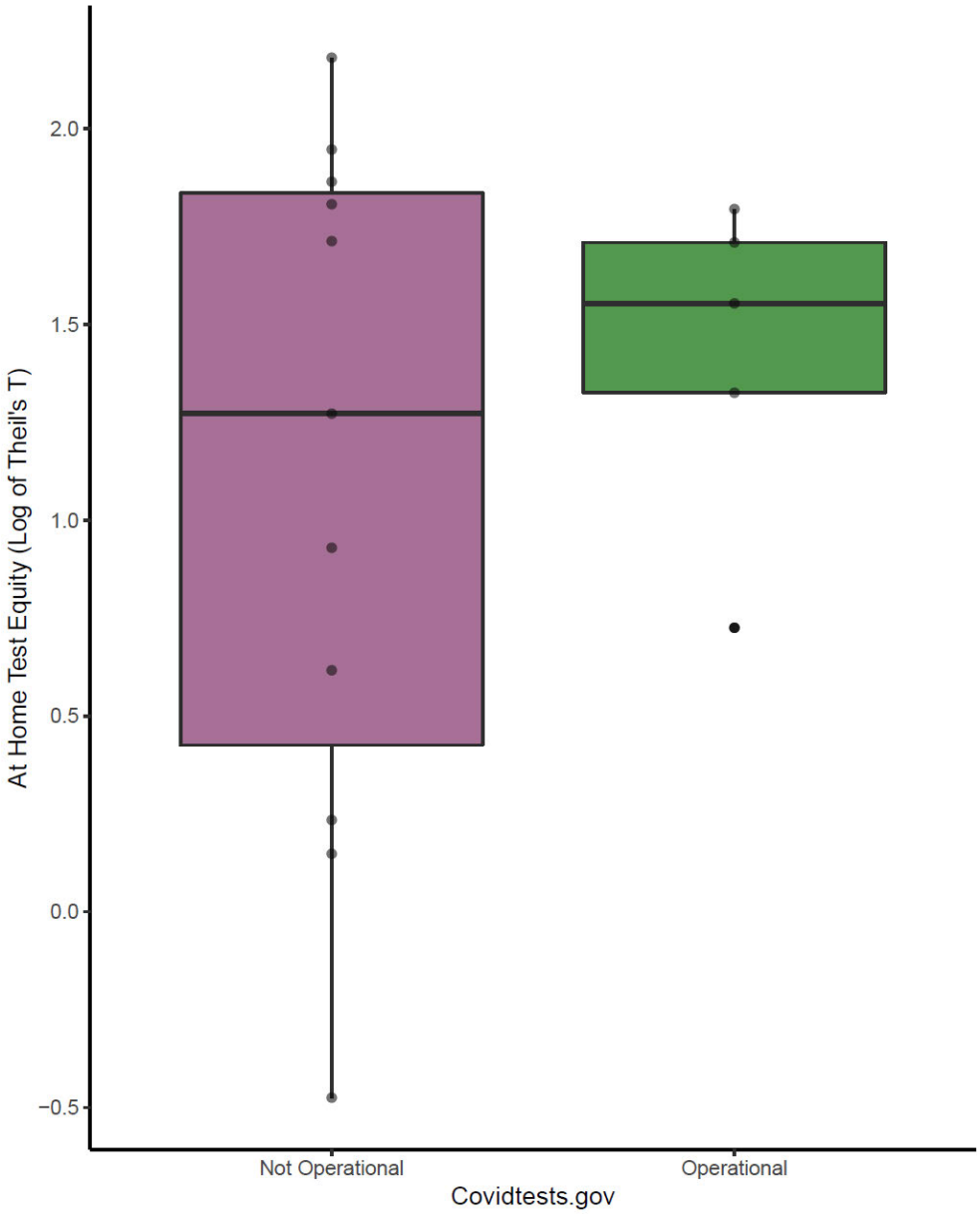

United States adults (N=742,244) self-reported utilization of at-home COVID-19 testing and acute experiences of medical symptoms via an online survey. Proportionality between at-home testing and burden of medical symptoms consistent with COVID-19 (Covid-like illness) across U.S. Census Division was measured by Theil's T. Sixteen of the weeks of the study period were identified (top 20th percentile) as weeks of peak COVID-19 burden. Distribution of Theil's T during the five of these weeks occurring during periods of Covidtest.gov operation were compared to the 11 that occurred outside programs operation. Higher Theil's T value suggests reduced equity.

Figure 4.13 At-home test utilization random group equity during periods of peak COVID-19 burden by operational status of Covidtests.gov in the United States, September 13, 2021, to March 4, 2023

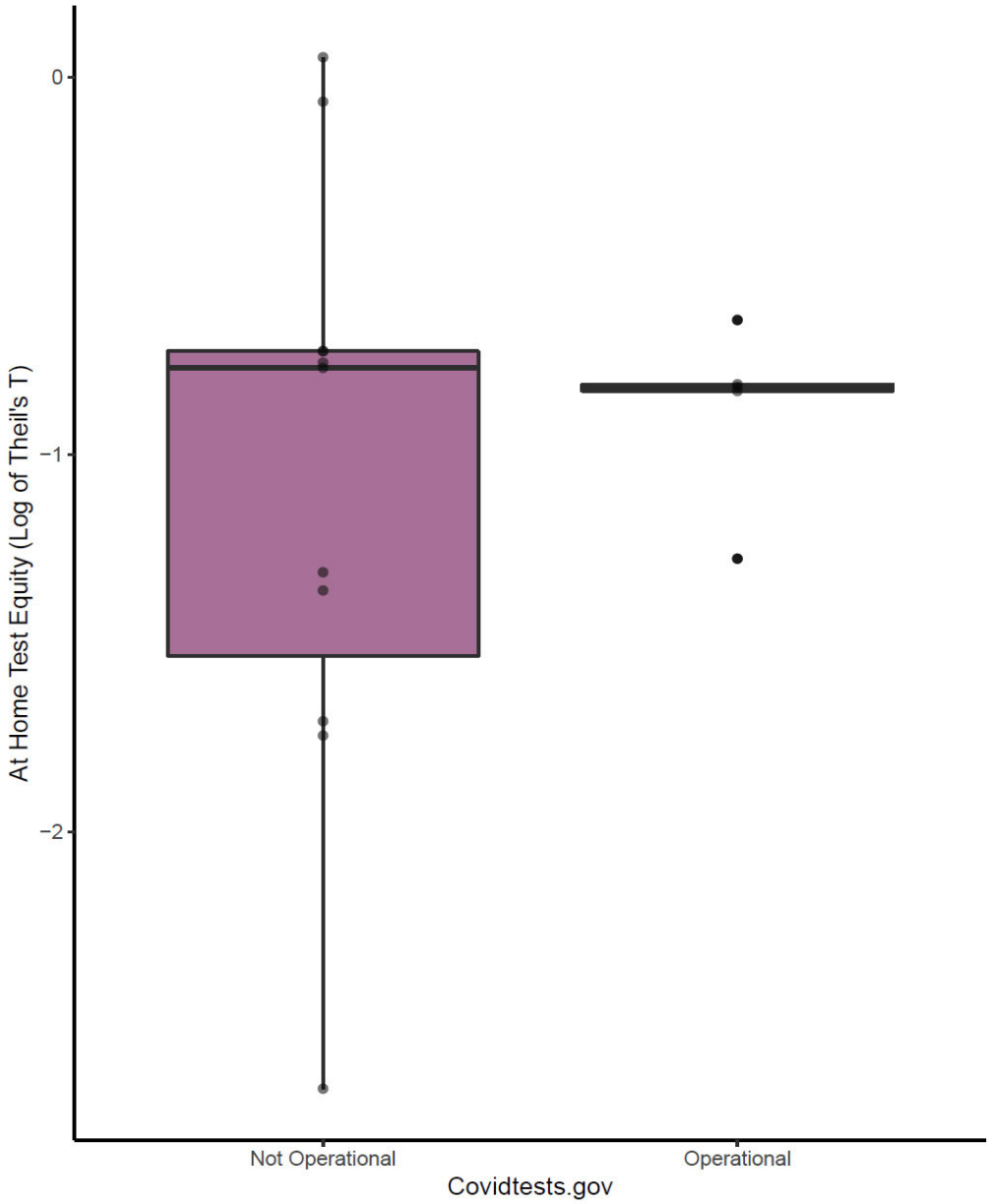

United States adults (N=742,244) self-reported utilization of at-home COVID-19 testing and acute experiences of medical symptoms via an online survey. Proportionality between at-home testing and burden of medical symptoms consistent with COVID-19 (Covid-like illness) across random group membership was measured by Theil's T. Sixteen of the weeks of the study period were identified (top 20th percentile) as weeks of peak COVID-19 burden. Distribution of Theil's T during the five of these weeks occurring during periods of Covidtest.gov operation were compared to the 11 that occurred outside programs operation. Higher Theil's T value suggests reduced equity.

4.6 REFERENCES

1. Centers for Disease Control and Prevention. COVID-19: Data & Surveillance. https://www.cdc.gov/coronavirus/2019-ncov/cases-updates/index.html
2. Astley CM, Tuli G, Mc Cord KA, Cohn EL, Rader B, Varrelman TJ, Chiu SL, Deng X, Stewart K, Farag TH, Barkume KM, LaRocca S, Morris KA, Kreuter F, Brownstein JS. Global monitoring of the impact of the COVID-19 pandemic through online surveys sampled from the Facebook user base. *Proceedings of the National Academy of Sciences*. 2021;118(51):e2111455118. doi:10.1073/pnas.2111455118
3. Nucleic Acid Amplification Tests (NAATs). Centers for Disease Control and Prevention. Published February 11, 2020. Accessed March 3, 2022. https://www.cdc.gov/coronavirus/2019-ncov/lab/naats.html
4. Rubin R. COVID-19 Testing Moves Out of the Clinic and Into the Home. *JAMA*. 2021;326(14):1362. doi:10.1001/jama.2021.15679
5. In Vitro Diagnostics EUAs - Antigen Diagnostic Tests for SARS-CoV-2. U.S. Food and Drug Administration. Published March 3, 2022. Accessed March 3, 2022. https://www.fda.gov/medical-devices/coronavirus-disease-2019-covid-19-emergency-use-authorizations-medical-devices/in-vitro-diagnostics-euas-antigen-diagnostic-tests-sars-cov-2
6. Rader B, Astley CM, Therese Sy KL, Sewalk K, Hswen Y, Brownstein JS, Kraemer MU. Geographic access to United States SARS-CoV-2 testing sites highlights healthcare disparities and may bias transmission estimates. *Journal of Travel Medicine*. 2020;2020:1–4. doi:10.1093/jtm/taaa076
7. Lieberman-Cribbin W, Tuminello S, Flores RM, Taioli E. Disparities in COVID-19 Testing and Positivity in New York City. *American Journal of Preventive Medicine*. 2020;59(3):326–332. doi:10.1016/j.amepre.2020.06.005
8. Tsai TC, Arik S, Jacobson BH, Yoon J, Yoder N, Sava D, Mitchell M, Graham G, Pfister T. Algorithmic fairness in pandemic forecasting: lessons from COVID-19. *npj Digital Medicine*. 2022;5(1):59. doi:10.1038/s41746-022-00602-z
9. Inward RPD, Jackson F, Dasgupta A, Lee G, Battle AL, Parag KV, Kraemer MUG. Impact of spatiotemporal heterogeneity in COVID-19 disease surveillance on epidemiological parameters and case growth rates. *Epidemics*. 2022;41:100627. doi:10.1016/j.epidem.2022.100627
10. Rader B, Gertz A, Iuliano AD, Gilmer M, Wronski L, Astley CM, Sewalk K, Varrelman TJ, Cohen J, Parikh R, Reese HE, Reed C, Brownstein JS. Use of At-Home COVID-19 Tests — United States, August 23, 2021–March 12, 2022. *MMWR Morbidity and Mortality Weekly Report*. 2022;71(13):489–494. doi:10.15585/mmwr.mm7113e1

11. The White House. Fact Sheet: The Biden Administration to Begin Distributing At-Home, Rapid COVID-19 Tests to Americans for Free. The White House. Published January 14, 2022. Accessed March 11, 2023. https://www.whitehouse.gov/briefing-room/statements-releases/2022/01/14/fact-sheet-the-biden-administration-to-begin-distributing-at-home-rapid-covid-19-tests-to-americans-for-free/

12. The White House. Fact Sheet: The Biden Administration Announces Americans Can Order Additional Free At-Home, Rapid COVID-19 Tests at COVIDTests.gov. The White House. Published May 17, 2022. Accessed March 11, 2023. https://www.whitehouse.gov/briefing-room/statements-releases/2022/05/17/fact-sheet-the-biden-administration-announces-americans-can-order-additional-free-at-home-rapid-covid-19-tests-at-covidtests-gov/

13. The White House. Press Briefing by White House COVID-19 Response Team and Public Health Officials. The White House. Published September 6, 2022. Accessed March 11, 2023. https://www.whitehouse.gov/briefing-room/press-briefings/2022/09/06/press-briefing-by-white-house-covid-19-response-team-and-public-health-officials-88/

14. The White House. Fact Sheet: Biden Administration Announces COVID-19 Winter Preparedness Plan. The White House. Published December 15, 2022. Accessed March 11, 2023. https://www.whitehouse.gov/briefing-room/statements-releases/2022/12/15/fact-sheet-biden-administration-announces-covid-19-winter-preparedness-plan/

15. The White House. Press Briefing by Press Secretary Karine Jean-Pierre. The White House. Published September 1, 2022. Accessed March 11, 2023. https://www.whitehouse.gov/briefing-room/press-briefings/2022/09/01/press-briefing-by-press-secretary-karine-jean-pierre-7/

16. Mody A, Pfeifauf K, Geng EH. Using Lorenz Curves to Measure Racial Inequities in COVID-19 Testing. *JAMA Network Open*. 2021;4(1):e2032696. doi:10.1001/jamanetworkopen.2020.32696

17. Gastwirth JL. The Estimation of the Lorenz Curve and Gini Index. *The Review of Economics and Statistics*. 1972;54(3):306. doi:10.2307/1937992

18. Woolhouse MEJ, Dye C, Etard JF, Smith T, Charlwood JD, Garnett GP, Hagan P, Hii JLK, Ndhlovu PD, Quinnell RJ, Watts CH, Chandiwana SK, Anderson RM. Heterogeneities in the transmission of infectious agents: Implications for the design of control programs. *Proceedings of the National Academy of Sciences*. 1997;94(1):338–342. doi:10.1073/pnas.94.1.338

19. Semega J, Kollar, Melissa. Increase in Income Inequality Driven by Real Declines in Income at the Bottom. United States Census Bureau. Published September 13, 2022. Accessed June 7, 2023. https://www.census.gov/library/stories/2022/09/income-inequality-increased.html

20. COVID-19 and Your Health. Centers for Disease Control and Prevention. Published February 11, 2020. Accessed June 7, 2023. https://www.cdc.gov/coronavirus/2019-ncov/symptoms-testing/testing.html

21. Pallikadavath S, Singh A, Ogollah R, Dean T, Stones W. Human resource inequalities at the base of India's public health care system. *Health & Place*. 2013;23:26–32. doi:10.1016/j.healthplace.2013.05.003

22. Harper S, Lynch J. Measuring health inequalities. *Methods in social epidemiology*. 2006;1:134.

23. Schaffer AL, Dobbins TA, Pearson SA. Interrupted time series analysis using autoregressive integrated moving average (ARIMA) models: a guide for evaluating large-scale health interventions. *BMC Medical Research Methodology*. 2021;21(1):58. doi:10.1186/s12874-021-01235-8

24. U.S. Census Bureau. *2015–2019 American Community Survey*. U.S. Census Bureau; 2021.

25. Arbel R, Wolff Sagy Y, Hoshen M, Battat E, Lavie G, Sergienko R, Friger M, Waxman JG, Dagan N, Balicer R, Ben-Shlomo Y, Peretz A, Yaron S, Serby D, Hammerman A, Netzer D. Nirmatrelvir Use and Severe Covid-19 Outcomes during the Omicron Surge. *New England Journal of Medicine*. 2022;387(9):790–798. doi:10.1056/NEJMoa2204919

26. Zerbo O, Lewis N, Fireman B, Goddard K, Skarbinski J, Sejvar JJ, Azziz-Baumgartner E, Klein NP. Population-based assessment of risks for severe COVID-19 disease outcomes. *Influenza and Other Respiratory Viruses*. 2022;16(1):159–165. doi:10.1111/irv.12901

5. CONCLUSION

Misestimation of respiratory infectious disease surveillance parameters is a threat to both descriptive epidemiology and outbreak response. Inadequate data on measures of disease occurrence and associated human behaviors can lead to flawed interpretations of causal relationships and suboptimal allocation of resources. Proper assessment in infectious disease surveillance requires high-quality data and appropriate methods. In this dissertation, we curated multiple high-resolution data streams across two respiratory pathogens of global health importance: tuberculosis, and SARS-CoV-2. We analyzed these data and adapted innovative methods across three distinct aims with the goal of improving our knowledge of pathogen transmission and understanding behavioral response.

Tuberculosis is a global health issue, but its complex disease dynamics, including extended periods of asymptomatic disease, make it difficult to study. In aim 1, we sought to accurately measure the reproductive number, which describes how a disease spreads in a population, for tuberculosis in the Greater Vitória metropolitan area in Brazil. This metric is crucial for guiding public health interventions in the region. In aim 1, we sought to overcome reproductive number estimation challenges by repurposing a routine tuberculosis surveillance system and using a newly developed reproductive number estimator. We also incorporated a human mobility model to account for the fact that individuals may present as a tuberculosis case in a region other than where they got infected. This approach allowed us to assess long-term disease dynamics and spatial variations in tuberculosis transmission within the region. In aim 1, we found that two

cities were the primary drivers of tuberculosis within Greater Vitória, highlighting how the combination of high-quality data and advanced methods can produce novel insights for disease mitigation.

The effectiveness of mask mandates in reducing COVID-19 transmission events is uncertain, and efforts to quantify this relationship have yielded mixed results. In aim 2, we tried to answer a more basic question on the causal pathway between mandates and health outcomes; do mandates change masking levels. We utilized a multi-million-person digital health survey on pandemic related behaviors to quantify the weekly percentage of the population masking across U.S. We combined this data with a comprehensive database on masking related mandates in the same counties to understand how, on a local level, mandates alter masking. In aim 2, we found that mandates produced a small increase in masking behavior, with larger effects observed in areas with lower pre-mandate mask usage. However, there was substantial heterogeneity in the effects of mandates across different counties and many locations had no change in masking post-mandate. These findings highlight the need for tailored and hyperlocal interventions to increase masking and help explain the mixed results seen in previous studies.

Disparities in access to nucleic acid amplification tests have been well-documented, favoring more affluent, insured, and white populations. At-home tests offer advantages such as affordability, convenience, and accessibility, but usage patterns have also shown disparities. In aim 3, we used the same nationally representative digital health survey as aim 2 to assess at-home test utilization across demographic groups, including income, age, race/ethnicity, and geography. We used two economic measures to quantify

distribution equity throughout the pandemic. In aim 3, we found disparities in at-home test utilization across income, age, race, and geography. We also found that the implementation of Covidtests.gov increased some of these disparities, indicating that although the program raised testing rates overall, the benefits were not equally distributed. Aim 3 helps demonstrates how high-resolution datasets can be leveraged to uncover biases in disease surveillance metrics, as well as how those biases change over time and because of exogenous influences.

This dissertation utilized a variety of high-spatial resolution and high-temporal resolution datasets to gain insight into the complexities of respiratory disease surveillance, focusing on uncovering biases and describing heterogeneity. In three aims, we underscore the critical role that granular data and tailored interventions play in controlling infectious diseases. In understanding and addressing these biases and the various sources of heterogeneity, we can facilitate more effective outbreak responses and better inform public health policymaking. Accurate and precise disease surveillance estimates are a vital component in efficient resource allocation, and ultimately in fostering healthier communities.

BIBLIOGRAPHY

Adjodah D, Dinakar K, Chinazzi M, Fraiberger SP, Pentland A, Bates S, Staller K, Vespignani A, Bhatt DL. *Association between COVID-19 Outcomes and Mask Mandates, Adherence, and Attitudes*. Cold Spring Harbor Laboratory Press; 2021:2021.01.19.21250132. doi:10.1101/2021.01.19.21250132

Angelo JR, Katsuragawa TH, Sabroza PC, de Carvalho LAS, Silva LHP da, Nobre CA. The role of spatial mobility in malaria transmission in the Brazilian Amazon: The case of Porto Velho municipality, Rondônia, Brazil (2010–2012). Mertens F, ed. *PLoS ONE*. 2017;12(2):e0172330. doi:10.1371/journal.pone.0172330

Arbel R, Wolff Sagy Y, Hoshen M, Battat E, Lavie G, Sergienko R, Friger M, Waxman JG, Dagan N, Balicer R, Ben-Shlomo Y, Peretz A, Yaron S, Serby D, Hammerman A, Netzer D. Nirmatrelvir Use and Severe Covid-19 Outcomes during the Omicron Surge. *New England Journal of Medicine*. 2022;387(9):790–798. doi:10.1056/NEJMoa2204919

Astley CM, Tuli G, Mc Cord KA, Cohn EL, Rader B, Varrelman TJ, Chiu SL, Deng X, Stewart K, Farag TH, Barkume KM, LaRocca S, Morris KA, Kreuter F, Brownstein JS. Global monitoring of the impact of the COVID-19 pandemic through online surveys sampled from the Facebook user base. *Proceedings of the National Academy of Sciences of the United States of America*. 2021;118(51):e2111455118. doi:10.1073/pnas.2111455118

Brauner JM, Mindermann S, Sharma M, Johnston D, Salvatier J, Gavenčiak T, Stephenson AB, Leech G, Altman G, Mikulik V, Norman AJ, Monrad JT, Besiroglu T, Ge H, Hartwick MA, Teh YW, Chindelevitch L, Gal Y, Kulveit J. Inferring the effectiveness of government interventions against COVID-19. *Science*. 2021;371(6531): eabd9338. doi:10.1126/science.abd9338

Centers for Disease Control and Prevention. COVID-19: Data & Surveillance. https://www.cdc.gov/coronavirus/2019-ncov/cases-updates/index.html

Clinton J, Cohen J, Lapinski J, Trussler M. Partisan pandemic: How partisanship and public health concerns affect individuals' social mobility during COVID-19. *Science Advances*. 2021;7(2):eabd7204. doi:10.1126/sciadv.abd7204

Cohen A, Einav L. The effects of mandatory seat belt laws on driving behavior and traffic fatalities. *Review of Economics and Statistics*. 2003;85(4):828–843. doi:10.1162/003465303772815754

Cori A, Ferguson NM, Fraser C, Cauchemez S. A New Framework and Software to Estimate Time-Varying Reproduction Numbers During Epidemics. *American Journal of Epidemiology*. 2013;178(9):1505–1512. doi:10.1093/aje/kwt133

Cowger TL, Murray EJ, Clarke J, Bassett MT, Ojikutu BO, Sánchez SM, Linos N, Hall KT. Lifting Universal Masking in Schools — Covid-19 Incidence among Students and Staff. *New England Journal of Medicine*. 2022;387(21):1935–1946. doi:10.1056/NEJMoa2211029

Cowling BJ, Zhou Y, Ip DKM, Leung GM, Aiello AE. Face masks to prevent transmission of influenza virus: a systematic review. *Epidemiology and Infection*. 2010; 138(4):449–456. doi:10.1017/S0950268809991658

Dowdy DW, Golub JE, Chaisson RE, Saraceni V. Heterogeneity in tuberculosis transmission and the role of geographic hotspots in propagating epidemics. *Proceedings of the National Academy of Sciences of the United States of America*. 2012;109(24): 9557–9562. doi:10.1073/pnas.1203517109

Doxsey-Whitfield E, MacManus K, Adamo SB, Pistolesi L, Squires J, Borkovska O, Baptista SR. Taking Advantage of the Improved Availability of Census Data: A First Look at the Gridded Population of the World, Version 4. *Papers in Applied Geography*. 2015;1(3):226–234. doi:10.1080/23754931.2015.1014272

Fischer CB, Adrien N, Silguero JJ, Hopper JJ, Chowdhury AI, Werler MM. Mask adherence and rate of COVID-19 across the United States. Tu WJ, ed. *PLoS ONE*. 2021;16(4):e0249891. doi:10.1371/journal.pone.0249891

Gastwirth JL. The Estimation of the Lorenz Curve and Gini Index. *The Review of Economics and Statistics*. 1972;54(3):306. doi:10.2307/1937992

Gebski V, Ellingson K, Edwards J, Jernigan J, Kleinbaum D. Modelling interrupted time series to evaluate prevention and control of infection in healthcare. *Epidemiology and Infection*. 2012;140(12):2131–2141. doi:10.1017/S0950268812000179

Gostic KM, McGough L, Baskerville EB, Abbott S, Joshi K, Tedijanto C, Kahn R, Niehus R, Hay JA, De Salazar PM, Hellewell J, Meakin S, Munday JD, Bosse NI, Sherrat K, Thompson RN, White LF, Huisman JS, Scire J, Bonhoeffer S, Stadler T, Wallinga J, Funk S, Lipsitch M, Cobey S. Practical considerations for measuring the effective reproductive number, Rt. Pitzer VE, ed. *PLoS Computational Biology*. 2020;16(12): e1008409. doi:10.1371/journal.pcbi.1008409

Guy GP, Lee FC, Sunshine G, McCord R, Howard-Williams M, Kompaniyets L, Dunphy C, Gakh M, Weber R, Sauber-Schatz E, Omura JD, Massetti GM, Bailey M, Brown A, Cramer R, Clodfelter C, Davison R, Dugmeoglu S, Fitts A, Gilchrist S, Hulkower R, Limeres A, Pepin D, Popoola A, Schroeder M, Tynan MA, Ukoha C, Williams M, Whitson CD, Jeong G, Landsman L, Moreland A, Shelburne J. Association of State-Issued Mask Mandates and Allowing On-Premises Restaurant Dining with County-Level COVID-19 Case and Death Growth Rates — United States, March 1–December 31,

2020. *MMWR: Morbidity and Mortality Weekly Report*. 2021;70(10):350–354. doi:10.15585/mmwr.mm7010e3

Haber NA, Clarke-Deelder E, Salomon JA, Feller A, Stuart EA. COVID-19 Policy Impact Evaluation: A Guide to Common Design Issues. *American Journal of Epidemiology*. 2021: kwab185. https://doi.org/10.1093/aje/kwab185

Harling G, Castro MC. A spatial analysis of social and economic determinants of tuberculosis in Brazil. *Health and Place*. 2014;25:56–67. doi:10.1016/j.healthplace.2013.10.008

Harper S, Lynch J. Measuring health inequalities. In J.M. Oakes and J.S. Kaufman (eds.), *Methods in social epidemiology,* pp. 134–168. San Francisco: Jossey-Bass, 2006.

Hart WS, Miller E, Andrews NJ, Waight P, Maini PK, Funk S, Thompson RN. Generation time of the alpha and delta SARS-CoV-2 variants: an epidemiological analysis. *The Lancet. Infectious Diseases*. 2022;22(5):603–610. doi:10.1016/S1473-3099(22)00001-9

Hedlund J, Gilbert SH, Ledingham K, Preusser D. *How States Achieve High Seat Belt Use Rates*. National Highway Traffic Safety Administration; 2008:1–170. Accessed May 17, 2021. https://crashstats.nhtsa.dot.gov/Api/Public/ViewPublication/810962

Hendrix MJ, Walde C, Findley K, Trotman R. Absence of Apparent Transmission of SARS-CoV-2 from Two Stylists After Exposure at a Hair Salon with a Universal Face Covering Policy — Springfield, Missouri, May 2020. *MMWR: Morbidity and Mortality Weekly Report*. 2020;69(28):930–932. doi:10.15585/mmwr.mm6928e2

Inward RPD, Jackson F, Dasgupta A, Lee G, Battle AL, Parag KV, Kraemer MUG. Impact of spatiotemporal heterogeneity in COVID-19 disease surveillance on epidemiological parameters and case growth rates. *Epidemics*. 2022;41:100627. doi:10.1016/j.epidem.2022.100627

Jefferson T, Dooley L, Ferroni E, Al-Ansary LA, Van Driel ML, Bawazeer GA, Jones MA, Hoffmann TC, Clark J, Beller EM, Glasziou PP, Conly JM. Physical interventions to interrupt or reduce the spread of respiratory viruses. Cochrane Acute Respiratory Infections Group, ed. *Cochrane Database of Systematic Reviews*. 2023;2023(4). doi:10.1002/14651858.CD006207.pub6

Katz J, Sanger-Katz M, Quealy K. A Detailed Map of Who Is Wearing a Mask in the U.S. The New York Times. Published 2020. Accessed August 5, 2020. https://www.nytimes.com/interactive/2020/07/17/upshot/coronavirus-face-mask-map.html

Leavitt SV, Lee RS, Sebastiani P, Horsburgh CR, Jenkins HE, White LF. Estimating the relative probability of direct transmission between infectious disease patients. *International Journal of Epidemiology*. 2020;49(3):764–775. doi:10.1093/ije/dyaa031

Leech G, Rogers-Smith C, Monrad JT, Sandbrink JB, Snodin B, Zinkov R, Rader B, Brownstein JS, Gal Y, Bhatt S, Sharma M, Mindermann S, Brauner JM, Aitchison L. Mask wearing in community settings reduces SARS-CoV-2 transmission. *Proceedings of the National Academy of Sciences of the United States of America*. 2022;119(23): e2119266119. doi:10.1073/pnas.2119266119

Lehtinen S, Ashcroft P, Bonhoeffer S. On the relationship between serial interval, infectiousness profile and generation time. *Journal of The Royal Society Interface*. 2021; 18(174):20200756. doi:10.1098/rsif.2020.0756

Lieberman-Cribbin W, Tuminello S, Flores RM, Taioli E. Disparities in COVID-19 Testing and Positivity in New York City. *American Journal of Preventive Medicine*. 2020;59(3):326–332. doi:10.1016/j.amepre.2020.06.005

Lillebaek T, Dirksen A, Baess I, Strunge B, Thomsen V, Andersen ÅB. Molecular evidence of endogenous reactivation of Mycobacterium tuberculosis after 33 years of latent infection. *Journal of Infectious Diseases*. 2002;185(3):401–404. doi:10.1086/338342

Lüdecke D. ggeffects: Tidy Data Frames of Marginal Effects from Regression Models. *Journal of Open Source Software*. 2018;3(26):772. doi:10.21105/joss.00772

Ma Y, Horsburgh CR, White LF, Jenkins HE. Quantifying TB transmission: A systematic review of reproduction number and serial interval estimates for tuberculosis. *Epidemiology and Infection*. 2018;146(12):1478–1494. doi:10.1017/S0950268818001760

Ma Y, Jenkins HE, Sebastiani P, Ellner JJ, Jones-López EC, Dietze R, Horsburgh, Jr. CR, White LF. Using Cure Models to Estimate the Serial Interval of Tuberculosis With Limited Follow-up. *American Journal of Epidemiology*. 2020;189(11):1421–1426. doi:10.1093/aje/kwaa090

Maas J, van Dillen SME, Verheij RA, Groenewegen PP. Social contacts as a possible mechanism behind the relation between green space and health. *Health and Place*. 2009;15(2):586–595. doi:10.1016/j.healthplace.2008.09.006

Maciel ELN, Pan W, Dietze R, Peres RL, Vinhas SA, Ribeiro FK, Palaci M, Rodrigues RR, Zandonade E, Golub JE. Spatial patterns of pulmonary tuberculosis incidence and their relationship to socio-economic status in Vitoria, Brazil. *International Journal of Tuberculosis and Lung Disease*. 2010;14(11):1395–1402.

McIntosh AI, Jenkins HE, White LF, Barnard M, Thomson DR, Dolby T, Simpson J, Streicher EM, Kleinman MB, Ragan EJ, van Helden PD, Murray MB, Warren RM, Jacobson KR. Using routinely collected laboratory data to identify high rifampicin-resistant tuberculosis burden communities in the Western Cape Province, South Africa: A retrospective spatiotemporal analysis. Suthar AB, ed. *PLoS Medicine*. 2018;15(8): e1002638. doi:10.1371/journal.pmed.1002638

McKelvey T. Coronavirus: Why are Americans so angry about masks? *BBC News*. https://www.bbc.com/news/world-us-canada-53477121. Published July 20, 2020. Accessed May 3, 2021.

Mody A, Pfeifauf K, Geng EH. Using Lorenz Curves to Measure Racial Inequities in COVID-19 Testing. *JAMA Network Open*. 2021;4(1):e2032696. doi:10.1001/jamanetworkopen.2020.32696

Moreno V, Espinoza B, Barley K, Paredes M, Bichara D, Mubayi A, Castillo-Chavez C. The role of mobility and health disparities on the transmission dynamics of Tuberculosis. *Theoretical Biology and Medical Modelling*. 2017;14(1):1–17. doi:10.1186/s12976-017-0049-6

Nunes MRT, Faria NR, de Vasconcelos JM, Golding N, Kraemer MUG, de Oliveira LF, da Silva Azevedo R do S, da Silva DEA, da Silva EVP, da Silva SP, Carvalho VL, Coelho GE, Cruz ACR, Rodrigues SG, da Silva Gonçalves Vianez JL, Nunes BTD, Cardoso JF, Tesh RB, Hay SI, Pybus OG, da Costa Vasconcelos PF. Emergence and potential for spread of Chikungunya virus in Brazil. *BMC Medicine*. 2015;13(1):102. doi:10.1186/s12916-015-0348-x

Pallikadavath S, Singh A, Ogollah R, Dean T, Stones W. Human resource inequalities at the base of India's public health care system. *Health & Place*. 2013;23:26–32. doi:10.1016/j.healthplace.2013.05.003

Parag KV. Improved estimation of time-varying reproduction numbers at low case incidence and between epidemic waves. Kosakovsky Pond SL, ed. *PLoS Computational Biology*. 2021;17(9):e1009347. doi:10.1371/journal.pcbi.1009347

Rader B, Astley CM, Therese Sy KL, Sewalk K, Hswen Y, Brownstein JS, Kraemer MU. Geographic access to United States SARS-CoV-2 testing sites highlights healthcare disparities and may bias transmission estimates. *Journal of Travel Medicine*. 2020; 2020:1–4. doi:10.1093/jtm/taaa076

Rader B, Gertz A, Iuliano AD, Gilmer M, Wronski L, Astley CM, Sewalk K, Varrelman TJ, Cohen J, Parikh R, Reese HE, Reed C, Brownstein JS. Use of At-Home COVID-19 Tests — United States, August 23, 2021–March 12, 2022. *MMWR: Morbidity and Mortality Weekly Report*. 2022;71(13):489–494. doi:10.15585/mmwr.mm7113e1

Rader B, Scarpino SV, Nande A, Hill AL, Adlam B, Reiner RC, Pigott DM, Gutierrez B, Zarebski AE, Shrestha M, Brownstein JS, Castro MC, Dye C, Tian H, Pybus OG, Kraemer MUG. Crowding and the shape of COVID-19 epidemics. *Nature Medicine*. 2020;28:1829–1834. doi:10.1038/s41591-020-1104-0

Rader B, White LF, Burns MR, Chen J, Brilliant J, Cohen J, Shaman J, Brilliant L, Kraemer MUG, Hawkins JB, Scarpino SV, Astley CM, Brownstein JS. Mask-wearing and control of SARS-CoV-2 transmission in the USA: a cross-sectional study. *The Lancet. Digital Health*. 2021;3(3):e148–e157. doi:10.1016/S2589-7500(20)30293-4

Randy Ludlow. Coronavirus in Ohio: DeWine requires masks in seven counties, including Cuyahoga. *Akron Beacon Journal*. https://www.beaconjournal.com/story/news/coronavirus/2020/07/07/coronavirus-in-ohio-dewine-requires-masks-in-seven-counties-including-cuyahoga/113367044/. Published July 7, 2020.

Robsky KO, Isooba D, Nakasolya O, Mukiibi J, Nalutaaya A, Kitonsa PJ, Kamoga C, Baik Y, Kendall EA, Katamba A, Dowdy DW. Characterization of geographic mobility among participants in facility- and community-based tuberculosis case finding in urban Uganda. Lebina L, ed. *PLoS ONE*. 2021;16(5):e0251806. doi:10.1371/journal.pone.0251806

Rubin R. COVID-19 Testing Moves Out of the Clinic and Into the Home. *JAMA: The Journal of the American Medical Association*. 2021;326(14):1362. doi:10.1001/jama.2021.15679

Schaffer AL, Dobbins TA, Pearson SA. Interrupted time series analysis using autoregressive integrated moving average (ARIMA) models: a guide for evaluating large-scale health interventions. *BMC Medical Research Methodology*. 2021;21(1):58. doi:10.1186/s12874-021-01235-8

Semega J, Kollar, Melissa. Increase in Income Inequality Driven by Real Declines in Income at the Bottom. United States Census Bureau. Published September 13, 2022. Accessed June 7, 2023. https://www.census.gov/library/stories/2022/09/income-inequality-increased.html

Simini F, González MC, Maritan A, Barabási AL. A universal model for mobility and migration patterns. *Nature*. 2012;484(7392):96–100. doi:10.1038/nature10856

The White House. Fact Sheet: The Biden Administration to Begin Distributing At-Home, Rapid COVID-19 Tests to Americans for Free. The White House. Published January 14, 2022. Accessed March 11, 2023. https://www.whitehouse.gov/briefing-room/statements-releases/2022/01/14/fact-sheet-the-biden-administration-to-begin-distributing-at-home-rapid-covid-19-tests-to-americans-for-free/

The White House. Fact Sheet: The Biden Administration Announces Americans Can Order Additional Free At-Home, Rapid COVID-19 Tests at COVIDTests.gov. The White House. Published May 17, 2022. Accessed March 11, 2023. https://www.whitehouse.gov/briefing-room/statements-releases/2022/05/17/fact-sheet-the-biden-administration-announces-americans-can-order-additional-free-at-home-rapid-covid-19-tests-at-covidtests-gov/

The White House. Press Briefing by Press Secretary Karine Jean-Pierre. The White House. Published September 1, 2022. Accessed March 11, 2023. https://www.whitehouse.gov/briefing-room/press-briefings/2022/09/01/press-briefing-by-press-secretary-karine-jean-pierre-7/

The White House. Press Briefing by White House COVID-19 Response Team and Public Health Officials. The White House. Published September 6, 2022. Accessed March 11, 2023. https://www.whitehouse.gov/briefing-room/press-briefings/2022/09/06/press-briefing-by-white-house-covid-19-response-team-and-public-health-officials-88/

The White House. Fact Sheet: Biden Administration Announces COVID-19 Winter Preparedness Plan. The White House. Published December 15, 2022. Accessed March 11, 2023. https://www.whitehouse.gov/briefing-room/statements-releases/2022/12/15/fact-sheet-biden-administration-announces-covid-19-winter-preparedness-plan/

Theron G, Jenkins HE, Cobelens F, Abubakar I, Khan AJ, Cohen T, Dowdy DW. Data for action: Collection and use of local data to end tuberculosis. *The Lancet*. 2015; 386(10010):2324–2333. doi:10.1016/S0140-6736(15)00321-9

Tsai TC, Arik S, Jacobson BH, Yoon J, Yoder N, Sava D, Mitchell M, Graham G, Pfister T. Algorithmic fairness in pandemic forecasting: lessons from COVID-19. *npj Digital Medicine*. 2022;5(1):59. doi:10.1038/s41746-022-00602-z

Tuite AR, Thomas-Bachli A, Acosta H, Bhatia D, Huber C, Petrasek K, Watts A, Yong JHE, Bogoch II, Khan K. Infectious disease implications of large-scale migration of Venezuelan nationals. *Journal of Travel Medicine*. 2018;25(1):1–8. doi:10.1093/jtm/tay077

U.S. Census Bureau. *2015–2019 American Community Survey*. U.S. Census Bureau; 2021.

Vieira RDCA, Fregona G, Palaci M, Dietze R, Maciel ELN. Epidemiological profile of multidrug-resistant tuberculosis cases in Espírito Santo. *Revista Brasileira de Epidemiologia*. 2007;10(1):56–65. doi:10.1590/s1415-790x2007000100007

Vinhas SA, Jones-López EC, Ribeiro Rodrigues R, Gaeddert M, Peres RL, Marques-Rodrigues P, de Aguiar PPL, White LF, Alland D, Salgame P, Hom D, Ellner JJ, Dietze

R, Collins LF, Shashkina E, Kreiswirth B, Palaci M. Strains of Mycobacterium tuberculosis transmitting infection in Brazilian households and those associated with community transmission of tuberculosis. *Tuberculosis*. 2017;104:79–86. doi:10.1016/j.tube.2017.03.003

Wagner AK, Soumerai SB, Zhang F, Ross-Degnan D. Segmented regression analysis of interrupted time series studies in medication use research. *Journal of Clinical Pharmacy and Therapeutics*. 2002;27(4):299–309. doi:10.1046/j.1365-2710.2002.00430.x

Wallinga J, Teunis P. Different epidemic curves for severe acute respiratory syndrome reveal similar impacts of control measures. *American Journal of Epidemiology* 2004;160 (6):509–516. doi:10.1093/aje/kwh255

Wang X, Ferro EG, Zhou G, Hashimoto D, Bhatt DL. Association Between Universal Masking in a Health Care System and SARS-CoV-2 Positivity Among Health Care Workers. *JAMA: The Journal of the American Medical Association*. 2020;324(7):703–704. doi:10.1001/jama.2020.12897

Wen TH, Hsu CS, Hu MC. Evaluating neighborhood structures for modeling intercity diffusion of large-scale dengue epidemics. *International Journal of Health Geographics*. 2018;17(1):9. doi:10.1186/s12942-018-0131-2

Wesolowski A, Buckee CO, Engø-Monsen K, Metcalf CJE. Connecting mobility to infectious diseases: The promise and limits of mobile phone data. *Journal of Infectious Diseases*. 2016;214(Suppl 4):S414–S420. doi:10.1093/infdis/jiw273

Whaley CM, Cantor J, Pera M, Jena AB. Assessing the Association Between Social Gatherings and COVID-19 Risk Using Birthdays. *JAMA Internal Medicine*. 2021; 181(8):1090. doi:10.1001/jamainternmed.2021.2915

White LF, Archer B, Pagano M. Estimating the reproductive number in the presence of spatial heterogeneity of transmission patterns. *International Journal of Health Geographics*. 2013;12(1):1–10. doi:10.1186/1476-072x-12-35

White LF, Moser CB, Thompson RN, Pagano M. Statistical Estimation of the Reproductive Number From Case Notification Data. *American Journal of Epidemiology*. 2021;190(4):611–620. doi:10.1093/aje/kwaa211

White LF, Pagano M. Reporting errors in infectious disease outbreaks, with an application to Pandemic Influenza A/H1N1. *Epidemiologic Perspectives and Innovations*. 2010;7(1). doi:10.1186/1742-5573-7-12

WHO. *Global Tuberculosis Report 2019*. World Health Organization; 2019:7. Accessed October 6, 2020. http://www.who.int/tb/publications/global_report/en/

Woolhouse MEJ, Dye C, Etard JF, Smith T, Charlwood JD, Garnett GP, Hagan P, Hii JLK, Ndhlovu PD, Quinnell RJ, Watts CH, Chandiwana SK, Anderson RM. Heterogeneities in the transmission of infectious agents: Implications for the design of control programs. *Proceedings of the National Academy of Sciences of the United States of America*. 1997;94(1):338–342. doi:10.1073/pnas.94.1.338

Wright AL, Chawla G, Chen L, Farmer A. Tracking Mask Mandates During the Covid-19 Pandemic. *SSRN Electronic Journal*. Published online August 7, 2020. doi:10.2139/ssrn.3667149

Zamudio C, Krapp F, Choi HW, Shah L, Ciampi A, Gotuzzo E, Heymann J, Seas C, Brewer TF. Public Transportation and Tuberculosis Transmission in a High Incidence Setting. Mokrousov I, ed. *PLoS ONE*. 2015;10(2):e0115230. doi:10.1371/journal.pone.0115230

Zerbo O, Lewis N, Fireman B, Goddard K, Skarbinski J, Sejvar JJ, Azziz-Baumgartner E, Klein NP. Population-based assessment of risks for severe COVID-19 disease outcomes. *Influenza and Other Respiratory Viruses*. 2022;16(1):159–165. doi:10.1111/irv.12901

Zhou Z, Kolaczyk E, Thompson R, White L. *Estimation of Heterogeneous Instantaneous Reproduction Numbers with Application to Characterize SARS-CoV-2 Transmission in Massachusetts Counties*. Infectious Diseases (except HIV/AIDS); 2021. doi:10.1101/2021.12.02.21267164

Zinszer K, Morrison K, Brownstein JS, Marinho F, Santos AF, Nsoesie EO. Reconstruction of zika virus introduction in Brazil. *Emerging Infectious Diseases*. 2017; 23(1):92–94. doi:10.3201/eid2301.161274

Zou G. A Modified Poisson Regression Approach to Prospective Studies with Binary Data. *American Journal of Epidemiology*. 2004;159(7):702–706. doi:10.1093/aje/kwh090

Sinopse Do Censo Demográfico: 2010. Brazilian Institute of Geography and Statistics; 2011.

Global Administrative Areas. GADM database of Global Administrative Areas. Published 2020. Accessed October 6, 2020. https://gadm.org/

CURRICULUM VITAE